

©Copyright 2018

Jesus E. Contreras Ocaña

Technical and Economic Models for Distributed Energy Resources Integration

Jesus E. Contreras Ocaña

A dissertation
submitted in partial fulfillment of the
requirements for the degree of

Doctor of Philosophy

University of Washington

2018

Reading Committee:

Baosen Zhang, Chair

Miguel A. Ortega-Vazquez, Chair

Daniel S. Kirschen

Program Authorized to Offer Degree:
Electrical Engineering

University of Washington

Abstract

Technical and Economic Models for Distributed Energy Resources Integration

Jesus E. Contreras Ocaña

Co-Chairs of the Supervisory Committee:

Assistant Professor Baosen Zhang

Electrical Engineering

Affiliate Assistant Professor Miguel A. Ortega-Vazquez

Electrical Engineering

The increase in distributed energy resources (DERs) in power systems presents society with both opportunities and challenges. On the one hand, DERs tend to reduce carbon emissions, introduce competition, and increase the flexibility to power systems. On the other hand, DERs fundamentally disrupt the technical and economic nature of power systems. As a result, they raise challenges such as less predictable load, more complex control of resources, disruption of power flow patterns, and obsolescence of market designs.

This dissertation addresses five of those challenges: i) the need for models of building load flexibility and ii) models of interaction between DERs and their aggregator, iii) the problem of coordination among DERs, iv) the risk of market power abuse, and v) the long-term DERs planning problem.

Regarding i), we present a data-driven and statistically robust model that describes the flexibility of thermostatically controlled loads in buildings. The model's simplicity makes it suitable for a wide-range of power system applications such as economic dispatch, optimal power flow, and reserve allocation problems.

Regarding ii), we present an interaction model for DERs and their aggregator that predicts their long-term equilibrium. Predicting the eventual equilibrium is valuable because

it predicts the aggregator’s behavior in the electricity market and profit allocation among players.

Regarding iii), we present a mixed-integer linear program adaptation of the Dantzig-Wolfe decomposition algorithm for decentralized coordination of a building and a fleet of electric vehicles (EVs). This algorithm is suitable for buildings and EVs whose operation is coupled (e.g., by common infrastructure) and cannot formulate a joint problem due to data privacy concerns or software impediments.

Regarding iv), we present a pricing mechanism that mitigates the market power of a generic firm (e.g., a generator, a demand-side bidder, or an aggregator of DERs). The pricing mechanism is attractive because it incentivizes socially optimal bids by the firm, requires no private information to be formulated, and provides an instrument for the regulation of the firm’s profit.

Finally, regarding v), we present a DER planning problem for deferral of capacity expansion (i.e., a non-wire alternatives planning problem) and an algorithm to solve it. Our contributions in this domain are twofold. We explicitly model deferral of capacity expansion an additional value stream of DERs and provide a scalable and tractable algorithm to solve this non-convex, large-scale problem.

TABLE OF CONTENTS

	Page
List of Figures	iv
List of Tables	vii
Glossary	viii
Chapter 1: Introduction	1
1.1 A motivating example	1
1.2 The trend of decentralization of electric power systems	2
1.3 DERs as disruptors of the old utility model	5
1.4 Potential benefits and challenges of DER adoption	5
Chapter 2: Contributions of this dissertation	14
2.1 Chapter 3: Modeling the Flexibility of Building Loads	14
2.2 Chapter 4: Modeling an Aggregator	17
2.3 Chapter 5: Coordination of Buildings and Electric Vehicles	22
2.4 Chapter 6: Market Power	24
2.5 Chapter 7: Non-wire Alternatives to Capacity Expansion	26
2.6 Organization of this dissertation	29
Chapter 3: Modeling the Flexibility of Buildings	30
3.1 Introduction	30
3.2 Preliminaries	34
3.3 A tractable and robust approximation of \mathcal{P}	37
3.4 Estimating the feasible region	39
3.5 Model validation	46
3.6 Case study: building flexibility for wind power balancing	51

3.7	Summary	56
Chapter 4:	Modeling an Aggregator	57
4.1	Introduction	57
4.2	Models	61
4.3	Single-shot game	62
4.4	Longterm cooperation	65
4.5	Profit split via Nash Bargaining	69
4.6	Summary	73
Chapter 5:	Coordination of Buildings and Electric Vehicles	74
5.1	Introduction	74
5.2	Organization of this chapter	77
5.3	Building model	77
5.4	Electric vehicles	82
5.5	The building-EV demand scheduling problem	85
5.6	Case studies	87
5.7	Summary	97
Chapter 6:	Market Power	99
6.1	Introduction	99
6.2	Strategic participant model	103
6.3	Market model	104
6.4	Market outcomes	107
6.5	Market power mitigation	110
6.6	Case study: the market power of an ESS in the IEEE 24 bus RTS	114
6.7	Summary	125
Chapter 7:	Non-Wire Alternatives to Capacity Expansion	126
7.1	Introduction	126
7.2	The capacity expansion problem	129
7.3	Non-wire alternatives	131
7.4	The non-wire alternatives planning problem	135
7.5	Solution techniques	139

7.6	Case study: non-wire alternatives for the University of Washington	142
7.7	Conclusion	149
Chapter 8:	Conclusion and Suggestions for Future Work	150
	Bibliography	154
Appendix A:	Dantzig-Wolfe Decomposition for Mixed-Integer Linear Programs	174
A.1	The master problem	175
A.2	The subproblems	176
A.3	Initialization	176
A.4	Phase I/II Algorithm	176
A.5	Terminating condition	177
Appendix B:	Training data clustering	179
Appendix C:	Estimate of the temperature and load limits	180
Appendix D:	Bounded least squares estimation	181
Appendix E:	Proofs	185
E.1	Proof of Lemma 1	185
E.2	Proof of Lemma 2	187
E.3	Proof of Theorem 1	188
E.4	Proof of Theorem 2	189

LIST OF FIGURES

Figure Number	Page
1.1 Forecasted demand in the Brooklyn-Queens area.	2
1.2 Forecast of annual distributed energy resources installations in the U.S.	3
1.3 Median installed price of ≤ 10 kW residential solar photovoltaic (PV) systems.	4
1.4 “Duck curve” and ramp requirements in CAISO.	9
2.1 Illustration of the feasible region of the load and a (hypothetical) thermal dynamics function.	16
2.2 Illustration of the robust approximation of the feasible region of the load and the RC circuit model.	18
2.3 Illustration of the market-aggregator-DERs relationship.	19
2.4 Illustration of DERs sharing infrastructure.	22
2.5 Visual representation of the building-EV demand scheduling problem.	23
3.1 High-level illustration of tractable and robust modeling of building flexibility.	33
3.2 Illustration of the feasible region of the load and a thermal dynamics function.	36
3.3 Illustration of the robust approximation of the feasible region and an RC model approximation.	37
3.4 Load and indoor temperature time-series simulated data of a small office building.	40
3.5 Illustration of the clustering and training algorithm.	42
3.6 Illustration of the BLSE and classical LSE.	42
3.7 Measured indoor temperature, indoor mean temperature estimate, and prediction bounds for a sample day.	43
3.8 Illustration of the data and algorithm to train $\hat{\xi}_t$	44
3.9 Training data grouped into three clusters.	45
3.10 Decision tree trained using points in Fig. 3.9.	46
3.11 MSE (for the cross-validation dataset) of the indoor temperature prediction for the three buildings and accuracy of the decision tree as a function of the number of clusters.	47

3.12	Percentage of measurements out of bounds, test error of the temperature prediction, and average bound width for each building type. These statistics are computed using test set data.	48
3.13	Test set RMSE for three different models: the RC circuit model, our model (central prediction), ($\alpha = 1$) and our model with $\alpha = 0.05$	50
3.14	Wind scenarios used in the case study.	51
3.15	Expected forecast error mitigation by all three buildings as a function of compensation v	53
3.16	Base load at different wind balancing compensation levels.	53
3.17	Expected forecast error mitigation and expected temperature violation by each building as a function of the robustness parameter.	55
3.18	Time required to solve Problem (3.4) under different number of buildings.	55
4.1	Market-aggregator-DETs framework.	58
4.2	Aggregator/storage unit Stackelberg and a Pareto-superior profits.	60
4.3	Cooperation regions.	70
4.4	Set of possible outcomes bargaining outcomes.	72
5.1	Visual representation of the building-EV demand scheduling problem structure.	85
5.2	Visual representation of the DWDA implementation information flow.	88
5.3	Southern California Edison hourly RTP schedule.	89
5.4	Case Study: demand limits. Aggregate building and EV demand for three different strategies.	90
5.5	Case Study: peak demand charge. Aggregate building and EV demand for two different strategies.	92
5.6	Case Study: itemized billing. Aggregate building and EV demand for two different strategies.	94
5.7	Objective function value vs number of iterations for each case study.	95
6.1	Social cost increase (with respect to the social optimum) due to strategic bidding of the ESS.	123
6.2	Surplus difference (with respect to the social optimum) due to the ESS's strategic bid for each power system actors. Positive differences denote gains while negative differences denote losses with respect to the social optimum.	124
7.1	Campus peak load scenarios.	144
7.2	NWAs planning problem objective value as a function of the protection level Γ	145

7.3	Year of expansion for traditional and NWAs-base planning as a function of the protection level Γ	145
7.4	Installed NWAs capacities for three values of Γ : 0, 0.5, and 1.	146
7.5	Load shed (as percentage of total load) as a function of Γ	147
7.6	Total as a function of Γ for two different values of lost load.	148
7.7	Optimal protection level as a function of VOLL.	148
A.1	Flow chart describing the Dantzig-Wolfe decomposition algorithm.	178

LIST OF TABLES

Table Number		Page
2.1	Description of planning and operating variables for a planning problem that considers four NWAs and a planning horizon of 20 years.	28
3.1	Summary of building characteristics.	46
5.1	Computational performance for the three Case Studies.	96
5.2	Computational performance for Case Study 1 with an increased number of buildings and EVs.	97
6.1	Welfare and profits for each market outcome: strategic bid and social optimum.	110
6.2	Surplus distribution among th four power system actors and social cost. . . .	125
7.1	Non-wire alternatives parameters	143

GLOSSARY

- AGC: Automatic generation control
- BLSE: Bounded least squares estimation
- BPA: Bonneville Power Administration
- CAISO: California Independent System Operator
- CHP: Combined heat and power
- COP: Coefficient of performance
- CPLEX: Optimization software package
- CPU: Central processing unit
- DER: Distributed energy resource
- DG: Distributed generation
- DSO: Distribution system operator
- DSR: Demand-side resource
- DR: Demand response
- DWDA: Dantzig-Wolfe decomposition algorithm
- ED: Economic dispatch
- EE: Energy efficiency
- ES: Energy storage

ESS: Energy storage system

ENERGYPLUSTM: Whole building energy simulation to model both energy consumption and water use in buildings

EMS: Energy management system

EPEC: Equilibrium problem with equilibrium constraints

EV: Electric vehicle

FERC: Federal Energy Regulatory Commission

HEMS: home energy management system

HHI: Herfindahl-Hirschman Index

HVAC: Heating, ventilation, and air conditioning

IEEE: Institute of Electrical and Electronics Engineers

ISO: Independent system operator

GAMS: General Algebraic Modeling System

GAN: Generative adversarial network

GUROBI: Optimization software package

JULIA: Programming language for numerical computing

JUMP: Optimization modeling environment in Julia

KKT: KarushKuhnTucker

LMP: Locational marginal price/pricing

LP: Linear program

LSE: Least squares error

MILP: Mixed-integer linear program

MLE: Maximum likelihood estimator

MPMP: Market power mitigating price

NE-ISO: New England Independent System Operator

NREL: National Renewable Energy Laboratory

NWA: Non-wire alternative

NYISO: New York Independent System Operator

MSE: Mean squared error

OPF: Optimal power flow

PCMI: Price-Cost Margin Index

PJM: Pennsylvania-Jersey-Maryland Interconnection

PV: Photovoltaic

RAM: Random-access memory

RC: Resistance-capacitance (used in the context of the RC circuit analogy for thermal dynamics)

RES: Renewable energy sources

RSI: Residual supply index

RTP: Real-time price

RTS: Reliability test system

SCL: Seattle City Light

SO: System operator

SOC: State-of-charge

SU: Storage unit

TLC: Thermostatically-controlled load

UC: Unit commitment

U-VALUE: A measure how effective a material is as an insulator

UW: University of Washington

V2B: Vehicle-to-Building

V2G: Vehicle-to-Grid

VOLL: Value of lost load

ACKNOWLEDGMENTS

I would first like to thank my parents for supporting me from the minute I was born to today and beyond. From them, I gained all the personal attributes that were essential to complete my Ph.D.

I would also like to thank Prof. Miguel Ortega-Vazquez guiding the first and mid stages of this Ph.D. and Prof. Baosen Zhang for taking me in during the final stages. In their own ways, their advice has been invaluable from academic, professional, and personal points of view.

I also thank my co-authors: Miguel, Baosen, Daniel, Mushfiq, Yishen, Uzma, and Yize. I appreciate their constructive criticism that has made my work better and pushed me to improve my writing and research skills.

I am incredibly grateful to have shared the last 4.75 years among the smart and handsome people from the REAL Lab: Daniel (Kirschen), Miguel, Chanaka, Ting, Yushi, Bolun, Ahmad, Abeer, Ryan (Elliott), Daniel (Olsen), Yao, Nam, Mareldi, Agata, Hrvoje, Pierre, Ricardo, Tu, Remy, Ahlmahz, Yury, Mushfiq, Yishen, Zeyu, Drew, Rebecca, Agustina, James, Kelly, Anna, Kevin, Kevin, Ryan (Hay), and anyone that I might have missed¹. I give Daniel Olsen credit for the title of this dissertation.

I would like to acknowledge the sources of funding that made my Ph.D. possible: the Clean Energy Institute, Dr. Kirsche, Dr. Ortega-Vazquez, Dr. Zhang, the Keith and Nancy Rattie Endowed Fellowship, Battery Informatics, Inc., Seattle City Light, and the Graduate & Professional Student Senate.

¹I blame Yushi if this is the case.

Last but not least, I would like to thank the fantastic faculty and staff of the Electrical Engineering Department, the friends I have made throughout this journey, and especially my azizam, Mina.

DEDICATION

A mis papás.

Chapter 1

INTRODUCTION

1.1 A motivating example

Brooklyn, Queens, and other boroughs of New York City have experienced a booming population during the past couple of decades. A consequence of fast growth is a sharp increase in electric load. Con Edison, the local utility, has seen overloads in sub-transmission feeders in Brooklyn since 2013. By the end of 2018, the utility expects overloads of circa 70 MW during peak summer days [75] (see Fig. 1.1). Traditional upgrades to alleviate overloads (e.g., reinforcing the overloaded feeders or rerouting flows) are estimated to cost approximately \$1 billion¹ [53].

As an alternative to distribution system upgrades, Con Edison has proposed a blend of DERs as “non-wire” alternatives (NWA). The proposal includes distributed generation (DG), demand response (DR), energy efficiency (EE), fuel cells, battery storage, etc. The basic idea is simple: shaping the load to keep it below capacity limits using DERs.

At a cost of \$200 million, Con Edison hopes to defer the \$1 billion in traditional infrastructure upgrades for up to 10 years. Con Edison asserts that the time-value of money resulting from deferred investment, environmental, and social benefits of clean DG [19] justify the \$200 million investment. While some of the NWAs are planned to be utility-owned and operated (e.g., utility-size energy storage), Con Edison anticipates that many would be customer ownership and control, i.e., “behind the meter²”.

On its surface, the difference of Con Edison’s non-wire approach and traditional solutions

¹This relatively high number is due to the difficulties of upgrading a complex underground distribution system located in one of the densest urban areas in North America.

²“Behind-the-meter” resources are devices that are connected downstream from a customer meter.

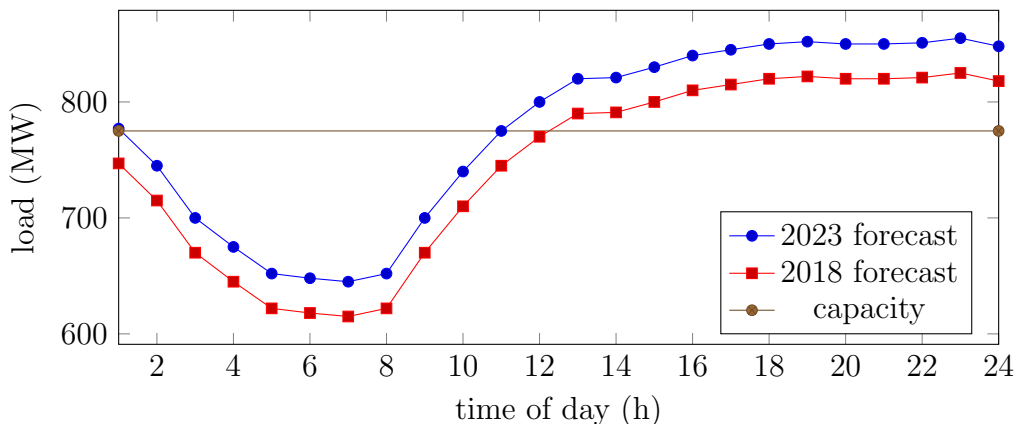


Figure 1.1: Forecasted demand in the Brooklyn-Queens area. (Image: Own elaboration. Data: courtesy of Con Edison.)

seems innovative yet relatively inconsequential on the grand scheme of things. Traditional solutions increase the system’s capacity (i.e., push up the capacity limit in Fig 1.1). Alternatively, a non-wire approach shapes the load to keep it below the capacity limit. However, a closer look raises questions about the simplicity of the trade-offs. The adoption of customer-owned, distribution-level DERs is leading to profound technical, regulatory, and economic changes in the utilities we conceive, plan, and operate electric power systems. These changes motivate this dissertation.

1.2 The trend of decentralization of electric power systems

The presence of “behind-the-meter,” customer-owned resources in Con Edison’s service territory is just a single example of a broader trend of decentralization and increasing adoption of DERs in electric power systems [38]. As shown in Fig. 1.2, new installations of DERs are expected to be about 80 GW for 2019 and just shy of 140 GW during the year 2024. A couple of macro-trends drive the increasing adoption of DERs: evolution preferences (by both the public and the government [150]) and technological improvements.

The evolution of preferences driving DER adoption manifests itself in a few ways. For instance, increased environmental concerns by governments have resulted in incentives for

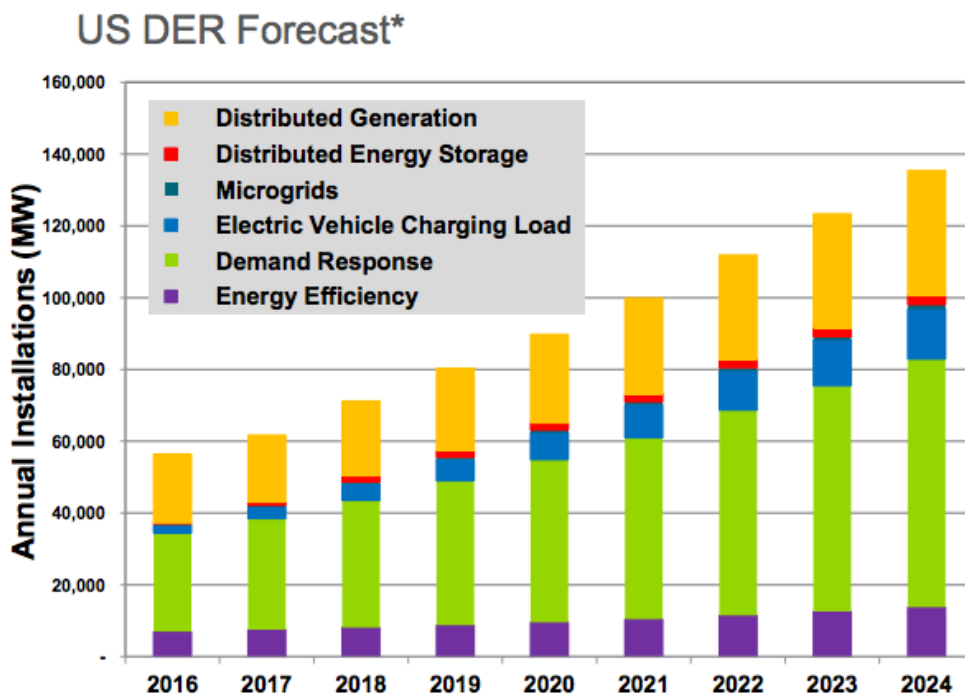


Figure 1.2: Forecast of annual DER installations in the U.S. (Image courtesy of Navigant Research Distributed Energy Resources Global Forecast, Q4 2015).

clean DG (e.g., the famously generous solar feed-in tariffs in Germany [18]) There is also data that suggests that younger generations are more interested in adopting clean DG than older ones are [83]. Another trend is the increasing interest among consumers in purchasing local goods [24]. In the electric industry, this trend has emerged in the form of increased peer-to-peer energy trading by DER owners, e.g., in [195]. The evolution of environmental preferences and attitudes towards locally produced goods are not the only ones that directly impact the propensity of the public to adopt DERs. According to a report by the consulting firm PwC, 75% of the consumers interested in smart home devices are motivated by perceived “enhanced security features” while 66% are motivated by “enhanced functionality [16]”.

The second macro-trend is improvements in DER technologies. The improvements lead to cost reduction, better performance, and financial innovations. Reduction of DER production and installation costs have occurred across virtually all technologies. For instance, as shown

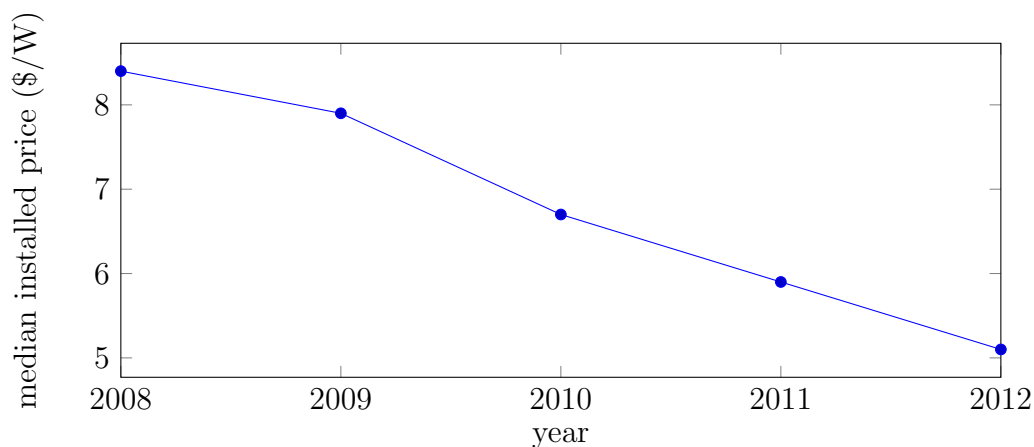


Figure 1.3: Median installed price of ≤ 10 kW residential PV solar systems. (Image: own elaboration. Data: [28].)

in Fig. 1.3, the median cost of a ≤ 10 kW residential PV solar system decreased from \$8.4/W in 2008 to \$5.1/W in 2012 [28]. The cost of battery energy storage (ES) has also plummeted. In less than ten years, the cost of ES decreased from \$2,000/kWh in 2009 [12] to about \$350/kWh in 2016 [15]. Technological improvements have also yielded increased performance (e.g., PV cell efficiency has improved by roughly a factor of 3 for most technologies [12]) and convenience (e.g., the energy density of lithium-ion batteries has increased more than three-fold since the 1990's [12]). Financial innovation plays no minor role in the deployment of DERs. New financial instruments such as power purchase agreements for small solar or demand charge savings agreements for distributed storage make DERs attractive by reducing complexity, risk, and upfront costs for customers [203].

Although macro-trends encourage DER adoption, the decision to buy an EV or install a solar panel ultimately rests in the hands of customers. The transfer of decision-making power from the utility to the customer is a pivotal change to the current utility model.

1.3 DERs as disruptors of the old utility model

The electric industry faces a profound question [160]: what is the role of the modern utility? Traditionally, a utility's core job was to forecast and plan for changes in load and replace equipment at the end of its useful life [136]. In the recent past, utilities have treated mild penetration levels of DERs as passive load and have not changed their practices in meaningful ways [160]. However, as projections show, future utilities will face higher levels of DER penetration. The question then becomes: does the utility's role include efficiently managing large penetrations of DERs?

Some experts propose the creation of distribution system operators (DSOs). DSOs, similar to Independent System Operators (ISOs), their transmission-level counterparts, would be responsible for efficiently managing DG, flexible loads, and other DERs [121]. Other experts avoid the restructuring distribution-level operations and instead propose aggregators that intervene between DERs and the wholesale electricity markets [43]. These two proposals, DSOs and aggregators, are not mutually exclusive and are not the only ones under discussion, e.g., fully decentralized peer-to-peer markets [195]. However the ultimate solution (or mix of solutions) may look, the existing approach for managing distributions systems must change to unlock the benefits and avoid the drawbacks of DERs [160].

1.4 Potential benefits and challenges of DER adoption

Although there is no single definition of the term DER, the New York Independent System Operator (NYISO) defines DERs as:

“ ... “behind-the-meter” power generation and storage resources typically located on the customers premises and operated for the purpose of supplying all or a portion of the customers electric load. Such resources may also be capable of injecting power into the transmission and/or distribution system, or into a non-utility local network in parallel with the utility grid. These DERs include such technologies as solar photovoltaic, combined heat and power (CHP) or co-generation systems,

microgrids, wind turbines, microturbines, backup generators, and ES [12].”

In this dissertation, and in line with the New York Public Service Commission, we consider a wider definition that includes DR, EE, and EVs [54]. In this section, we provide an extensive (although non-exhaustive) list of the previously alluded to potential benefits and challenges brought about by the adoption of DERs.

1.4.1 Potential benefits from adoption of distributed energy resources

In general, the benefits of adopting DERs can be either private or system-wide. However, the magnitude and beneficiaries of the benefits are case-dependent. For instance, private benefits are dependent on local incentive structures, utility rates, DER cost, etc. System-wide benefits, on the other hand, can depend on the generation mix of the system, the degree of DER control by the SO, among others. Some of the private benefits of DER adoption are:

- Customer **electric bill reduction** [12]. The means of reducing a customer’s electric bill vary depending on the characteristics of the DER in question and on the environment at which they operate. Some DERs (e.g., ES, DR) are effective at reducing peak demand charges [95, 115] while others (e.g., solar PV, EE) reduce the energy portion of the bill, e.g., in [31]. Of course, decisions of how to invest on and operate DERs are dependent on tariff structure, DER cost, etc [182].
- Increases in **resiliency and reliability** [12]. In fact, using small generators to maintain service during disruption of service is perhaps the oldest and most common application of DERs [85]. Regarding newer technologies, ES (and even EVs [192]) is often proposed to serve as backup generation. For example, Tesla³ heavily markets its home ES device, the Powerwall, as a backup source of power during outages [6].
- Improving **power quality**. Many DERs interact with the grid via power electronic-based inverters which can be controlled to improve power quality. For instance, the authors of [20, 26] show how power electronic converters can be used to mitigate various

³Tesla is a Palo Alto-based company that specializes in electric vehicles, solar energy, and energy storage.

power quality problems such as harmonic distortion and voltage fluctuations.

- **Remuneration for the provision** of goods and services on wholesale or local markets. For instance, Ortega-Vazquez et al. propose an aggregator-based framework whereby EV owners are compensated for providing services in the wholesale electricity market [156]. In [57], we show how a building can receive remuneration for wind-balancing services.
- Private entities can take advantage of **regulatory incentives** of DERs. For instance, thousands of German customers have taken advantage of solar incentives in the form of generous feed-in tariffs [18]. In the United States, the federal government provides up to \$7,500 in tax credits for EV purchases [3].
- Finally, new **business opportunities**. Tesla’s solar division (formerly SolarCity), provides various solar-related services including financing, integration, and PV panel design [7]. Furthermore, aggregator/energy services/energy analytics companies such as Drift [2], Centrica [1], EnerNOC [4], and others have recently emerged to fulfill formerly inexistent (or unidentified) gaps in the electric energy industry.

Even when DERs are installed and controlled in pursuit of private benefits, they may produce secondary system-wide benefits. For instance, locally, DR allows customers to reduce peak demand charges. From a system-level point of view, DR can increase the efficiency of a power system by introducing elasticity to the demand side. In other cases, however, the benefits may be more exclusive to the power system-level, e.g., increased renewable hosting capacity. Some system-wide benefits of DER adoption are:

- **Increased economic efficiency.** At its core, the business of being a utility is to sell energy and capacity at an acceptable level of reliability. Some experts argue that DERs will slowly permeate the market, erode the natural monopoly of the utility, and ultimately compete with utilities [62] to bring down electricity prices. Additionally, DERs introduce elasticity and price-responsiveness to the electricity demand. Evidence suggests that price-responsive demand helps mitigate the risk of market power [172, 223]. DERs such as DR and ES can also reduce the need for expensive peaking generation

by “flattening” the load.

- **Reduced greenhouse gas emissions** via decreased transmission and distribution losses⁴, increased efficiency (e.g., through CHP technologies), cleaner generation (e.g., rooftop solar and wind), among others [12] .
- **Increased power system flexibility**⁵. From an economic point of view, some DERs introduce elasticity and price-responsiveness to the demand. However, from a technical point of view, they introduce flexibility to the power system. Flexibility is crucial to increase the system’s capacity to host renewable energy resources.
- **Increased reliability, resiliency, and power quality**. For instance, microgrids with DG have been proposed to increase the reliability and resiliency of service to customers in distribution systems [51, 126]. Furthermore, under proper coordination techniques, DERs contribute to improved power quality in distribution systems, e.g., in [194].
- Ability to **substitute traditional infrastructure projects**. As discussed in depth in Chapter 7, DERs can serve as NWAs to capacity expansion projects. In essence, DERs can curb peak load growth to avoid or defer expensive projects.
- DERs can spur **economic growth and job creation** in economically depressed areas. The New York Times article [167] points out that while current President Donald “Don the Con” Trump, focuses on making America great again by sending people back to the coal mines, the wind and solar industry employ three times as many Americans as coal. Furthermore, renewable energy jobs tend to be relatively high-paying (e.g., solar panel installers) while coal mining jobs are notoriously dangerous.
- **National security**. Distributed renewable generation can contribute to national security by lessening the nation’s dependence on foreign fuels [217].

⁴DG tends to reduce flows in the transmission and distribution system because it tends to be closer to the load.

⁵Power system flexibility is the ability of the system to respond to changes in demand or supply within a given time frame [52].

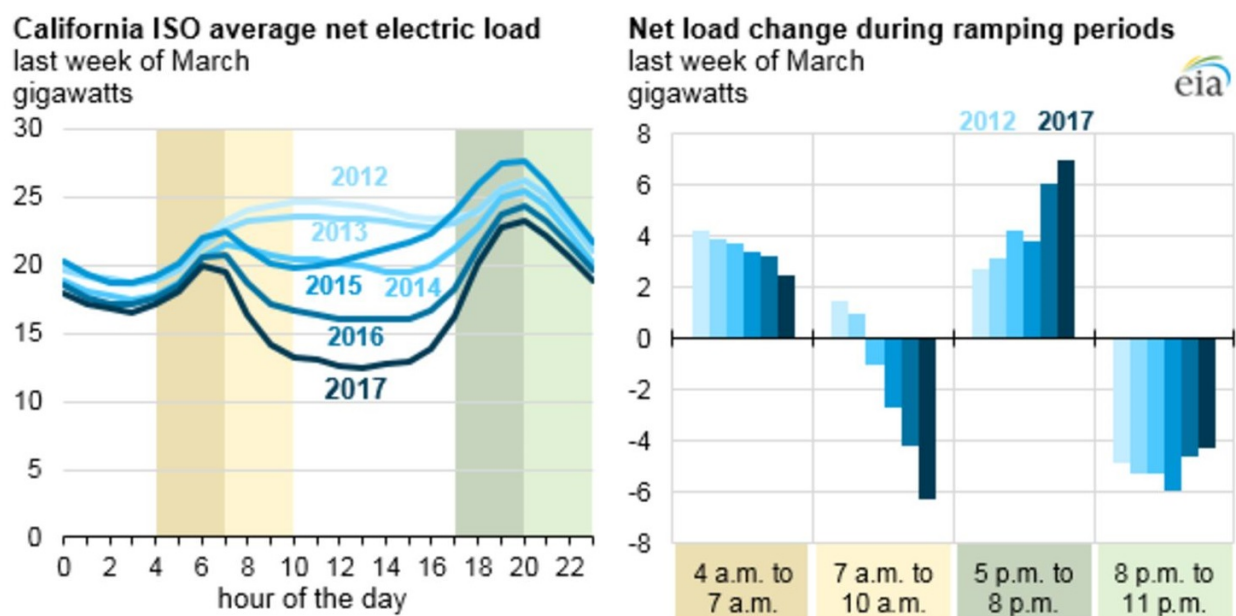


Figure 1.4: Illustration of the “duck curve” (left) and ramp requirements (right) in California ISO (image courtesy of Greentech Media and data from the U.S. Energy Information Administration).

1.4.2 Challenges of increased penetration of distributed energy resources

The many potential benefits of DERs are accompanied by just as many challenges. Some of the challenges include:

- **Changes to load patterns and increased uncertainty.** A well-known example is the so-called California “duck curve” which is caused by large injections of solar power at midday (see Fig. 1.4). The duck curve is a challenge to both operators and planners. Operators now must schedule more ramping and reserves to cover rapid and uncertain changes in net load. From a long-term standpoint, a new load pattern likely obsoletes California’s current generation mix.
- **Changes in the nature of the load.** Traditionally, load composition, individual (or business) preferences, and weather dictate load patterns. Except for load-shedding events, state of the power system does not affect the load [76]. However, customer

g exposure to power system variables (e.g., prices, direct load control signals [22]) increasingly makes the load behave in a closed loop-like fashion.

- **Complex planning for utilities.** One traditionally job squarely in the hands of a utility is to decide when to expand the distribution system and generation capacity to meet growing load [86, 173]. However, the decision to adopt DERs often rests in the hands of the customers. The decentralized nature of DER adoption poses significant changes to the utility planning process: uncertainty on the characteristics of the distribution network, impact of the changing behavior of the downstream distribution grid, new interconnection studies and procedures, etc [109].
- **The evolving nature of the utility-customer relationship and the emergence of new players.** The load and customers are traditionally passive actors. Nowadays, the demand is becoming more active [160], to the point that some are envisioning a widespread emergence of “prosumers [170]”. Furthermore, new players in the distribution system are emerging as a result of widespread adoption of DERs, e.g., aggregators. Chapter 4 explores how these changes and new players influence the customer-utility relationship.
- **More complex coordination processes.** For instance, absent two-way power flow capabilities, DG must be coordinated to ensure that no reverse flows occur in distribution systems. Furthermore, some of the system-wide benefits of DER adoption (e.g., improved power quality) involve DER coordination. Without proper coordination, intended benefits can become disadvantages. For instance, Olsen et al. argue that the roll-out of home energy management systems (HEMS) must be coordinated to avoid damages to distribution infrastructure [153]. Similarly, but from an operational point of view, Sarker et al. show that without coordination of HEMS and EVs, distribution transformers risk an accelerated loss of life [181].
- **Financial regulation and utility incentives.** Two major incentives drive much of the decision-making of regulated utilities: 1) capital investments (to set rates as high as possible) and 2) the sale of as much energy as possible (to maximize revenue) [161].

These incentives are in direct contradiction to the adoption of DERs because 1) DERs are usually installed not by the utility but by private or third parties, and 2) most DERs decrease the amount of energy sold by the utility (e.g., EE, DG). Regulation and utility incentives must be modified to achieve a socially desirable number of DERs.

- **Obsolete market designs.** Current markets must be modified to properly value DERs and mitigate undesirable side-effects of their adoption. For instance, Negash et al. identify cases where conventional cost allocation techniques for DR are “unfair [145].” An example of an undesirable side-effect of DER adoption is that generators in the U.S. faced a \$2 billion revenue shortfall in 2015 due to rooftop PV generation [204]. Furthermore, without proper DER compensation schemes, socially unjust cross-subsidies can emerge [74] and the infamous “utility death spiral” [63] can negatively affect utilities. Another problem is that strategic actions by DER aggregators can negatively affect system welfare [58, 151, 178], e.g., by exerting market power.

Of the many challenges and potential benefits that come alongside DERs, this dissertation investigates five of them:

1. One promising DER is DR. According to the Federal Energy Regulatory Commission (FERC), is defined as “*Changes in electric usage by demand-side resources from their normal consumption patterns...*” Heating, ventilation, and air conditioning (HVAC) systems are widely considered as some of the most promising sources of DR. However, to attain effective DR control strategies, one must understand the capabilities of flexible HVAC systems. Chapter 3 presents a data-driven methodology to estimate the flexibility of HVAC systems in buildings.
2. DERs are almost always too small to participate in wholesale markets. A common way to enable DERs to participate in the market is through *aggregators* who amass enough capacity and then act as middlemen between the DERs and the market. Chapter 4 presents a model of the interactions between the aggregator and its constituent DERs. We show that although short-term of this relationship can be inefficient, Pareto-optimal cooperative outcomes are achievable when DERs and aggregators interact continuously

- (which it is likely to occur in practice). Sound models of the aggregator-DER relationship are indispensable to predict their effects on the rest of the power system.
3. In some cases, multiple DERs may need to coordinate to achieve a goal, satisfy common operating constraints, bid into the market as a single block, etc. However, privacy concerns or software incompatibilities may make it impossible to formulate a joint optimization problem to achieve optimal coordination. In Chapter 5, we propose a mixed-integer linear programming adaptation of the Dantzing-Wolfe Decomposition Algorithm (DWDA) that solves the joint problem of an EV aggregator and an energy management system of a building. The algorithm is guaranteed to reach the optimal solution⁶, preserves the privacy of both entities, and is shown to be scalable.
 4. A notorious problem of imperfect markets is *market power* – the ability to act strategically (in a market) for private gains at the expense of social welfare. Up to now, most work focuses on the market power of generators. While some partial mitigation techniques exist, no definitive solution exists. As we show in Chapter 4, aggregators can achieve cooperation with a large number of DERs, making them potentially large players in the energy market. Furthermore, a heterogeneous composition of their constituent DERs make the aggregator’s behavior completely different from that of large generators, e.g., aggregators could be net producers, consumers of energy, or both. Chapter 6 proposes a pricing mechanism that mitigates the market power of an arbitrary firm (e.g., large generator, flexible demand, ES, etc.) acting strategically in an electricity market. Under the assumptions outlined in the chapter, we show that the proposed pricing mechanism incentivizes socially optimal bids, requires no private information to be formulated, and allows for the regulation of the firm’s profit.
 5. Finally, Chapter 7 addresses the NWA’s planning problem. We propose a long-term planning problem of NWA’s for deferment of traditional capacity expansion. Because we consider both investment and operation cost over planning-length horizons (decades),

⁶In a finite number of iterations. Every iteration delivers a feasible solution.

the problem is very high-dimensional. Furthermore, the time-value of money of traditional capacity expansion makes the problem non-convex. We tackle the dimensionality issue by decomposing the problem using the DWDA. We tackle the non-convexities by decomposing the DWDA master problem. All in all, the contributions of Chapter 7 are from a modeling perspective (because we consider delaying traditional investments as an additional value stream) and computational perspective (for the solving algorithm).

Chapter 2

CONTRIBUTIONS OF THIS DISSERTATION

This chapter provides background to each of the problems addressed in each chapter and summarizes our contributions.

2.1 Chapter 3: Modeling the Flexibility of Building Loads

The increasing presence of control and communication equipment in the demand-side has allowed it to take part in the vital task of balancing supply and demand. For instance, controllable electric vehicle (EV) chargers [108], grid-connected thermostats [111], and other “smart” appliances [171] could receive signals from an operator (e.g., building manager, utility, or system operator) and modify their behavior to match the electricity supply.

However, the system operator (SO) must have predict which load profiles are attainable to formulate effective load control policies. That is, the operator would like to know the set \mathcal{P} of feasible load profiles from which to choose the “best” one¹.

For instance, on its most basic form, the economic dispatch (ED) problem is typically formulated as the convex, linearly constrained optimization problem [118]

$$\min_{\mathbf{g}_i} \sum_{i \in \mathcal{G}} C_i(\mathbf{g}_i) \tag{2.1a}$$

$$\text{s.t.} \sum_{i \in \mathcal{G}} \mathbf{g}_i = \mathbf{p} \tag{2.1b}$$

where the objective is to minimize the dispatch cost of the set of generators \mathcal{G} while satisfying a total hourly fixed load of \mathbf{p} . The variable \mathbf{g}_i is a vector of hourly output of generator i and

¹The best load profile could be, for instance, the one that achieves the lowest system cost or the higher renewable energy utilization.

C_i is its cost function.

In the classical ED problem described by Eqs. (2.1), only the supply-side of the problem can be adjusted to minimize costs. In the old days, when hand-operation of loads by end users was the only way to adjust the demand-side of the power balance equation, it made sense to focus on optimizing the supply-side of the problem and treat the hard-to-control demand side as a fixed parameter. However, with controllable demand, we could reformulate the classical ED problem as

$$\min_{\mathbf{g}_i, \mathbf{p}} \sum_{i \in \mathcal{G}} C_i(\mathbf{g}_i) \quad (2.2a)$$

$$\text{s.t.} \sum_{i \in \mathcal{G}} \mathbf{g}_i = \mathbf{p} \quad (2.2b)$$

$$\mathbf{p} \in \mathcal{P} \quad (2.2c)$$

where \mathbf{p} are decision variables constrained by \mathcal{P} . Under this reformulation, the operator now has the ability to choose the \mathbf{p} that achieves a lower cost.

2.1.1 Problem

Unfortunately, knowing \mathcal{P} is practically impossible. The set \mathcal{P} may depend on hard-to-predict factors like building occupancy, ever-changing characteristics like appliance performance, or hard-to-quantify physical processes such as thermal dynamics. Moreover, create a perfect model of \mathcal{P} , its complexity may be an impediment to common power system frameworks like the ED problem.

Then it is reasonable to use a simpler model of \mathcal{P} for decision-making purposes. The model $\hat{\mathcal{P}}$ must have two important properties: *tractability* and *robustness*. What we mean by the former is that the model must be computationally tractable when used in typical power system applications. For instance, since the traditional ED problem described by Eqs. (2.1) is a linearly constrained convex optimization problem, $\hat{\mathcal{P}}$ needs to be described using linear constraints. What we mean by robustness is that a load profile \mathbf{p} contained in $\hat{\mathcal{P}}$ must also

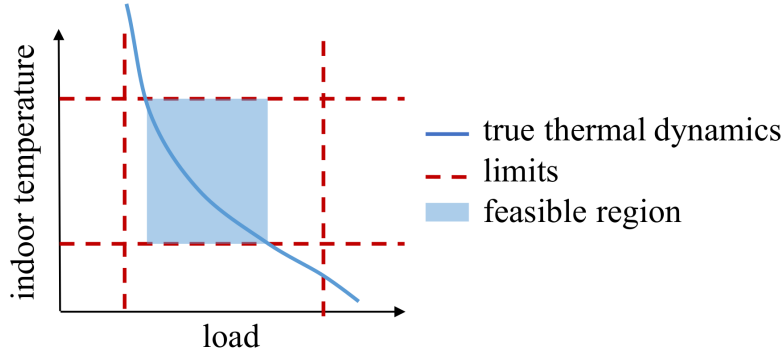


Figure 2.1: Illustration of the feasible region of the load and a (hypothetical) thermal dynamics function. With a complicated non-linear dynamics function such as the one illustrated here, \mathcal{P} is too complex for common power system frameworks.

be included in \mathcal{P} to an α -degree of confidence. Tractability is an important property because we want $\hat{\mathcal{P}}$ to be usable. Robustness is important because we do not want to choose load profiles not contained in \mathcal{P} . When \mathbf{p}^* is $\notin \mathcal{P}$ two things may happen:

1. \mathbf{p}^* is not realized in operation, causing a deviation in the operator’s plan or
2. \mathbf{p}^* is “forced” by violating some of the constraints that describe \mathcal{P} , e.g., by violating indoor temperature requirements.

2.1.2 Proposed solution

In Chapter 3, we consider buildings whose source of flexibility is their HVAC load and propose a data-driven methodology to find a *tractable* and *robust* model of their load. Besides tractability and robustness, the methodology requires only easy-to-gather and coarse data (e.g., building load and average indoor temperature). This last quality makes our method widely applicable and not exclusive to buildings equipped with sophisticated data-gathering equipment.

One of the reasons \mathcal{P} for HVAC loads may be complicated is the complexity of the load-indoor temperature relationship (see Fig. 2.1). This relationship is relevant the building load is constrained to be in the set of load profiles that deliver acceptable indoor temperatures. We

achieve tractability by describing the model $\hat{\mathcal{P}}$ as a polyhedron, i.e., using *exclusively* linear constraints. Then, we can reformulate Problem (2.2) by using $\hat{\mathcal{P}}$ in lieu of the complicated \mathcal{P} :

$$\min_{\mathbf{g}_i, \mathbf{p}} \sum_{i \in \mathcal{G}} C_i(\mathbf{g}_i) \quad (2.3a)$$

$$\text{s.t.} \sum_{i \in \mathcal{G}} \mathbf{g}_i = \mathbf{p} \quad (2.3b)$$

$$\mathbf{p} \in \hat{\mathcal{P}}. \quad (2.3c)$$

The simplicity of $\hat{\mathcal{P}}$ makes the transition from the classical formulation shown in Problem (2.1) to the controllable-demand formulation of Eqs. (2.3) straightforward. Like the former, the latter is a linearly-constrained problem. Our method stands in contrast to works like those in [48, 93] which employ complicated neural network functions to describe $\hat{\mathcal{P}}$.

We achieve robustness by estimating the load-indoor temperature relationship (an example is shown in Fig. 2.1) of a building via a *prediction band*. The prediction band stands in contrast to the well-known resistance-capacitance (RC) circuit model which provides a *central prediction* [89, 96, 133, 169]. As illustrated in Fig. 2.2, a central prediction risks scheduling load profiles that are not feasible during operation. A prediction band, on the other hand, provides higher confidence that the planned load is attainable during operation.

2.2 Chapter 4: Modeling an Aggregator

Individual DERs are typically too small to participate in wholesale electricity markets [14, 166]. The DERs' inability to participate in the market is unfortunate for both the DERs and the power system. On the one hand, DERs are deprived of potential revenue streams. On the other hand, the power system misses out on potentially more efficient providers of energy and services. However, DERs can indirectly participate in the market by joining an aggregator. The aggregator amasses enough capacity and participates on the DERs' behalf [43]. Fig. 2.3 illustrates the framework whereby DERs participate in the market through an aggregator.

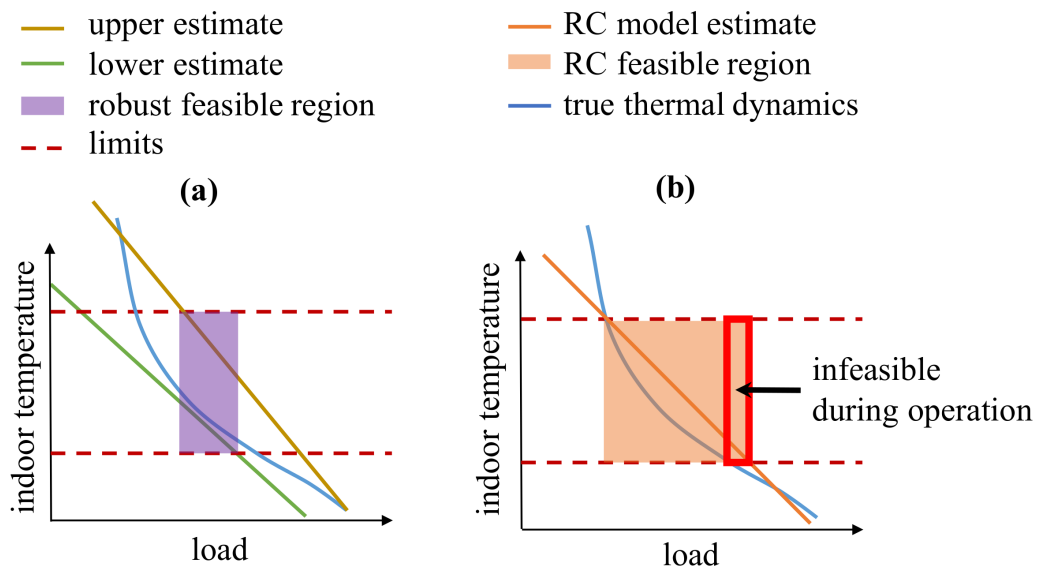


Figure 2.2: Illustration of the robust approximation of the feasible region of the load (plot a) and the feasible region based on the RC circuit model (plot b). In the proposed approximation, the upper temperature estimate is upper bounded by the maximum temperature limit. Similarly, the lower temperature estimate is lower bounded by the minimum temperature limit. The RC circuit model, on the other hand, limits a central estimate to be within the minimum and maximum temperatures. Note that the RC circuit model may overestimate the feasible region and lead to load profiles that are infeasible during operation.

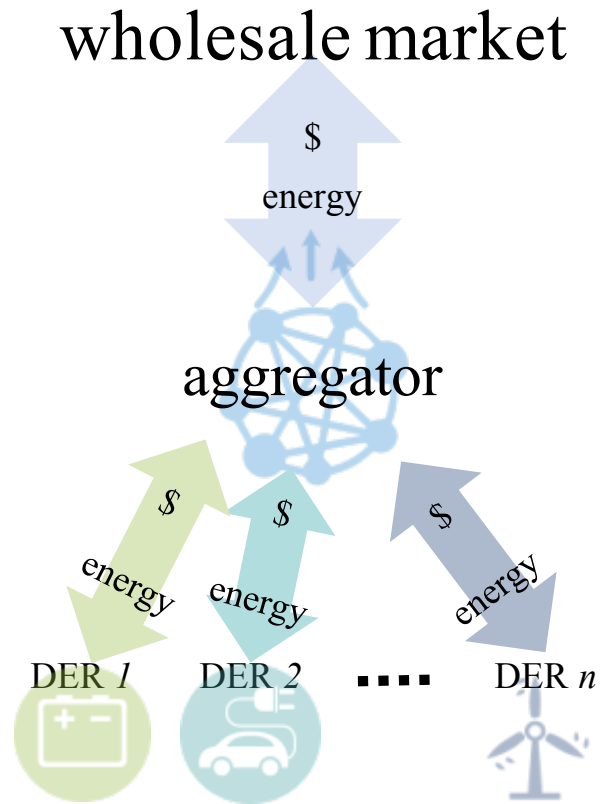


Figure 2.3: Illustration of the market-aggregator-DETs relationship.

2.2.1 Research question

Modeling a traditional power plant's bid into the market is relatively straightforward. For instance, if we assume that the market is reasonably close to perfect competition, it is reasonable to assume that generator will bid close to their marginal cost. In the case of an oligopolistic market, one can model generators as strategic and self-interested players. Modeling how an aggregator bids into a market, however, more complicated. An aggregator's bids result from n DERs and at least one aggregator taking strategic actions. The central question of Chapter 4 is:

Q1: How do we model an aggregator's market bids?

2.2.2 Our answer

The answer to **Q1** depends on a second question:

Q2: What relationship does the aggregator (the bidder) have with its DERs (the energy providers/consumers)?

For a traditional generator, the answer to **Q2** is trivial: the bidder and the energy provider are the same. However, this is not the case for aggregators and DERs. In Chapter 4 we start with the reasonable assumption that the DERs and aggregator are rational players. Under this assumption, we quickly find out that their short-term relationship is “adversarial.”

We illustrate the adversarial nature of the relationship between the aggregator and its DERs using a small example. Suppose a market price of $\lambda = 2$ and a small, behind-the-meter generator with a production cost function of $c(x) = \frac{1}{2}x^2$. If the generator sells directly into the market, the first order conditions of its profit maximization problem², $\lambda - x = 0$, dictates that it should bid 2 units of energy into the market. In this case, the generator’s profit is

$$\text{generator profit} = 2.$$

Suppose, on the other hand, that the generator does not have access to the market and has to participate through an aggregator who offers the generator a price τ . If we assume perfect information, the aggregator knows that the generator’s best move is to bid the energy price. Then, if the aggregator offers a price of τ to the generator, the aggregator’s profit is

$$\pi(\tau, x) = (\lambda - \tau) \cdot x = (\lambda - \tau) \cdot \tau$$

where the second equality follows from the generator’s first order optimality condition. Then, the aggregator’s profit-maximizing price is $\tau = 1$ and the generator’s best move is to offer

²The generator’s profit is $\lambda \cdot x - \frac{1}{2}x^2$.

the aggregator 1 unit of energy. In this case, the generator's profit is

$$\text{generator profit 2} = \frac{1}{2}$$

and the aggregator's profit is

$$\text{aggregator profit 2} = 1$$

with a combined profit (generator profit 2 + aggregator profit 2) of $1\frac{1}{2}$.

Notice that the combined profit is smaller than the generator's profit were it able to bid into the wholesale market. The smaller profit is the result of an adversarial relationship of sorts in which an increase in τ results in gains for the aggregator but losses for the generator.

A natural question is, could the aggregator and the generator agree on an arrangement that is better on a Pareto-sense? For instance, a generator offer of 2 units of energy a $\tau = 1.5$ would result in a Pareto-superior generator profit of 1 and an aggregator profit of 1. Unfortunately, the answer to this question is no. A better arrangement is not compatible with rational players in the short term. The generator would see the price $\tau = 1.5$, and instead of offering the agreed 2 units of energy, it would maximize its profit by offering 1.5 units of energy.

In Chapter 4, however, we take a long-term view of the aggregator-DER relationship and show that better strategies are compatible with rational players when they interact continuously. This feature of continuous interaction is, we believe, more reasonable than the single-game setting: aggregators and DERs are likely to interact for extended periods of time. Then, using Nash Bargaining Theory [144], we show that the aggregator and DERs are inclined to agree on a Pareto-efficient strategy and cooperate in the long term.

The results presented in Chapter 4 have a few implications:

1. We can model a cooperative aggregator and its DERs as a single entity that adopts the Pareto-efficient strategy. This result is convenient from a modeling and a computational point of view: modeling 1 player is easier than modeling $n + 1$.
2. The statement above implies that many DERs acting as a single entity could, in theory,

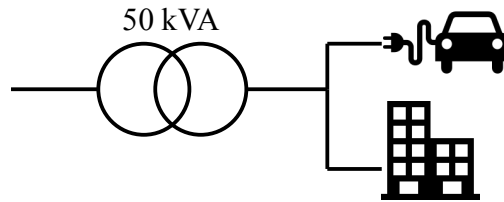


Figure 2.4: Illustration of DERs sharing infrastructure. In this case, a building and an electric vehicle share a transformer.

exert market power. We explore this implication further in Chapter 6.

3. They serve as the starting point of a theoretical justification for the existence of direct load control programs. These programs implicitly assume cooperation by loads and an aggregator or utility.

2.3 Chapter 5: Coordination of Buildings and Electric Vehicles

As described in [141], multiple DERs can form energy collectives or microgrids and interact with an aggregator, the system operator (SO), and/or the electricity market as if it were a single DER. While a microgrid may interact with the “outside world” as a single entity, its internal components may not be willing nor able to fully share information with each other. The unwillingness or inability to share information can be a major impediment to centrally formulate a coherent and optimal strategy to interact with the aggregator, SO, or electricity market. This impediment is especially true if the DERs share common constraints. For instance, Fig. 2.4 illustrates a case where an EV and a building share a transformer. Thus, any feasible strategy needs to observe the transformer limit.

2.3.1 Problem

In Chapter 5, we consider a building and an EV fleet that face a problem with the structure illustrated in Fig. 2.5. The building and EV fleet face a shared objective and share a set of constraints, both functions of the building load, d_t^b , and EV load, d_t^{ev} . However, they also

$$\min f(d_t^b, d_t^{ev})$$

$$\mathbf{A}_b \mathbf{x}_b = \mathbf{b}_b$$

$$\mathbf{x}_b \geq \mathbf{0}$$

$$\mathbf{A}_{ev} \mathbf{x}_{ev} = \mathbf{b}_{ev}$$

$$\mathbf{x}_{ev} \geq \mathbf{0}$$

$$g(d_t^b, d_t^{ev}) = 0$$

Figure 2.5: Visual representation of the building-EV demand scheduling problem. The function $f(d_t^b, d_t^{ev})$ represents the common objective. Equations $\mathbf{A}_b \mathbf{x}_b = \mathbf{b}_b$ and $\mathbf{x}_b \geq \mathbf{0}$ represent the building constraints while $\mathbf{A}_{ev} \mathbf{x}_{ev} = \mathbf{b}_{ev}$ and $\mathbf{x}_{ev} \geq \mathbf{0}$ represent the EV constraints. Function $g(d_t^b, d_t^{ev}) = 0$ represents the coupling constraints.

have internal variables (\mathbf{x}_b and \mathbf{x}_{ev}) and data (\mathbf{A}_b , \mathbf{b}_b , \mathbf{A}_{ev} , and \mathbf{b}_{ev}) that might encode data that is private to either party. Furthermore, even if the building and EV fleet could share private information, their algorithms, databases, or software may be incompatible or hard to consolidate. Therefore, building and solving the problem illustrated in Fig. 2.5 in a centralized manner may not be possible.

2.3.2 Solution

We propose a mixed-integer linear programming (MILP) adaptation of the Dantzig-Wolfe Decomposition Algorithm (DWDA) to solve the problem depicted in Fig. 2.5. The solution method allows us to treat the building and the EV constraints independently. The coupling constraints, g , are handled by an independent master problem.

Our solution method addresses the following.

- **Privacy** concerns. Only essential information to build the coupling constraints needs to be shared with the master problem solver. Thus, it is not necessary to share internal variables/parameters such as appliance-level loads or individual EV charge/discharge rates.
- **Incompatibility** of software, data, and algorithms. One of the virtues of the DWDA

is that it allows us to deal with $\mathbf{A}_b \mathbf{x}_b = \mathbf{b}_b$ and $\mathbf{A}_{ev} \mathbf{x}_{ev} = \mathbf{b}_{ev}$ independently. Thus, databases containing relevant data do not have to be merged. Furthermore, our method allows us to solve each subproblem using algorithms and software of choice.

Furthermore, the DWDA has the following advantages.

- It delivers a feasible solution at each iteration (unlike Lagrangian-based approaches).
- It is a well-known algorithm. Computational [80, 98, 101] and privacy-related [77, 102] enhancements are readily available.
- Its convergence is guaranteed³ in a finite number of iterations [66].

2.4 Chapter 6: Market Power

One of the most notable phenomena that can arise in non-ideal markets is *market power*. Market power can take on a few different forms (see Section 6.1 for a brief overview). However, we consider *firms bidding strategically* to alter market prices for *short-term gains*.

Most of the studies, metrics, and solutions that concern to market power are aimed at the generation side of the power system. For instance, CAISO uses the correlation of the Residual Supply Index (RSI) with above-competitive-rates-markups by generators to detect abuses in market power [190]. The focus on generation as a source of market power is reasonable since generators have historically been the largest players in electricity markets.

However, market power from aggregators of DERs may become an issue as some researchers have pointed out, e.g., in [58, 151, 178]. Notably, our work in Chapter 4 shows how a robust DER-aggregator coalition can arise even from self-interested agents in non-cooperative settings. Thus, in theory, an aggregator could amass enough DERs to rival the size of a large power plant and exercise market power.

³For the LP case.

2.4.1 Problem statement

We consider a single profit-maximizing strategic bidder (the “firm”) under a perfect information setting and a market operator that maximizes social welfare as revealed by the bids. By definition, strategic bidding increases (or at worst, does not decrease) the short-term profit of the firm. However, society as a whole suffers, i.e., the social welfare is lower than the social optimum. We model the two cases as the following optimization problems.

Strategic bidding	Social optimum
$\max \{ \text{utility} - q \cdot \lambda \} \tag{2.4a}$	$\max \left\{ \sum_i \text{utility}_i \right\} \tag{2.5a}$
$\text{s.t.} \tag{2.4b}$	$\text{s.t. system constraints.} \tag{2.5b}$
$\text{MC:} \left\{ \begin{array}{l} \lambda, q = \max \{ \sum_i \text{utility}_i \} \\ \text{s.t. system constraints} \end{array} \right. \tag{2.4c}$	

Under strategic bidding, the firm’s objective is to maximize its utility minus costs. The cleared quantity, q , and price, λ , are outcomes of the market clearing (MC) process. The MC process is an optimization problem whose objective is to maximize the social welfare as revealed by each player’s bid. In contrast, the socially optimal case maximizes the *true* social welfare, i.e., when every player bids according to its real utility function.

2.4.2 Main contribution

The efficiency gap that results from strategic bids (i.e., the difference in social welfare for the two cases) motivates the central contribution of this chapter: our market power mitigating price (MPMP). In a nutshell, the MPMP is a pricing mechanism that induces the firm to bid the social optimum.

The MPMP has the following characteristics:

1. it induces the firm to bid according to its true utility function,
2. its formulation requires no private information,
3. it is firm-agnostic, i.e., it applies to firms that are producers, consumers, or prosumers,
4. it allows for the regulation of the firm's profit.

The key insight that allows us to formulate the MPMP is that Problems (2.4) and (2.5) can be recast as follows.

Strategic bid (1-level equivalent)	Social optimum (with redundant optimality conditions)
$\max \{ \text{utility} - q \cdot \lambda \}$	$\max \left\{ \sum_i \text{utility}_i \right\}$
s.t. system constraints (primal feasibility)	s.t. system constraints (primal feasibility)
stationarity condition of MC	stationarity condition of MC
dual feasibility of MC	dual feasibility of MC
complimentary slackness of MC	complimentary slackness of MC.

Both of the problems above are equivalent to their counterparts from (2.4) and (2.5). We recast the strategic bidding problem as a single-level equivalent by replacing the lower-level problem by its Karush-Kuhn-Tucker (KKT) optimality conditions. For Problem (2.5) we included its own KKT conditions as redundant constraints. Notice that the strategic bid and the social optimum problems above have the same feasible solution space, but their objectives differ. The MPMP equalizes both objectives when substituted for λ .

2.5 Chapter 7: Non-wire Alternatives to Capacity Expansion

Electric utility distribution systems are typically built for peak load which usually happens for a small number of hours per year. When the system load reaches capacity, the traditional solution is to install more wires or reinforce existing ones [187]. While decades of experience make this solution reliable and safe, it is often associated with enormous capital costs, hostile

public opinion, and time-consuming legal issues [196].

However, planners today are increasingly considering DERs to reduce peak load and avoid or defer traditional investments. In a long-term planning context, DERs are often referred to as NWAs. For instance, the Bonneville Power Administration (BPA) is considering DR, EE, and distributed roof-top solar as alternatives to a billion dollar transmission line along the I-5 corridor [112]. At the distribution level, Con Edison deferred a 1.2 billion dollar substation in Brooklyn, NY by contracting 52 MW of demand reduction and 17 MW of distributed resources [212].

There are several reasons why NWAs are becoming more popular. The first is that the cost of technologies such as solar photovoltaics (PV) and ES is now at a point where they can compete with traditional capacity expansion solutions. The second is that some DER technologies are not new anymore and are slowly gaining the trust of system operators. Third, the time-value of money makes deferring substantial traditional investments economically attractive. The fourth reason is that delaying investments can mitigate risks of expected load growth not materializing. The fifth and last reason is that projects like new transmission lines are often politically infeasible. It is worth noting that these reasons are not exhaustive and that each case has its own particularities.

2.5.1 Problem

The traditional capacity expansion problem at a single point in a radial network is relatively simple: expand capacity as late as possible but in time to handle peak load. In contrast, planning NWAs is significantly more complicated: one needs to determine both investment decisions and operating decisions to predict their impact on peak load. Then, we decide whether and *when* to expand capacity. Note the emphasis on the “*when*” question. We explicitly model the present cost of capacity expansion to account for the benefits of deferring infrastructure investment.

The NWA approach considers load shape, not just the peak load like the traditional problem. We must recognize load shape in part because the operation of some NWAs like

Table 2.1: Description of planning and operating variables for a planning problem that considers four NWAs and a planning horizon of 20 years.

NWA	planning variables	operating vars./hr	approx. # of variables
ES	<ul style="list-style-type: none"> energy capacity 	<ul style="list-style-type: none"> charge discharge state-of-charge 	$\approx 3 \times 20 \times 24 \times 365$ $\approx \mathbf{525,600}$
solar PV	<ul style="list-style-type: none"> installed capacity 	<ul style="list-style-type: none"> solar output 	$\approx 20 \times 24 \times 365$ $\approx \mathbf{175,200}$
DR	<ul style="list-style-type: none"> DR capacity 	<ul style="list-style-type: none"> DR deployment demand rebound 	$\approx 2 \times 20 \times 24 \times 365$ $\approx \mathbf{350,400}$
EE	<ul style="list-style-type: none"> increased efficiency (%) 	<ul style="list-style-type: none"> load reduction 	$\approx 20 \times 24 \times 365$ $\approx \mathbf{175,200}$
		total	$\approx \mathbf{1,226,400}$

ES is coupled across time periods. Also, most NWAs have additional value streams that traditional expansion does not. For example, solar generation reduces energy purchases from the utility, DR may reduce the peak demand charge, and on-site dispatchable generation may improve reliability, and so on. Therefore, a good plan must consider the multiple benefits of NWAs and their operation over long periods of time (e.g., a few decades).

Simulating the operation of various DERs over a long-term planning horizon leads to a large problem. For instance table, Table 2.1 approximates the dimension of a problem that considers four NWAs (ES, PV, DR, and EE) and a planning horizon of 20 years. The planning variables refer to investment decisions such as: is ES a viable option? If so, how big should the system be? Or, should we invest in EE measures? The operating variables, on the other hand, concern the short-term operation of each NWA and are typically made on an hourly basis⁴. Note from Table 2.1 that even a problem that considers a small number of relatively simple NWAs can be significantly large (more than 1×10^6 -dimensional). Additionally, the variables and constraints that describe the timing of capacity expansion introduce further difficulties in the form of non-convexities to the feasible solution space of the problem.

⁴For simplicity we consider hourly operating time-steps. In some cases, however, longer or shorter (e.g., 15 minutes) time-steps may be desirable.

2.5.2 Solution

The NWAs planning problem is hard to solve because it is large and non-convex. We tackle the size issue by decomposing it into n subproblems and a master problem using the DWDA. Each of the subproblems handles the investment and operating decisions of a NWA. The master problem manages the timing of capacity expansion and is small because its variables and constraints are in the order of years. Unfortunately, however, the master problem is non-convex. Chapter 7 presents an algorithm to solve the master problem by decomposing it into a small number of small linear problems.

2.6 Organization of this dissertation

The rest of this dissertation is organized as follows. Chapter 3 presents a tractable and robust model of the flexibility of a building. Chapter 4 presents a model of the relationship between an aggregator and its constituent DERs. We show how a self-interested DERs and aggregators could end up engaging in a cooperative relationship. Chapter 5 presents a MILP adaptation of the DWDA that can be used to coordinate a building and an EV fleet. Chapter 6 presents a pricing mechanism that mitigates the market power of a strategic actor in power system. Chapter (7) presents a NWA planning problem that minimizes the investment and operating costs of NWAs and the present cost of traditional capacity expansion. We also present an algorithm to solve this large-scale non-convex problem. Finally, Chapter 8 concludes this dissertation and provides suggestions for future extension of our work.

Chapter 3

MODELING THE FLEXIBILITY OF BUILDINGS

3.1 Introduction

Power system flexibility is the ability to respond to changes in demand or supply within a given time frame [52]. Traditionally, the primary (and usually sole) source of flexibility in power systems is flexible generation resources, e.g., simple and combined cycle gas turbines. Meanwhile, the load is treated as a fixed quantity to be followed by a flexible supply-side. However, thermostatically-controlled loads in buildings (e.g., heating, ventilation, and air-conditioning units, refrigerators, and water heaters) have the potential to provide flexibility from the demand-side by altering their consumption to accommodate power variations [128, 133].

Benefits of increased power system flexibility include: infrastructure investment deferral [22,60], increased renewable energy hosting capacity [130], higher economic efficiency [90], and others (see, e.g., [30,179] and the references therein). However, to fully harvest the flexibility of TCLs, challenges still exist. For example, the need for building models, data privacy issues, and state estimation of flexible loads, [8,30,164]. The central contribution of this chapter is a method that uses easy-to-collect data find **tractable** and **robust** building models of **load flexibility**.

The concepts in bold font in the previous paragraph seem simple but are loaded with meaning. We start by introducing the concept of **load flexibility**. Similar to [143], we define load flexibility, or equivalently, the feasible region of the load \mathcal{P} , as the collection of load profiles that satisfy the user requirements, e.g., thermal comfort, technical limits.

We then turn to the concept of robustness. A model of \mathcal{P} , denoted by $\hat{\mathcal{P}}$, is said to be **robust** if an arbitrary element (i.e., a load profile) of $\hat{\mathcal{P}}$ is also contained in \mathcal{P} to a degree

of certainty. Robustness is important because it ensures, to said degree of certainty, that a load profile in the model is attainable by the physical building.

In this work, a model $\widehat{\mathcal{P}}$ is said to be **tractable** if it is easily incorporated into a desired power system analysis frameworks. For instance, a model is said to be tractable with respect to a mixed-integer linear program (MILP)-based unit commitment (UC) problem if it is described by linear constraints. Other typical power system analysis frameworks include optimal power flow (OPF), economic dispatch (ED), etc. [52, 213, 214].

3.1.1 Flexibility of heating, ventilation, and air-conditioning (HVAC) loads

We consider buildings whose source of flexibility is their HVAC loads¹ and indoor temperature is the only controllable comfort index. Since indoor temperature is typically allowed to be in an allowable range, e.g., from 20°C to 25°C, it is possible that multiple HVAC load profiles achieve proper indoor temperatures. Then, the building operator could choose a load profile among the set of possibilities that accomplishes a power system-level objective, e.g., demand response (DR), and satisfies indoor temperature requirements. However, the relationship between indoor temperature and the electrical power consumption can be complex [27], and finding the set of load profiles that map to appropriate temperatures is nontrivial.

This chapter presents a *data-driven* approach to *appropriately* model the feasible region of a building load. We develop a model of demand-side flexibility that *i*) is computationally tractable, *ii*) does not compromise occupant comfort, and *iii*) requires relatively simple and easy-to-obtain sets of data. The model is easy to incorporate into common power system analysis frameworks because it is described by a set of linear constraints and continuous variables. The model is robust in the sense that it ensures (to a degree of confidence) that a feasible load profile does not violate temperature limits. Finally, the approach uses small amounts of relatively coarse data²: average indoor temperatures rather than zone-specific

¹We consider heating and cooling loads because they are the most significant component of commercial loads [207].

²Gathering fine-grained data may be expensive or not viable.

temperatures and total building load rather than individual appliance loads. Not needing fine-grained data makes the approach attractive to model buildings without instrumentation at the appliance level (which is still the mostly the case). Our data-driven approach does not rely on human inputs of architectural parameters.

3.1.2 *Related works*

Perhaps the most popular model of the relation between indoor temperature and HVAC load is the resistance-capacitance (RC) circuit model (or RC model) [89, 96, 133, 169]. The RC parameters are typically calculated from building specifications such as volume, insulation, wall area, etc. The RC model is an easy-to-use linear representation of a building’s thermal dynamics but its form is restrictive and calculating it may be costly and labor intensive. In contrast, our method identifies the model using building-level metered data.

The works in [27, 91, 93, 105, 177] use metered data to identify building models. The authors of [27] propose a maximum likelihood estimation of the RC parameters. Reference [105] proposes an identification method of a “virtual battery” building model for system-wide frequency regulation. Both models in [27] and [105] are well-suited for short prediction horizons, e.g., 5 minutes. However, we are interested in longer prediction horizons, e.g., 24 hours. The authors of [91] present a model of internal building thermal dynamics identified with room-level temperature data. In contrast, our model uses coarser data (e.g., average zonal temperature rather than individual room temperature) that are easier to obtain.

Furthermore, models are mathematically simple and can be readily adopted in a wide range of power system frameworks, unlike the artificial neural network models in [48, 93]. Our model is mathematically simple because exclusively employs linear relations. Thus it can be easily embedded in most power system optimization and control frameworks. The work in [177] is closely related to ours because it identifies a coarse (e.g., facility-level) model of thermal dynamics that provides a single indoor temperature estimate. In contrast, our approach offers robustness by modeling upper and lower indoor temperature estimates.

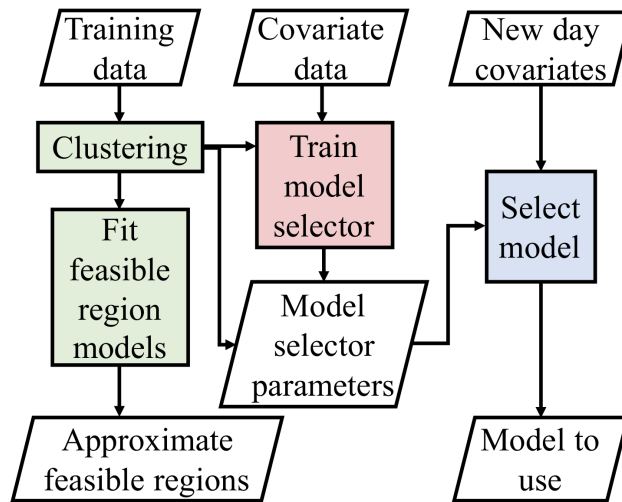


Figure 3.1: High-level illustration of the method presented in this chapter. First (green blocks), we cluster the training data. Each cluster identifies a model of the feasible region. Then (red block), explanatory variables and training data clusters train the parameter of a “model selecting function.” Finally (blue block), we use expected explanatory variable values to select an appropriate feasible region model. The first two steps (green and red blocks) are the training stages. The last step is performed during operation.

3.1.3 Overview of the proposed method

We divide our method into three tasks: data clustering, model fitting, and model selection. First, we group similar training data points into a number of clusters. Clustering segregates the training data by classes of thermal behaviors. Each data cluster fits a model of the feasible region.

Each training data point is associated with a set of explanatory variables (e.g., outdoor temperature, solar irradiation, or day of the week). The explanatory variables and the training data clusters train a “model selecting function” that maps the explanatory variables to feasible region models. During operation, the expected value of the explanatory variables determines the feasible region model to use. Fig. 3.1 illustrates these three major tasks.

The major contributions of our work are:

- A method that describes the feasible region of a building’s load. First, we group the

training data into C clusters of similar days. Then, we C train models of building thermal dynamics using a technique we call bounded least squares estimation (BLSE). Rather than providing a central indoor temperature prediction, the BLSE provides a prediction band, i.e., upper and lower estimates of indoor temperatures.

- Validation of our models using EnergyPlus building data [64].
- A demonstration of how the proposed model can be used to mitigate discrepancies between expected and actual wind power generation.

3.1.4 Organization of this chapter

This Chapter is organized as follows. Section 3.2 describes the model of a generic building and defines the feasible region of the load. Section 3.3 introduces the tractable and robust model of the feasible region. Section 3.4 describes the data and outlines the procedure to estimate the feasible regions. Section 3.5 validates the model and compares it to the traditional RC circuit model. Section 3.6 shows how our model can be used to mitigate discrepancies between expected and actual wind power generation.. Section 3.7 summarizes this chapter.

3.2 Preliminaries

We define the feasible region of the load as the set load profiles that meet power and indoor temperature limits. The maximum power limit is the non-HVAC building load (or base load) plus the installed capacity of the HVAC system. The minimum power limit is the base load plus the minimum power of the HVAC system. The temperature limits are predefined comfort limits.

3.2.1 Building thermal dynamics

The building thermal dynamics model describes the behavior of indoor temperatures of as functions of the heating, cooling, and internal/external disturbances. There are two

quantities of interest per thermal zone: the stored energy and the temperature. The stored energy, denoted by \mathbf{x} , represents the thermal state of the building. The temperature of each zone is denoted by $\boldsymbol{\theta}$ and is constrained by comfort preferences of users. The thermal input is denoted by \mathbf{u} and represents actions of the HVAC system (energy is injected when heating and withdrawn when cooling). The state \mathbf{x} evolves as:

$$\mathbf{x}_t = \mathbf{g}_t(\mathbf{x}_{t-1}, \mathbf{u}_{t-1}),$$

where \mathbf{g} is the state transition function. The indoor temperature at time t is a function of the state and the input at the current time, i.e., $\boldsymbol{\theta}_t(\mathbf{x}_t, \mathbf{u}_t)$.

We express the total building load, p_t , as the sum of the HVAC load and the base load $p_t = p_t^{\text{hvac}} + p_t^{\text{base}}$. Then, \mathbf{u}_t a function of the total building load p_t . Thus, we express the indoor temperature at time t as a function of the load at t , the load at $t - 1$ and the state at $t - 1$, written as $\boldsymbol{\theta}_t(\mathbf{x}_{t-1}, p_{t-1}, p_t)$. Rolling out this relationship backward in time until $t = 0$, we eliminate the dependencies on $\mathbf{x}_1, \dots, \mathbf{x}_T$, and write $\boldsymbol{\theta}_t$ as function of \mathbf{x}_0 and p_0, p_1, \dots, p_t ,

$$\boldsymbol{\theta}_t(\mathbf{x}_0, \mathbf{p}_{0:t}),$$

where $\mathbf{p}_{0:t} = \begin{bmatrix} p_0 & \dots & p_t \end{bmatrix}^\top$.

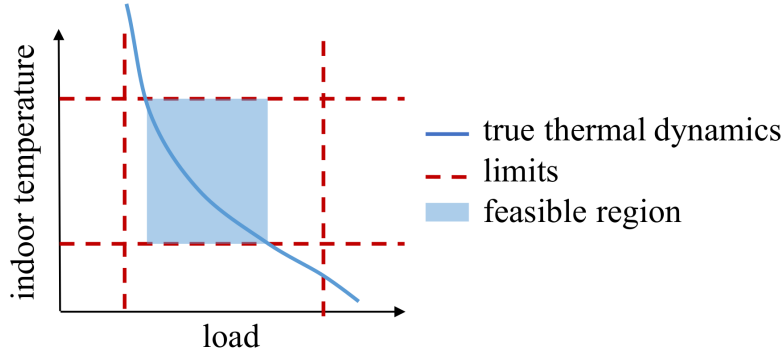


Figure 3.2: Illustration of the feasible region of the load and a (hypothetical) thermal dynamics function. With a complicated non-linear dynamics function such as the one illustrated here, the feasible region described by Eqs. (3.1) is too complex to be used in typical power system frameworks.

3.2.2 Feasible region of the load

Given that the building operation is constrained by load and temperature limits, the feasible set of load profiles is

$$\mathcal{P} = \{\mathbf{p} \mid p_t^{\min} \leq p_t \leq p_t^{\max} \forall t = 1, \dots, T \quad (3.1a)$$

$$\theta_t(\mathbf{x}_0, \mathbf{p}_{0:t}) \geq \theta_t^{\min} \forall t = 1, \dots, T \quad (3.1b)$$

$$\theta_t(\mathbf{x}_0, \mathbf{p}_{0:t}) \leq \theta_t^{\max} \forall t = 1, \dots, T \quad (3.1c)$$

$$\mathbf{p}_{0:t} = [p_0 \ \dots \ p_t]^\top \forall t = 1, \dots, T \quad (3.1d)$$

$$\mathbf{p} = \mathbf{p}_{1:T}. \quad (3.1e)$$

The symbol \mathcal{P} describes set of load profiles that are within the minimum and maximum load limits (\mathbf{p}^{\min} and \mathbf{p}^{\max}) and whose associated indoor temperatures are within comfort limits (θ_t^{\min} and θ_t^{\max}).

The set \mathcal{P} is hard to characterize primarily due to the function θ_t (Fig. 3.2 for an example). Finding a good approximation \mathcal{P} motivates this work.

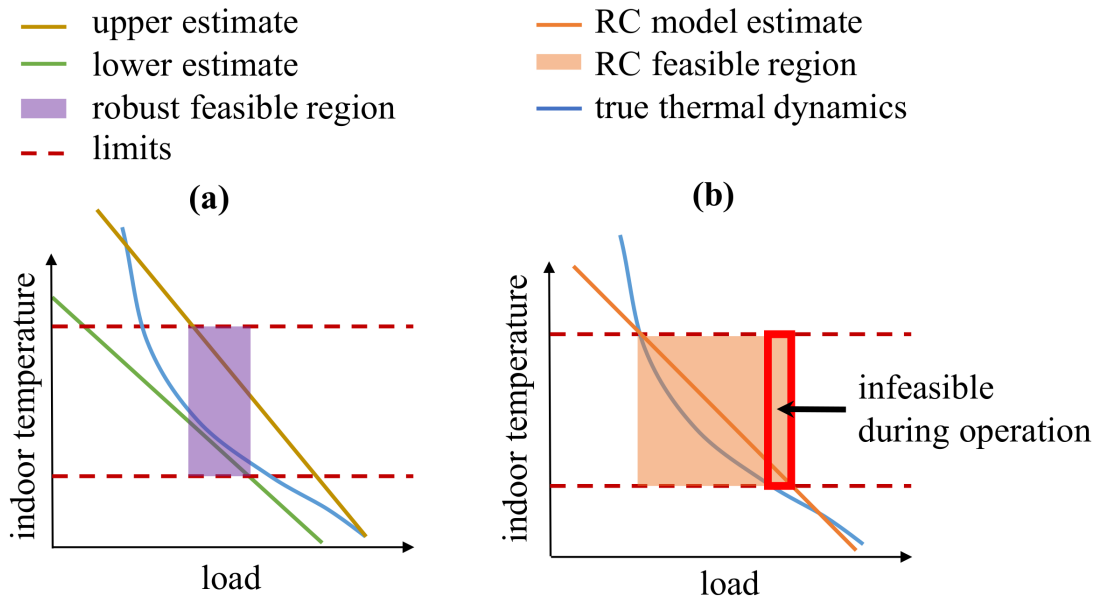


Figure 3.3: Illustration of the robust approximation of the feasible region (plot a) and RC approximation (plot b). In (a), the maximum temperature limits the upper temperature estimate. Similarly, the minimum temperature limits the lower temperature estimate. The RC approximation, on the other hand, bounds a central estimate to be between the minimum and maximum temperatures. Note that the RC model may overestimate the feasible region.

3.3 A tractable and robust approximation of \mathcal{P}

We look for two features of an approximation: robustness and tractability. The former is important because the primary purpose of the HVAC system is to meet comfort levels while servicing the grid is of secondary priority (if at all). The latter is important because a model of \mathcal{P} should be tractable in grid-related optimization and control problems.

An indoor temperature *prediction band* of arbitrary confidence achieves model robustness. We limit an *upper estimate* to be under the maximum allowable temperature and a *lower estimate* to be over the minimum. Our method stands in contrast to an *central estimate* from the RC model [59, 89, 96, 133, 169]. Thus, the maximum temperature limit could be violated when the RC model underestimates the indoor temperature. Similarly, the minimum

temperature limit could be violated when the temperature is overestimated.

Incidentally, a prediction band is that it allows handling a diverse set of temperature dynamics functions. Rather than linearly fit a potentially complicated thermal dynamics function, we upper and lower bound the function. Fig. 3.3 illustrates how a linear prediction band handles a complex function.

Tractability is essential to seamlessly incorporate our model of flexibility into existing power system frameworks, e.g., the UC problem, OPF, among others. For instance, the PJM Interconnection and California ISO implement their UC problems using MILPs [157, 175]. Similarly, most European market models are MILPs [46]. We achieve tractability by a polyhedral approximating the feasible region of the load, \mathcal{P} (i.e., described linear relations). Furthermore, the approximation is low-dimensional because we model average indoor temperatures and building-level load.

Remark 1. *In this work, we weigh zonal temperature by volume to determine the average indoor temperature.*

The mathematical simplicity of our model stands in contrast to neural network-based models like the ones in [48, 93]. While such models are useful for applications like local load control, their non-linearities ill-suites them for MILPs.

Let the robust approximation feasible region be denoted by

$$\widehat{\mathcal{P}} = \{\mathbf{p} \mid \hat{p}_t^{\min} \leq p_t \leq \hat{p}_t^{\max} \forall t = 1, \dots, T\} \quad (3.2a)$$

$$\hat{\theta}_t^{\text{U}}(\phi_0^{\text{in}}, \phi_t^{\text{out}}, \mathbf{p}_{1:t}) \leq \hat{\theta}_t^{\max} \forall t = 1, \dots, T \quad (3.2b)$$

$$\hat{\theta}_t^{\text{L}}(\phi_0^{\text{in}}, \phi_t^{\text{out}}, \mathbf{p}_{1:t}) \geq \hat{\theta}_t^{\min} \forall t = 1, \dots, T \quad (3.2c)$$

$$\mathbf{p}_{1:t} = \begin{bmatrix} p_1 & p_2 & \dots & p_t \end{bmatrix}^{\top} \quad (3.2d)$$

$$\mathbf{p} = \mathbf{p}_{1:T}. \quad (3.2e)$$

The approximation has a similar structure to the set described by Eqs. (3.1). In (3.2), however, the load \mathbf{p} is constrained by load limit approximations ($\hat{\mathbf{p}}^{\min}$ and $\hat{\mathbf{p}}^{\max}$). A more

consequential difference is that upper and lower estimates describe indoor temperatures ($\hat{\theta}_t^U$ and $\hat{\theta}_t^L$). The approximations of the maximum and minimum temperature limits ($\hat{\theta}_t^{\max}$ and $\hat{\theta}_t^{\min}$) constraint the upper and lower indoor temperature estimates, respectively Fig. 3.3(a) illustrates the approximation of \mathcal{P} in one load dimension.

We achieve tractability by modeling $\hat{\theta}_t^U$ and $\hat{\theta}_t^L$ as affine functions of the initial indoor temperature ϕ_0^{in} , outdoor temperature ϕ_t^{out} , and load from 1 to t :

$$\hat{\theta}_t^U(\phi_0^{\text{in}}, \phi_t^{\text{out}}, \mathbf{p}_{1:t}) = \bar{\mathbf{a}}_t^\top \mathbf{p}_{1:t} + \bar{\mathbf{b}}_t^\top \begin{bmatrix} \phi_0^{\text{in}} & \phi_t^{\text{out}} & 1 \end{bmatrix}^\top \quad (3.3a)$$

$$\hat{\theta}_t^L(\phi_0^{\text{in}}, \phi_t^{\text{out}}, \mathbf{p}_{1:t}) = \underline{\mathbf{a}}_t^\top \mathbf{p}_{1:t} + \underline{\mathbf{b}}_t^\top \begin{bmatrix} \phi_0^{\text{in}} & \phi_t^{\text{out}} & 1 \end{bmatrix}^\top. \quad (3.3b)$$

The vectors $\bar{\mathbf{a}}_t, \underline{\mathbf{a}}_t \in \mathbb{R}^t$ relate the building load from time 1 to t , $\mathbf{p}_{1:t}$, to upper and lower estimates of indoor temperature at time t , respectively. The vectors $\bar{\mathbf{b}}_t, \underline{\mathbf{b}}_t \in \mathbb{R}^3$ relate outside ambient temperature and the initial indoor temperature to upper and lower approximations indoor temperature at time t , respectively. The last element of $\bar{\mathbf{b}}_t$ and $\underline{\mathbf{b}}_t$ is the offset.

For each time period, the feasible region is described by the 6-tuple

$$\Phi_t = \left(\hat{p}_t^{\min}, \hat{p}_t^{\max}, \hat{\theta}_t^{\min}, \hat{\theta}_t^{\max}, \hat{\theta}_t^L, \hat{\theta}_t^U \right)$$

and the collection of all Φ_t 's from $t = 1$ to $t = T$ describe $\hat{\mathcal{P}}$. The next section shows how to find Φ_t from data.

3.4 Estimating the feasible region

We use time-series data of total building load, indoor temperature, and outdoor temperature to find $\hat{\mathcal{P}}$. The source of the data is EnergyPlus³ simulations of typical U.S. commercial buildings [70]. While the data itself is simulated, the underlying data to construct the models is real and characteristic of buildings in the U.S.

³EnergyPlus is widely used instead of building measurements that are rarely available to academic researchers, e.g., in References [35, 177, 224]

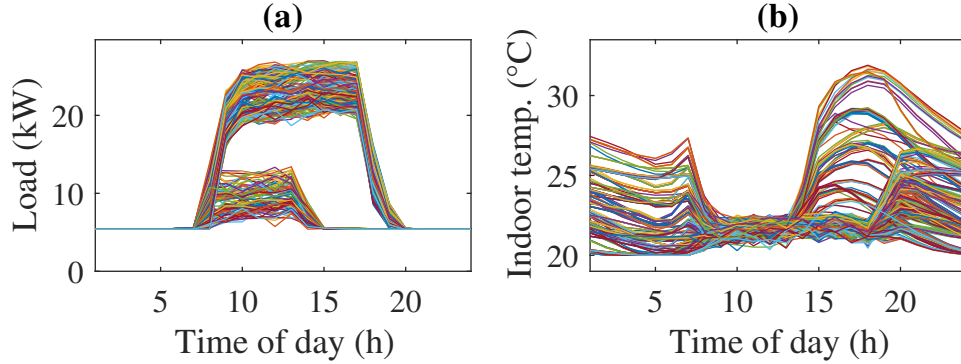


Figure 3.4: Load and indoor temperature time-series simulated data of a small office building. Plot a shows load data for 300 summer days and plot b shows indoor temperature.

Fig. 3.4 shows simulated load and indoor temperature data for a small office building. In our work, we find that using 300 training days is sufficient to identify most of the behaviors. Since buildings are typically designed to operate for years without significant renovations [107], lack of data should not be a problem after a few months of operation.

While there are other pieces of information that could help to better approximate \mathcal{P} , we are interested in using small amounts of data. For instance, HVAC rather than total load could result in more accurate approximations of the thermal dynamics. However, HVAC data may not be readily available or gathering it may be costly [119].

3.4.1 Clustering

Each one of the training days is different from each other. For instance, the outdoor temperatures of two days are never *exactly* the same. Therefore, each day k is associated with a different $\mathcal{P}_k \forall k \in \mathcal{K}$ where \mathcal{K} is the set of K training days. However, fitting one model per day is difficult and of little use since no future day is exactly like any previous one. Instead, we fit C_t different values of the Φ_t to capture the characteristics of distinct types of days. In general, C_t is significantly smaller than K .

Denote the C_t different parameters of the load-indoor temperature relation, load, and

temperature limits as $\{\Phi_{1,t}, \Phi_{2,t}, \dots, \Phi_{C_t,t}\}$ where

$$\Phi_{c,t} = \left(\hat{p}_{c,t}^{\min}, \hat{p}_{c,t}^{\max}, \hat{\theta}_{c,t}^{\min}, \hat{\theta}_{c,t}^{\max}, \hat{\theta}_{c,t}^L, \hat{\theta}_{c,t}^U \right).$$

Intuitively, one would like each set of parameters to model days that are similar to each other. Thus, we cluster days that exhibit similar load-indoor temperature-outdoor temperature relationships.

Specifically, we use the K-means clustering algorithm to partition the training set

$$\mathcal{D}_t = \left\{ (\mathbf{p}_{k,1:t}, \phi_{k,0}^{\text{in}}, \phi_{k,t}^{\text{in}}, \phi_{k,t}^{\text{out}}) \right\}_{k \in \mathcal{K}}$$

into subsets used to train the different models. The training set contains data in different units (temperature and power units) and likely different magnitudes. To accommodate the magnitude differences, we normalize the training set to have an ℓ_2 norm of 1. We denote the clusters of \mathcal{D}_t that result from the K-means algorithm as $\{\mathcal{D}_{1,t}, \mathcal{D}_{2,t}, \dots, \mathcal{D}_{C_t,t}\}$ where each set $\mathcal{D}_{c,t}$ is associated with a subset of \mathcal{K} denoted as $\mathcal{K}_{c,t}$. The functions $(\hat{\theta}_{c,t}^L, \hat{\theta}_{c,t}^U)$ and the rest of the parameters in $\Phi_{c,t}$ are trained from the data in $\mathcal{D}_{c,t}$. The clustering method is detailed in Appendix B.

3.4.2 Robust model of the load-indoor temperature relationship

The inputs of this portion of the algorithm are the training data \mathcal{D}_t , the number of clusters C_t , and the robustness tuning parameter $\alpha \in (0, 1)$. The robustness parameter α represents the proportion of temperature observations allowed outside the prediction band. Thus, a smaller alpha leads to a wider, more robust band. Conversely, a larger alpha leads to a tighter band. The Case Study demonstrates how a small α leads to more aggressive provision of flexibility but also to a higher risk of violating temperature limits. Appendix D details the mechanism whereby α influences the robustness of the prediction band.

We use the data subset $\mathcal{D}_{c,t}$ to learn the parameters $\Phi_{c,t}$ (Fig. 3.5 provides an illustration).

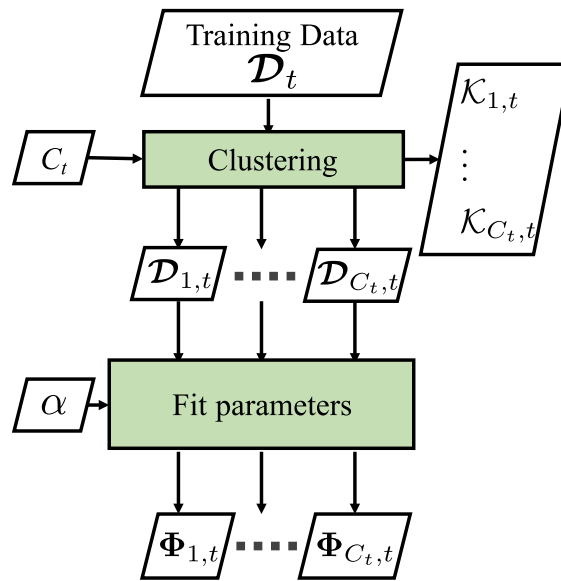


Figure 3.5: Illustration of the clustering and training algorithm. Each cluster of training data $\mathcal{D}_{c,t}$ trains a corresponding set $\Phi_{c,t}$.

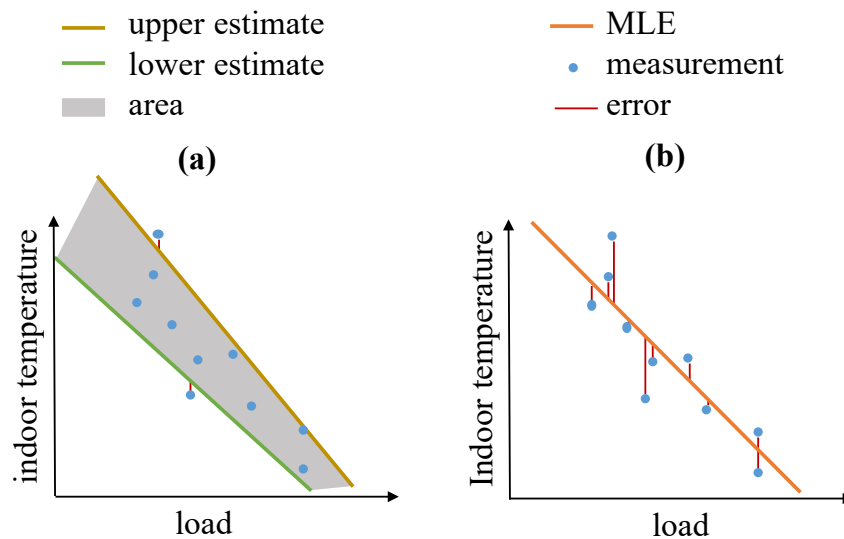


Figure 3.6: Illustration of (a) the BLSE and (b) traditional LSE. The former provides upper and a lower predictions that minimize two weighted objectives: 1) the area between the predictions and 2) the MSE of the points outside the prediction band. The latter provides a central maximum likelihood estimator (MLE).

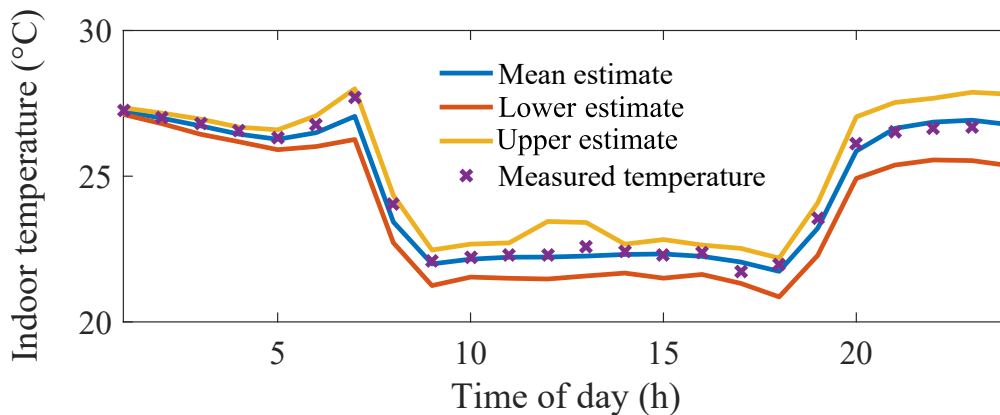


Figure 3.7: Measured indoor temperature, indoor mean temperature estimate, and prediction bounds for a sample day.

We use a least squares estimation (LSE)-inspired algorithm called “bounded least squares estimation (BLSE)” to train the parameters $\bar{\mathbf{a}}_{c,t}$, $\underline{\mathbf{a}}_{c,t}$, $\bar{\mathbf{b}}_{c,t}$, and $\underline{\mathbf{b}}_{c,t}$.

The classic LSE calculates a line that minimizes the prediction mean squared error (MSE). The BLSE finds *two* lines (an upper and a lower prediction) that minimize two objectives: 1) the squared error of the points outside of the prediction band and 2) a measure of the band area. The robustness tuning parameter α determines the weight of each objective and influences the tightness of the prediction band. The tightness of the predictions affects the outcomes of the model: overly tight predictions may overestimate the building flexibility while looser predictions may deliver an overly conservative $\hat{\mathcal{P}}$. Figure 3.6 illustrates the classical LSE and contrasts it with the BLSE. Figure 3.7 shows measured indoor temperature, mean indoor temperature estimate, and prediction bounds for a sample day. Appendix D details the BLSE algorithm. .

3.4.3 Estimates of the temperature and load limits

In some ways, estimating the parameters of the functions $\hat{\theta}_{c,t}^U$ and $\hat{\theta}_{c,t}^L$ is easier than estimating the temperature and load limits. The former is a supervised learning problem, while the latter is unsupervised (since we do not directly observe the limits). We approximate the

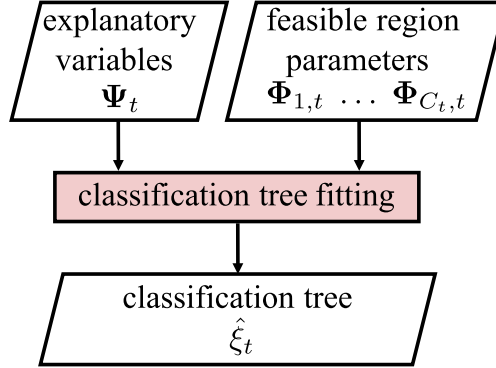


Figure 3.8: Illustration of the data and algorithm to train $\hat{\xi}_t$, an approximation of ξ_t . The function $\hat{\xi}_t$ selects the best set of feasible region parameters given the expected values of a set of explanatory variables (e.g., outdoor temperature, day of the week).

temperature and load limits of cluster c as the highest/lowest observed values during days in $\mathcal{K}_{c,t}$. See Appendix C for details.

3.4.4 Model selection

Suppose we would like to estimate the building's flexibility during day $K + 1$, i.e., during a day outside the training set. The first question is: for each time period t , which set of parameters in $\{\Phi_{1,t}, \Phi_{2,t}, \dots, \Phi_{C_t,t}\}$ should constitute $\hat{\mathcal{P}}_{K+1}$?

Recall that we use load, indoor temperatures, and outdoor temperature relationships to group the elements of the training dataset. Naturally, we have no load nor indoor temperature data *before* the new day. However, each data point in the training set is associated with the explanatory variables $\Psi_t = \{\psi_{1,t}, \dots, \psi_{K,t}\}$. The information encoded in $\psi_{k,t}$ is anything that might influence the feasible region of the load during day k . For instance, $\psi_{k,t}$ may include information on whether k is a weekday, weekend, or a holiday, outdoor temperature during time t , solar irradiation levels, or building occupancy. In this work, explanatory variables are hourly outdoor temperatures, solar radiation, and day of the week. Considering a different set of explanatory variables might be appropriate in some cases.

We use expected values of the explanatory variables of day $K + 1$ to select which $\Phi_{c,t}$'s

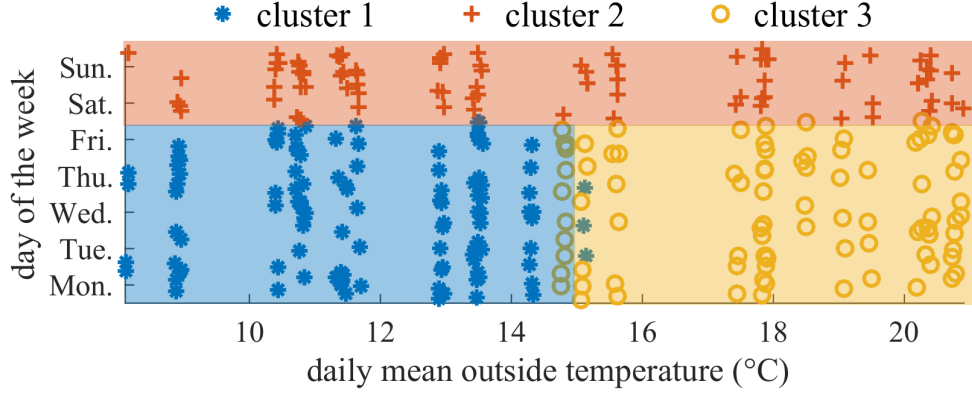


Figure 3.9: Training data grouped into three clusters. Each point in the plot represents a training data point.

to use. We assume there exists a function

$$\xi_t : \psi_{k,t} \rightarrow \{\Phi_{1,t}, \Phi_{2,t}, \dots, \Phi_{C_t,t}\}$$

that maps the set of explanatory variables $\psi_{k,t}$ to its associated set of parameters. Here, $\xi_t(\psi_{k,t}) = \Phi_{c,t}$ when k belongs in the set $\mathcal{D}_{c,t}$ (recall that $\mathcal{D}_{c,t}$ is used to train $\Phi_{c,t}$). We estimate ξ_t using a *classification tree* [127]. Fig. 3.8 illustrates the training algorithm of an approximation of ξ_t , denoted by $\hat{\xi}_t$.

Let $\{\psi_{K+1,1}, \psi_{K+1,2}, \dots, \psi_{K+1,T}\}$ denote the set of explanatory variables for each time period of day $K + 1$ and the predicted model to use is $\Phi_{\hat{c}_t,t} = \hat{\xi}_t(\psi_{K+1,t})$. Then, the set

$$\{\Phi_{\hat{c}_1,1}, \Phi_{\hat{c}_2,2}, \dots, \Phi_{\hat{c}_T,T}\}$$

describes the building's flexibility model during day $K + 1$.

Take the data in Fig. 3.9 as an example. In this case, the explanatory variables are the day of the week and mean outside temperature. Notice training data points in cluster 2 come exclusively from weekends. Training data points in clusters 1 and 3 come from colder and warmer weekdays, respectively. Thus, a reasonable decision rule is: use the parameters

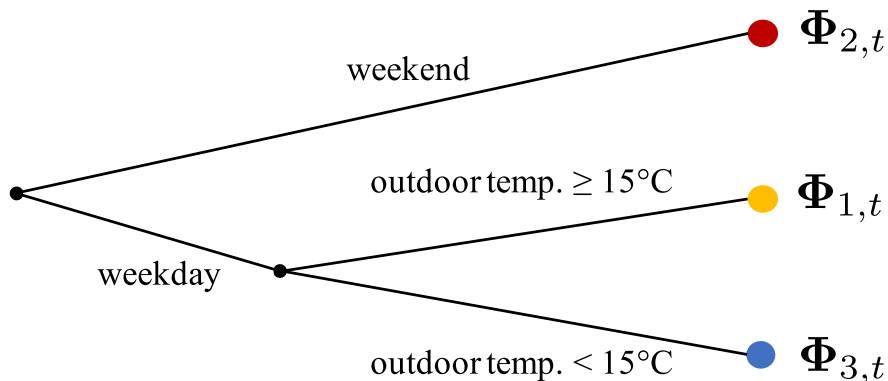


Figure 3.10: Decision tree trained using points in Fig. 3.9.

$\Phi_{2,t}$ if day $K + 1$ is a weekend; use $\Phi_{1,t}$ if $K + 1$ is a weekday and if the daily mean temperature is expected to be under 15°C ; and use $\Phi_{3,t}$ otherwise. Fig. 3.10 illustrates the the aforementioned decision rule.

3.5 Model validation

We test the proposed method using data from EnergyPlus simulation of three different buildings [70]. Table 3.1 provides a brief summary of important characteristics of each building: peak load, average load, and thermal mass (the amount of electric energy needed to cool the building by 1°C).

Table 3.1: Summary of building characteristics.

Type	Peak / avg. load	Thermal mass
Office 1	27/ 10 kW	2.7 kWh/ $^\circ\text{C}$
Office 2	15/ 6.7 kW	7.7 kWh/ $^\circ\text{C}$
Supermarket	140/ 86 kW	77 kWh/ $^\circ\text{C}$

The sizes of the training, cross-validation, and test datasets for each building are 300, 100, and 100, respectively. The explanatory variables for the model selection stage are the

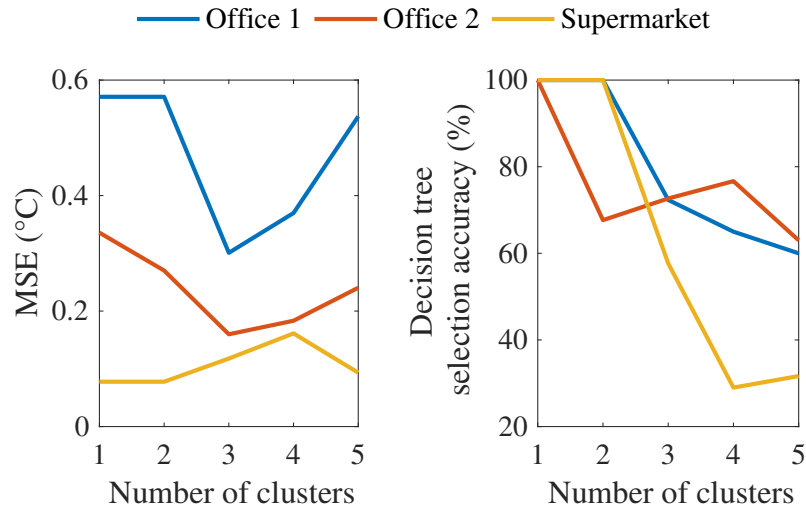


Figure 3.11: The left-hand plot shows mean square error (for the cross-validation dataset) of the indoor temperature prediction for the three buildings at period $t = 19$ as a function of the number of training data clusters. In this case, the optimal number of clusters for office 1, office 2 and the supermarket are 3, 3, and 1, respectively. The right-hand plot shows the accuracy of the decision tree as a function of the number of clusters.

day of the week (e.g., Monday), outdoor temperature, and solar irradiation.

3.5.1 Test error and the optimal number of clusters

There is a trade-off in the number of training data clusters C_t . On the one hand, a small C_t implies that more training data is available for each approximation. On the other hand, a large C_t means that each approximation models days that are more like each other. Similar to references [82, 202] and as a special case of the hyperparameter tuning problem in machine learning, we define the optimal number clusters C_t^* as the number that minimizes the temperature prediction MSE over the cross-validation dataset. Then, we use the test dataset to measure the actual prediction performance. For instance, the cross-validation error of temperature prediction for Office 1 is at a minimum when the number of clusters is $C_t^* = 2$ (see the left-hand plot of Fig. 3.11).

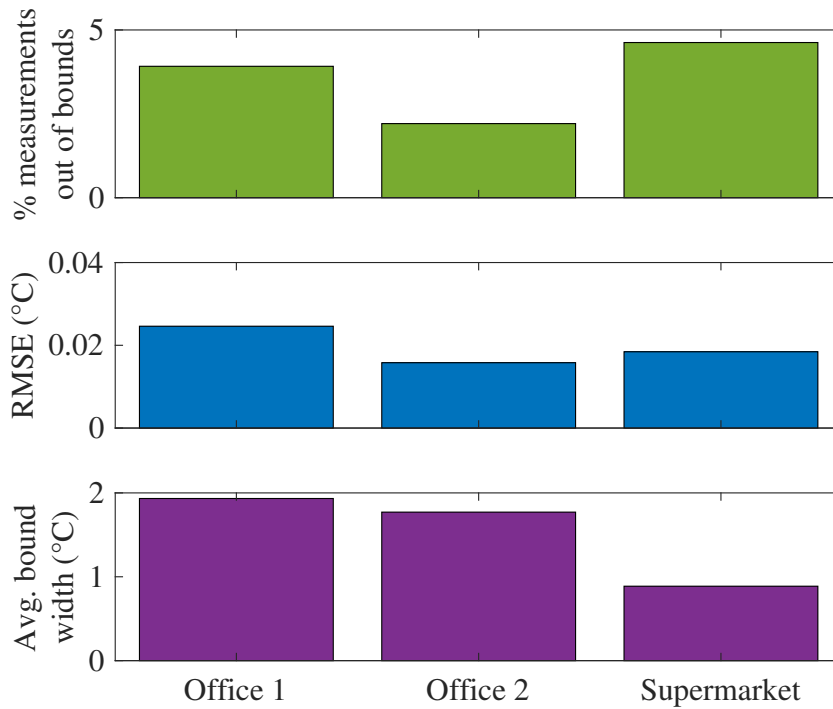


Figure 3.12: Percentage of measurements out of bounds, test error of the temperature prediction, and average bound width for each building type. These statistics are computed using test set data.

The cross-validation initially decreases error with the number of clusters because, as we divide the training data into more groups, each data cluster approximates functions that are more like each other. However, at some point, increasing the number of data clusters increases the cross-validation error (see the left-hand plot in Fig. 3.11). There are two main reasons for this phenomenon. The first one is that a higher number of clusters decreases the number of data points in each cluster and increases the risk of over-fitting. The second reason is that as the number of clusters increases, the accuracy of the decision tree $\hat{\xi}_t$ decreases (see the right-hand plot in Fig. 3.11).

3.5.2 Error analysis on the test set

Fig. 3.12 shows the percentage of indoor temperature measurements outside the prediction band, the temperature prediction error, and tightness of the band (all for the test set). The percentage of measurements outside the band is closely linked to the robustness parameter α . Recall that an α -level of robustness restricts the percentage of *training* data points outside the prediction band to be less than $100 \cdot \alpha$ %.

We define the error of each measurement used to compute the root-mean-squared error (RMSE), as zero if the measurement is inside the prediction band and as the distance to the nearest band if the measurement otherwise (see Fig. 3.6 for an illustration and Appendix D for details). The RMSE of our model is lower than the error given by the RC circuit model (we compare our approach against the RC circuit model in greater detail in Sec. 3.5.3). However, the lower error of our model is not free. It comes at the cost of more conservative models of building flexibility, (we explore this further in Sec. 3.6).

3.5.3 Comparison against the RC circuit model

The most widely adopted alternative to our method is the RC circuit model. The RC model expresses the indoor temperature change from time t to $t + 1$ as a linear function of the indoor-outdoor temperature difference, HVAC power⁴, and an independent thermal disturbance [59, 89, 96, 133, 169] and is written as

$$\phi_{t+1}^{\text{in}} - \phi_t^{\text{in}} = A_t \cdot (\phi_t^{\text{in}} - \phi_t^{\text{out}}) + B_t \cdot p_t^{\text{hvac}} + D_t$$

where A_t and B_t relate indoor-outdoor temperature difference and HVAC power, respectively, to change in indoor temperature from t to $t + 1$ and D_t is a thermal disturbance [59, 133]. We estimate A_t , B_t , and D_t via a linear regression where the dependent variable is the temperature change $\phi_{t+1}^{\text{in}} - \phi_t^{\text{in}}$ and the regressors are $\phi_t^{\text{in}} - \phi_t^{\text{out}}$ and p_t^{hvac} .

⁴In some cases, HVAC cooling/heating load is used instead of HVAC power, e.g. [133].

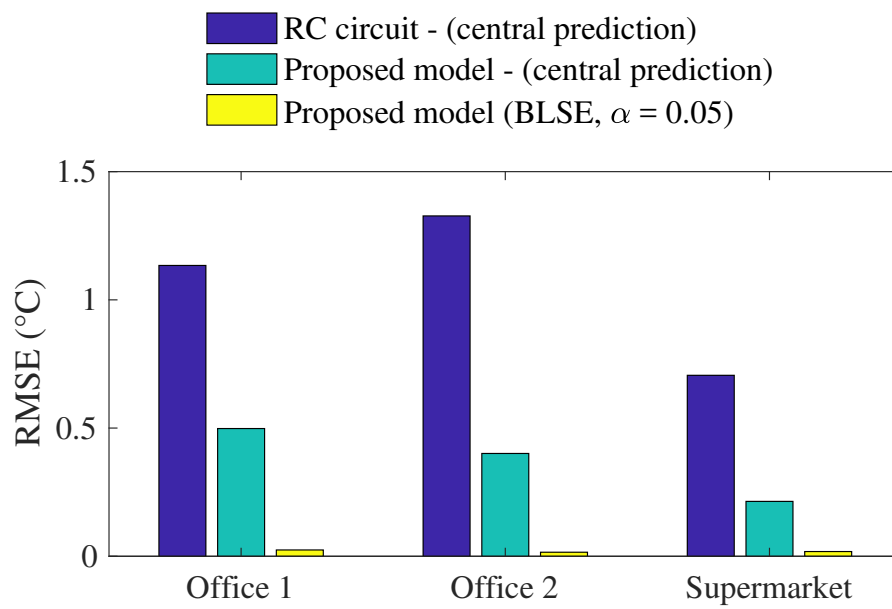


Figure 3.13: Test set RMSE for three different models: the RC circuit model, our model (central prediction), ($\alpha = 1$) and our model with $\alpha = 0.05$.

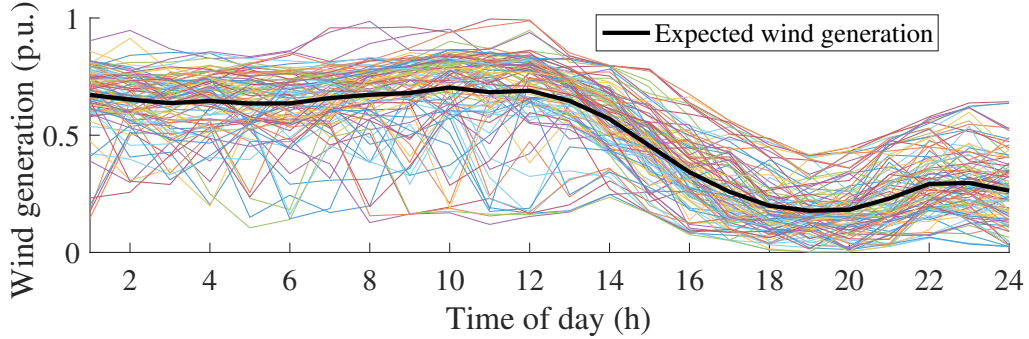


Figure 3.14: Wind scenarios used in the case study.

Fig. 3.13 shows the test set RMSE for three different models: the RC model, and our approach with $\alpha = 1$ and with $\alpha = 0.05$. It is natural that the $\alpha = 0.05$ model RMSE is orders of magnitude smaller: by definition, close to 95% of the predictions fall in the prediction band. Less intuitive is the fact that our model with $\alpha = 1$, equivalent to a central estimate, also outperforms the RC model. There are two reasons why our model outperforms the alternative. The first is that we cluster our data to model several, rather than one, thermal models. The second is that the traditional RC circuit model fails to use p_t^{hvac} at time t to predict indoor temperature during that same time period [59, 133, 169].

3.6 Case study: building flexibility for wind power balancing

We consider a setting where a wind power producer contracts an aggregator of buildings to use the flexibility of its loads to compensate deviations from expected production. Let Ω^w represent the set of scenarios and each generation scenario be denoted by the vector $\boldsymbol{\nu}_{\omega^w} \in \mathbb{R}_+^T$. The t^{th} entry of $\boldsymbol{\nu}_{\omega^w}$ represents wind power at time t in scenario ω^w . Then, the expected wind production is given by $\mathbb{E}[\boldsymbol{\nu}_{\omega^w}]$ and the wind production deviation of scenario ω by $\boldsymbol{\Delta}_{\omega^w} = \boldsymbol{\nu}_{\omega^w} - \mathbb{E}[\boldsymbol{\nu}_{\omega^w}]$. Fig. 3.14 shows 100 wind scenarios from [42, 165].

Additionally, we consider uncertainty in the building load. We model the stochastic load component of building i via a T -dimensional normally distributed parameter $\boldsymbol{\epsilon}_i \sim \mathcal{N}(\mathbf{0}, \boldsymbol{\Sigma}_i)$.

We assume that the stochastic components of the N buildings are independent. Then, the aggregate stochastic load component is $\sum_i^N \epsilon_i = \epsilon \sim \mathcal{N}(\mathbf{0}, \sum_i^N \Sigma_i)$. We represent ϵ via scenarios $\{\epsilon_{\omega^b}\}_{\omega^b \in \Omega^b}$.

The aggregator's problem is as follows. In the first stage, e.g., in the day-ahead market, the aggregator schedules an aggregate base load $\mathbf{p}^b \in \mathbb{R}_+^T$ at an energy price $\boldsymbol{\tau} \in \mathbb{R}^T$. When the uncertainty in wind production materializes in the second stage, e.g., in the real-time, the aggregator can deviate from the base load to accommodate deviations and be remunerated by v per unit energy. For instance, suppose that the wind production for a particular hour is expected to be 10 kWh, but the actual output is 12 kWh. Then, the buildings deviate from their base load of 50 kWh to 51 kWh to partially accommodate the 2 kWh surplus. In this case, the building pays $50 \cdot \tau_t$ for day-ahead energy and receives $1 \cdot v$ for balancing services. The aggregator's problem is written as:

$$\min_{\substack{\boldsymbol{\tau}, \mathbf{p}^b \\ \mathbf{p}_i^b, \mathbf{p}_{i, \omega^w} \\ \mathbf{p}^b, \mathbf{p}_{\omega^w, \omega^b}}} \boldsymbol{\tau}^\top \mathbf{p}^b + \mathbb{E}[v \cdot |\mathbf{p}^b - \mathbf{p}_{\omega^w, \omega^b} + \boldsymbol{\Delta}_{\omega^w}|] \quad (3.4a)$$

s.t.

$$\mathbf{p}^b = \sum_{i=1}^N \mathbf{p}_i^b \quad (3.4b)$$

$$\mathbf{p}_{\omega^w, \omega^b} = \sum_{i=1}^N \mathbf{p}_{i, \omega^w} + \epsilon_{\omega^b} \quad \forall \omega^w \in \Omega^w, \omega^b \in \Omega^b \quad (3.4c)$$

$$\mathbf{p}_i^b \in \widehat{\mathcal{P}}_i \quad \forall i = 1, \dots, N \quad (3.4d)$$

$$\mathbf{p}_{i, \omega^w} \in \widehat{\mathcal{P}}_i \quad \forall i = 1, \dots, N, \omega^w \in \Omega^w. \quad (3.4e)$$

The objective function (3.4a) has two components: the cost of energy, $\boldsymbol{\tau}^\top \mathbf{p}^b$, and the expected foregone revenue from balancing wind power deviations $\mathbb{E}[v \cdot |\mathbf{p}^b - \mathbf{p}_{\omega^w, \omega^b} + \boldsymbol{\Delta}_{\omega^w}|]$. The second stage variable $\mathbf{p}_{\omega^w, \omega^b}$ is the aggregate building load for wind scenario ω^w and load uncertainty scenario ω^b . Eq. (3.4b) defines the aggregate base load (first stage) as the sum of the base loads of each building. Similarly, Eq. (3.4c) defines the aggregate load when scenarios ω^w and

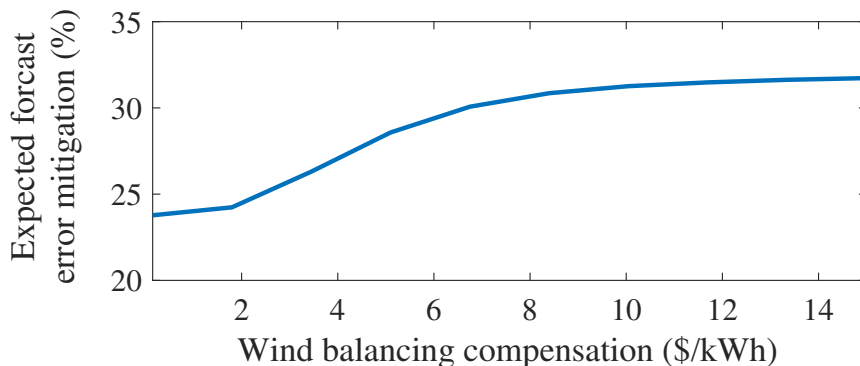


Figure 3.15: Expected forecast error mitigation by all three buildings as a function of compensation v .

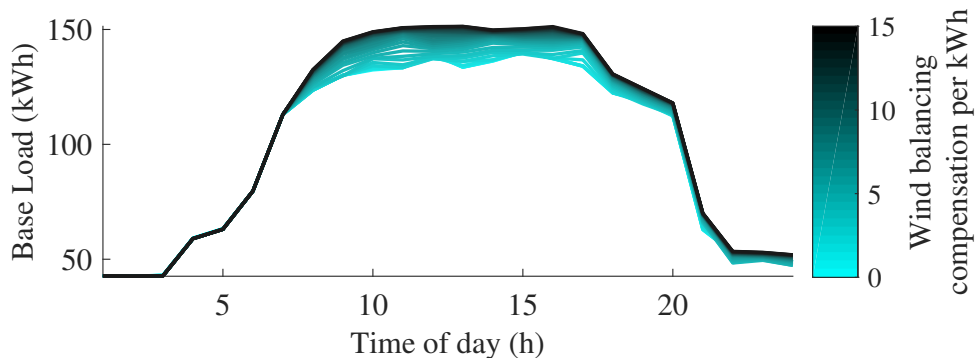


Figure 3.16: Base load at different wind balancing compensation levels.

ω^b materialize (second stage). Finally, Eqs. (3.4d) and (3.4e) restrict the first and second stage load of each building, respectively, to be within their respective approximate feasible region. The feasible regions $\hat{\mathcal{P}}_i$ are defined by Eqs. (3.2) and (3.3).

We formulate Problem (3.4) as a stochastic linear program (LP) and modeled using Julia's JuMP environment [71]. We use Gurobi Optimizer [94] on a desktop computer running on a Intel(R) Xenon(R) CPU E3-1220 v3 @ 3.10 GHz with 16 GB of RAM to solve the problem.

3.6.1 Wind forecast error mitigation and balancing compensation

Let the cost of energy be 1 throughout the day and the installed wind capacity be one-third of peak load. Depending on the wind balancing compensation, the three buildings mitigate around 25–30 % of the wind forecast errors. As expected, and as shown in Fig. 3.15, the amount of error mitigation increases as with compensation. This result can be explained as follows. When the compensation is low, the base load tends to be low to minimize energy costs (see the lighter shades in Fig. 3.16). Low base load is poorly positioned to compensate wind shortages by further decreasing load in the real-time. As compensation increases, however, it becomes economically attractive to position base load at higher levels and increase the ability to accommodate wind shortages.

3.6.2 Demonstration of robustness and tractability

Robustness and tractability of are the two central characteristics of $\hat{\mathcal{P}}$. The former claims that a building load profile in $\hat{\mathcal{P}}$ does not violate temperature limits during building operation (to a degree of confidence determined by α). The latter claims that our model is easily, and without significant computational burden, incorporated into typical power system analysis frameworks (such as the one presented in this case study).

First, we analyze the effect of the parameter α on the building operation. As shown in Fig. 3.17(a), the expected forecast error mitigation increases with α . That is, as the robustness of the model decreases, it allows a more aggressive operation to compensate forecast errors. However, less robust models such as the RC circuit model, risk scheduling load profiles that are not feasible during operation (see an illustration of this phenomenon in Fig. 3.3). As shown in Fig. 3.17(b), as the robustness parameters α increases so does the expected indoor temperature limits violations. All in all, the user faces a trade-off when tuning the robustness parameter: a larger α leads to higher error mitigation but also increases the risk of indoor temperature limit violations.

We demonstrate that the proposed model is tractable by increasing the number of build-

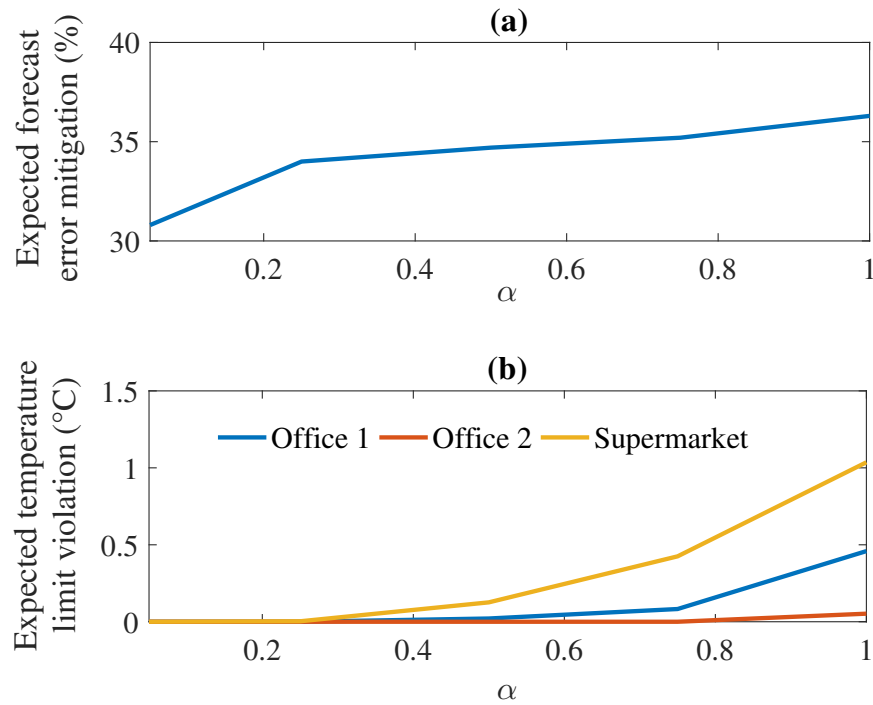


Figure 3.17: Plot a shows the expected forecast error mitigation by all three buildings and plot b shows expected temperature violation by each building as a function of the robustness parameter α . Notice that there is a trade-off between error mitigation and robustness to indoor temperature prediction errors.

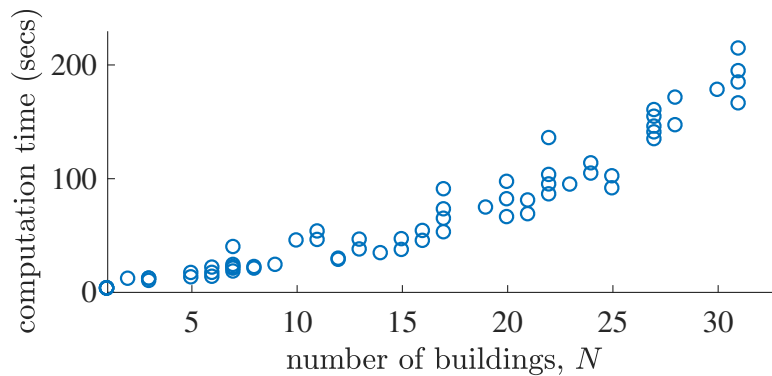


Figure 3.18: Time required to solve Problem (3.4) under different number of buildings. Note that each building is represented by 101 scenarios : one base load, \mathbf{p}_i^b , and one for each wind power scenario, \mathbf{p}_{i,ω^w} .

ings in Problem (3.4). We show that computational burden remains manageable even with a large number of buildings (see Fig. 3.18). It is worth noting that each building is represented by 101 scenarios: one base load, \mathbf{p}_i^b , and one for each wind power scenario, \mathbf{p}_{i,ω^w} . Thus, Problem (3.4) with $N = 10$, for instance, is equivalent to a deterministic problem with 1010 buildings.

3.7 Summary

In this chapter, we propose a method to estimate a robust feasible region of the building load using simple linear relations. Our approach ensures that a building HVAC system maintains acceptable occupant comfort while providing flexibility to the power system. Our model is mathematically simple and tractable because it can be easily incorporated into common power system optimization and control environments. For instance, our model can be seamlessly incorporated into problems such as the ED, DR scheduling and control, OPF, and UC, among others. Furthermore, the model training algorithm requires coarse and generic data and can be applied to many kinds of buildings. We compare our model's performance to the RC circuit model and demonstrate its use in a practical application.

Chapter 4

MODELING AN AGGREGATOR

4.1 *Introduction*

A prominent trend in power systems is the increase of “behind-the-meter,” customer-owned and controlled distributed energy resources (DERs) such as distributed solar photovoltaic (PV), dispatchable generation, electric vehicles (EVs) [38]. These DERs are typically installed to accomplish local objectives like reducing electric bills [182] or improving local reliability [122]. While DERs have the potential to contribute to the operation of the grid by participating in wholesale markets [69, 156], they are not able for two main reasons: their capacities are typically smaller than the required minimum [14, 166]; and the large number of DERs would make their management difficult [183]. The exclusion of DERs from electricity markets is of detriment to both their owners and society as a whole. On the one hand, DERs miss potentially profitable revenue streams (e.g., reserve provisions or energy arbitrage). On the other hand, society is unable to tap into assets that potentially provide services more efficiently than market incumbents. A commonly proposed solution is aggregators that act as mediators between DERs and the power system [43]. See Fig. 4.1 for an illustration of the market-aggregator-DER relationships.

A proper understanding of DER-aggregator relationship is fundamental to explain an aggregator’s market behavior. On the one hand, an aggregator participates in the market on behalf of its constituent DERs. On the other hand, however, the aggregator does not own and may not have direct control of the resources. This dynamic is unlike traditional generators where the bidder and the resource are a single entity. In this chapter, we study the relationship between an aggregator and its constituent DERs. We assume that all players are rational and use game theoretic tools to explain their relationship. The result is a sound

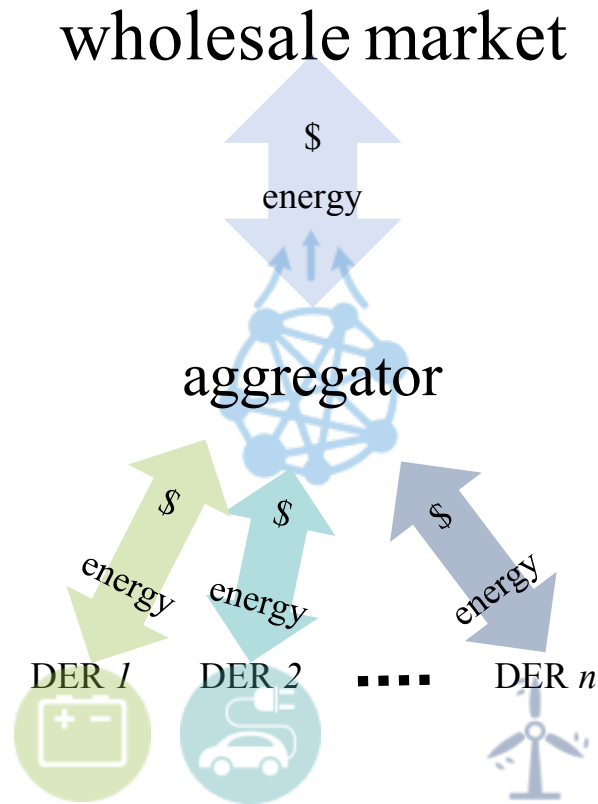


Figure 4.1: Market-aggregator-DETs framework.

model of the aggregator's market behavior and the profit split between aggregator and DETs.

4.1.1 Related works

One can find many studies of the operation and market strategies of aggregators in the literature. For instance, [156,183] studies the aggregation and market participation of a fleet of electric vehicles. Chen et al. study the problem of coordination of residential consumers for demand response [47]. The studies above focus on the short-term interactions between aggregator and grid. However, they pay little attention to the interactions between the aggregator and its constituents.

On a topic closely related to our work [148] uses Nash Bargaining Theory to determine

the compensation of reactive power providers. In [140], the authors focus on the distributed optimization problem of an EV aggregator. The authors of [209, 216] study the problem subjected to power flow constraints. The work in [218] studies the interactions of an EV aggregator and its EVs when providing frequency regulation. However, these studies do not address how profits the aggregator and its DERs share profits. The problem of profit allocation is not trivial since neither party can participate in the market alone: the aggregator has no physical assets, and the individual DERs are too small to participate. In this work, we use Nash Bargaining Theory to derive a profit-split model between the aggregator and DERs.

In contrast, we take a closer look at the relationship between DERs and an aggregator operating in a market environment. Not only we consider the aggregator as a strategic and profit-maximizing actor, but we also assume that each DER is rational and autonomous. More concretely, the aggregator decides how to bid into the market and the prices to offer each DER while the DERs react to the aggregator prices. Furthermore, we study the *long-term* relationship between DER and aggregator since this is reasonable to assume that their interactions are sustained over time. Studying the longterm is essential because the short-term relationship may be a lousy predictor of the aggregator and DER actions.

4.1.2 Contributions

In summary, the contributions of this work are:

- i) *A model of interactions between an aggregator, its DERs, and the electricity market.*

First, we introduce the short-term interaction DER-aggregator interaction model: they play a single-leader, multi-follower Stackelberg Game. We show that the outcome of this non-cooperative game can be Pareto-inefficient (see Fig. 4.2). In practice, however, the aggregator and DERs are likely to interact repeatedly. We demonstrate the existence of profit-splitting schemes in which cooperation by rational agents is stable in the long-term. Finally, we use Nash Bargaining Theory to show that the aggregator and DERs split a Pareto-optimal profit and cooperate in the long term.

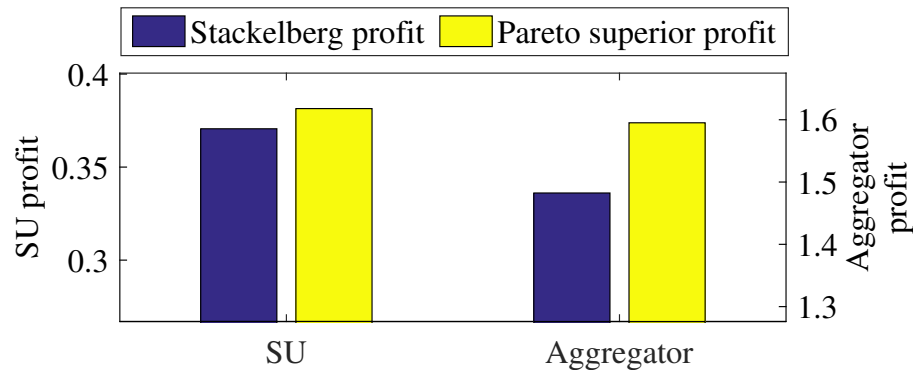


Figure 4.2: Aggregator/storage unit (SU) Stackelberg and a Pareto-superior profits. The blue bars are the SU and the aggregator profits under the parameters defined in Example 1. These profits are Pareto-inefficient because we can find operating points where both parties receive higher profits (yellow bars).

- ii) *A simplified model of DERs managed by an aggregator.* The Pareto-optimal agreement permits replacing a complicated system composed of many agents (i.e., the aggregator and DERs) with a simpler aggregate profit maximization problem. The benefits of the simplified model are two-fold. First, it provides a model of the aggregator market participation strategy. Second, it provides a computationally tractable model of the actions of many DERs under an aggregator.

4.1.3 Organization of this chapter

This chapter is organized as follows. Section 4.2 introduces the market, DER, and aggregator models. Section 4.3 introduces the short-term interaction model between the aggregator and the DERs. Section 4.4 introduces model long-term interaction model between. In Section 4.5, we use Nash Bargaining to model aggregator market bids and determine the long-term equilibrium. Section 4.6 summarizes and concludes the chapter.

4.2 Models

This section introduces the models used in this chapter: the market structure, the DERs, and the aggregator. We assume that DERs do not participate directly in the market. Instead, they interact with an aggregator that participates in the wholesale market. The structure of these interactions is illustrated in Fig. 4.1.

4.2.1 The market structure

We consider a locational marginal price (LMP)-based electricity market that balances supply and demand at the minimum cost over multiple time periods. We the set of time periods as \mathcal{T} . We assume that the supply at each node b and time t is an increasing function known by all participants. The SO dispatches generation to minimize cost, and the market clears at prices λ_t . Then, a participant that supplies x amount of energy during period t at node b is paid $x \cdot \lambda_{b,t}$ and a participant consuming y amount of energy is charged $y \cdot \lambda_{b,t}$.

4.2.2 The distributed energy resources

Let \mathcal{I} denote the set of n DERs. Let $x_{i,t}^+$ ($x_{i,t}^-$) denote the energy produced (consumed) by DER i at time t . We define the net production as $x_{i,t} = x_{i,t}^+ - x_{i,t}^-$, that is, positive $x_{i,t}$ implies power injection while a negative $x_{i,t}$ implies power absorption.

Let $\tau_{i,t}$ denote the aggregator price that DER i faces at time t . Then, DER i 's profit is:

$$\pi_i^{\text{der}}(\mathbf{x}_i; \boldsymbol{\tau}_i) = \sum_{t \in \mathcal{T}} \tau_{i,t} \cdot x_{i,t} - c_i(\mathbf{x}_i), \quad (4.1)$$

where $\mathbf{x}_i = \{x_{i,t}^+, x_{i,t}^-\}_{t \in \mathcal{T}}$ and $\boldsymbol{\tau}_i = \{\tau_{i,t}\}_{t \in \mathcal{T}}$. The function $c_i(\cdot)$ models the cost of DER i . For instance, $c_i(\cdot)$ may represent the production cost of distributed generation or the discomfort cost due to demand-response deployment [87]. In this work, $c_i(\cdot)$ is a non-negative and strictly convex function of \mathbf{x}_i .

The actions \mathbf{x}_i DER i are limited by a set of operating constraints that constitute a

feasible operating region $\mathcal{X}_i^{\text{der}}$. Finally, the profit maximization problem DER i is expressed as

$$\max_{\mathbf{x}_i \in \mathcal{X}_i^{\text{der}}} \pi_i^{\text{der}}(\mathbf{x}_i; \boldsymbol{\tau}_i). \quad (4.2)$$

We focus on energy exchange between DERs, the aggregator, and the wholesale market and consider additional revenue streams (e.g., payments for frequency regulation and reserves [220]), or benefits delivered by DERs (e.g., improvement of power quality [186]) as high-priority tasks modeled by constraints on the DER operation. For instance, a storage unit (SU) can reserve some of its capacity for frequency regulation and contract the remainder for market participation through the aggregator.

4.2.3 The aggregator

Let the vector $\mathbf{x}_t^{\text{bus}}$ denote net nodal energy injections/absorptions by the DERs and be defined as

$$\mathbf{x}_t^{\text{bus}} = \sum_{i \in \mathcal{I}} \mathbf{m}_i \cdot x_{i,t}.$$

Here, the b^{th} element of the vector \mathbf{m}_i is 1 if DER i is connected to bus b and 0 otherwise. The b^{th} element of $\mathbf{x}_t^{\text{bus}}$ denotes net injection (if positive) or absorption (if negative) of the DERs connected to node b . Then, the aggregator's net revenue from market participation is

$$\sum_{t \in T} \boldsymbol{\lambda}_t^\top \mathbf{x}_t^{\text{bus}}.$$

In this work, we assume that an aggregator is a profit-maximizing agent and has the ability to select the prices $\boldsymbol{\tau}_i$ accordingly.

4.3 Single-shot game

In this section, we present a single-shot Stackelberg Game used to model the aggregator-DERs short-term interaction and show that the equilibria could be unsatisfactory for all parties.

4.3.1 Aggregator-DETs Stackelberg Game

We model the interaction between the aggregator and DETs as a single leader multi-follower game with perfect information [65]. The aggregator leads by announcing prices $\boldsymbol{\tau}_i$, and the DETs respond by deciding their actions \boldsymbol{x}_i .

For a price schedule $\boldsymbol{\tau}_i$ chosen by the aggregator, each DET chooses a production/consumption schedule

$$\boldsymbol{x}_i^{\text{SE}} = \arg \max_{\boldsymbol{x}_i \in \mathcal{X}_i^{\text{der}}} \pi_i^{\text{der}}(\boldsymbol{x}_i; \boldsymbol{\tau}_i) \quad (4.3)$$

that maximizes its profit¹.

The aggregator's objective is to choose a set of prices $\boldsymbol{\tau} = \{\boldsymbol{\tau}_i\}_{i \in \mathcal{I}}$ that maximize its profit given by

$$\pi^{\text{a}}(\boldsymbol{\tau}; \boldsymbol{x}) = \sum_{i \in \mathcal{I}} \sum_{t \in \mathcal{T}} \{\boldsymbol{\lambda}_t^\top \boldsymbol{m}_i \cdot x_{i,t} - \tau_{i,t} \cdot x_{i,t}\} \quad (4.4)$$

where $\boldsymbol{x} = \{\boldsymbol{x}_i\}_{i \in \mathcal{I}}$. That is, it chooses

$$\boldsymbol{\tau}^{\text{SE}} = \arg \max_{0 \leq \tau \leq M} \pi^{\text{a}}(\boldsymbol{\tau}; \{\boldsymbol{x}_i^{\text{SE}}\}_{i \in \mathcal{I}}).$$

For technical convenience, we assume that aggregator can set prices within a range $[0, M]$. Then, there exists a (price, storage action) pair that constitutes the *Stackelberg Equilibrium* for the single-shot game [65].

A natural question about the Stackelberg Equilibrium is how *efficient* it is. In this work, we measure efficiency via the notion of Pareto optimality.

Definition 1. *A strategy A is Pareto-superior to B if at least one player is strictly better off with A and no one is worst-off. We say a strategy is Pareto-inefficient if there exists a Pareto-superior strategy.*

The following example shows that the equilibrium can be Pareto-inefficient. For simplicity, we consider a single SU under an aggregator.

¹The equilibrium $\boldsymbol{x}_i^{\text{SE}}$ is a unique maximizer because the DET objective is strictly concave.

Example 1. *In this and the rest of the examples in this chapter, we assume that an aggregator interacts with one SU ($n = 1$) in a single-node system and that the time horizon is composed by two time periods ($n_t = 2$). The round-trip efficiency of the SU is $\eta = 0.95$, its charge and discharge limits are 1, its SoC must be in $[0, 1]$ at all times, and its cost function is*

$$c(\mathbf{d}) = \frac{1}{2} \cdot \sum_{t=1}^2 x_t^2.$$

Naturally for a SU, the energy purchased must be equal to the energy sold plus losses. The price at each time period is given by $\lambda_t(q_t) = q_t \forall t = 1, 2$ where q_t is the net load at time t . The net load is $-x_1$ when $t = 1$ and $5 - x_2$ when $t = 2$. We consider a single SU and a single node to reduce notational clutter and suppress the indices i and b .

The single-shot game proceeds as follows. The aggregator sends a price schedule such that $\Delta\tau^{\text{SE}} = \tau_1^{\text{SE}} - \eta \cdot \tau_2^{\text{SE}} = -1.19$. The SU, on the other hand, charges 0.62 units of energy during the first period. Because of the energy neutrality, the SU discharges $0.95 \cdot 0.62$ units of energy during the second period. These strategies constitute the Stackelberg Equilibrium. The Stackelberg profits are $\pi^{\text{a SE}} = 1.48$ and $\pi^{\text{der SE}} = 0.37$, respectively.

However, suppose that the aggregator and SU agree to the following: The SU charges 0.7 units of energy during the first period, and the aggregator sets a price schedule $\Delta\tau = \tau_1 - \eta \cdot \tau_2 = -1.25$. In this case, the both the SU's and the aggregator's profits are higher than the Stackelberg profits (see Fig. 4.2). This agreement is a Pareto-superior to the Stackelberg Equilibrium: both the aggregator and SU are better off as compared to the single-shot game outcome.

Any strategy other than a Stackelberg Equilibrium, however, is necessarily unstable. Thus, cooperation during a single-shot game is not necessarily compatible with rational players. It is also important to note that the overall system cost may suffer from the adversarial relationships between aggregators and DERs.

However, it is unlikely that the aggregator and DERs interact only once. In fact, it is reasonable to assume that aggregators maintain longterm relationships with its DERs.

The DER-aggregator situation is not unlike the long-term relationship between utilities and their rate-payers. In the context of a long-term relationship, aggregators and DERs may be induced to cooperate and adopt equilibria that are at least Pareto-superior to the Stackelberg Equilibrium.

4.4 Longterm cooperation

The previous section shows that the Stackelberg Equilibrium may not be Pareto-efficient and that other solutions are not stable. In practice, this view may be pessimistic and not necessarily reasonable: most aggregators and DERs do not play a single-shot game. Instead, we assume that the aggregator repeatedly interacts with its DERs. Thus, the totality of the single-shot outcomes determines the *longterm* outcome.

In this section, we show that the aggregator and DERs may reach a cooperative equilibrium that is stable and Pareto-superior to the Stackelberg Equilibrium. Furthermore, we establish the conditions that lead to stable cooperative equilibria.

Remark 2. *It is trivial to show that all cooperative equilibria are Pareto-superior to the Stackelberg Equilibrium since a worst-off player could repeatedly play the Stackelberg Equilibrium.*

4.4.1 Repeated game model

For simplicity, we assume that the exact same single-shot game is played repeatedly and define the longterm profit as the discounted sum of the single-shot profits. The longterm profit of the aggregator is denoted by

$$\pi^{a,\infty} = \sum_{k=0}^{\infty} \delta^k \cdot \pi^a(\boldsymbol{\tau}^{(k)}; \mathbf{x}^{(k)})$$

where $\delta \in (0, 1)$ is the discount rate². The symbols $\boldsymbol{\tau}^{(k)}$ and $\boldsymbol{x}^{(k)}$ denote strategy decisions for the k^{th} time the single-shot game is played. Similarly, the longterm profit of DER i is denoted by

$$\pi_i^{\text{der}, \infty} = \sum_{k=0}^{\infty} \delta^k \pi_i^{\text{der}}(\boldsymbol{x}_i^{(k)}; \boldsymbol{\tau}_i^{(k)}).$$

We reduce the dimensionality of the repeated game strategy space by defining only two strategies: cooperation and defection. Under cooperation, each DER plays an agreed action if the aggregator has honored previous commitments. Otherwise, the DER reverts to the Stackelberg Equilibrium. The same is true for the aggregator. It cooperates (i.e., plays the agreed action) if the DER honored previous commitments. Otherwise, the aggregator reverts to the Stackelberg Equilibrium. At every step, each player has the opportunity to defect (i.e., play an action that differs from the previously agreed action).

Cooperation strategies

In the cooperation strategy,

$$\boldsymbol{\tau}_i^{(k)} = \begin{cases} \widehat{\boldsymbol{\tau}}_i & \text{if } \boldsymbol{x}_i^{(m)} = \widehat{\boldsymbol{x}}_i \quad \forall m < k \\ \boldsymbol{\tau}_i^{\text{D}} & \text{otherwise} \end{cases} \quad \forall i \in \mathcal{I}, \quad (4.5)$$

the aggregator sends DER i previously agreed prices $\widehat{\boldsymbol{\tau}}_i$ if the DER has played agreed actions $\widehat{\boldsymbol{x}}_i$ during all previous times. If the DER failed to uphold its commitment during previous games, the aggregator plays the defection strategy $\boldsymbol{\tau}_i^{\text{D}}$ (defined shortly).

Likewise,

$$\boldsymbol{x}_i^{(k)} = \begin{cases} \widehat{\boldsymbol{x}}_i & \text{if } \boldsymbol{\tau}_i^{(m)} = \widehat{\boldsymbol{\tau}}_i \quad \forall m \leq k \\ \boldsymbol{x}_i^{\text{D}} & \text{otherwise} \end{cases} \quad (4.6)$$

²The discount rate reflects the time value of money. It can also encode the probability that the repeated game ends.

describes the cooperation strategy of DER i . The DER plays agreed actions $\widehat{\mathbf{x}}_i$ if the aggregator upheld its commitment to send agreed prices $\widehat{\boldsymbol{\tau}}_i$ during previous times the game was played. Otherwise, the DER i plays the defection strategy \mathbf{x}_i^D .

Defection strategies

We assume that a player defects by maximizing the single-shot profit. This assumption is reasonable since cooperation stops regardless of how the player defects. The DER's defection strategy is given by

$$\mathbf{x}_i^D = \arg \max_{\mathbf{d}_i \in \mathcal{X}_i^{\text{der}}} \pi_i^{\text{der}}(\mathbf{x}_i; \widehat{\boldsymbol{\tau}}_i).$$

. Similarly, the aggregator maximizes the profit derived from DER i by playing

$$\boldsymbol{\tau}_i^D = \arg \max_{0 \leq \tau_i \leq M} \pi^{\text{a}}(\{\boldsymbol{\tau}_i, \widehat{\boldsymbol{\tau}}_{-i}\}; \widehat{\mathbf{x}})$$

where the subscript $-i$ represents all DERs except i .

Defection equilibrium

From the strategies defined by (4.6) and (4.5), if and when the aggregator deviates from agreed prices to DER i , the DER defects from cooperation. Similarly, if and when the DER deviates from agreed actions, the aggregator defects from cooperation.

Both players defect by maximizing their single-shot profits. Thus, they fall into playing a single leader, single follower sequential game while the actions of the rest of the DERs remain fixed. The Stackelberg Equilibrium of this single leader, single follower game is given by

$$\mathbf{x}'_i = \arg \max_{\mathbf{d}_i \in \mathcal{X}_i^{\text{der}}} \pi_i^{\text{der}}(\mathbf{x}_i; \boldsymbol{\tau}_i) \quad \text{and} \quad \boldsymbol{\tau}'_i = \arg \max_{0 \leq \tau_i \leq M} \pi^{\text{a}}(\{\boldsymbol{\tau}_i, \boldsymbol{\tau}_{-i}\}; \{\mathbf{x}'_i, \mathbf{x}_{-i}\}).$$

Denote the defection equilibrium profit of the aggregator as $\pi_i^{\text{a}'}$ and the defection equilibrium profit of the DER as $\pi_i^{\text{der}'}$.

4.4.2 Cooperation in an infinitely repeated game

Here, we characterize the strategies that ensure long-term cooperation by a rational aggregator and DERs. Then, we use the Nash Bargaining Model to conclude that the profit split is Pareto-efficient (i.e., the aggregator and DERs cooperate to maximize their aggregate profit) and to predict the profit allocation among all players.

A set of agreed prices $\widehat{\boldsymbol{\tau}}_i$ and storage actions $\widehat{\boldsymbol{x}}_i$ is a cooperative equilibrium in the infinitely repeated game if they incentivize both the aggregator and DERs to never defect. Given a set of agreed prices and storage actions, all players decide whether (and when) to defect by following the strategy defined by (4.6) and (4.5). A player cooperates if no finite time of defection maximizes its long-term profit.

Lemma 1. *The aggregator cooperates with DER i if its profit is greater than its defection equilibrium profit $\pi_i^{\text{a}'}$. DER i cooperates with the aggregator when its agreed profit is greater than*

$$(1 - \delta) \cdot \pi_i^{\text{der}}(\boldsymbol{x}_i^{\text{D}}; \boldsymbol{\tau}_i) + \delta \cdot \pi_i^{\text{der}'}$$

The set of agreed profits that incentivize both the DER and the aggregator to cooperate define the cooperative equilibria.

The proof of Lemma 1 is included in Appendix E.1. As shown in the proof, there are infinitely many cooperative equilibria. Thus, there are infinitely many profits splitting schemes that foster long-term cooperation by both parties.

Section 4.5 shows how the Nash Bargaining Model predicts the profit allocation among all players and the actions agreed by the DERs. Predicting the profit allocation is interesting for the aggregator and DERs. However, profit allocation does not have clear repercussions in the wholesale market. Predicting the actions of the DERs, however, has strong repercussions on the electricity market since it affects the aggregator bidding behavior.

Example 2. *This continues the previous example. Let the discount rate be $\delta = 0.98$ and let*

$$\alpha_a(\widehat{\Delta\tau}, \widehat{x}_1) = \pi^a(\widehat{\boldsymbol{\tau}}; \widehat{\boldsymbol{x}}) - \pi^{a'}.$$

From Lemma 1, the aggregator cooperates when $\alpha_a(\widehat{\Delta\tau}, \widehat{x}_1) \geq 0$. Similarly, let

$$\alpha_{\text{der}}(\widehat{x}_1, \widehat{\Delta\tau}) = \pi^{\text{der}}(\widehat{\boldsymbol{x}}; \widehat{\boldsymbol{\tau}}) - (1 - \delta) \cdot \pi_i^{\text{der}}(\boldsymbol{x}_i^{\text{D}}; \boldsymbol{\tau}_i) - \delta \cdot \pi^{\text{der}'}$$

Also from Lemma 1, the SU cooperates when $\alpha_{\text{der}}(\widehat{x}_1, \widehat{\Delta\tau}) \geq 0$.

Let the sets

$$\mathcal{A}^{\text{der}} = \{(\widehat{x}_1, \widehat{\Delta\tau}) | \alpha_{\text{der}}(\widehat{x}_1, \widehat{\Delta\tau}) \geq 0\}$$

and

$$\mathcal{A}^a = \{(\widehat{x}_1, \widehat{\Delta\tau}) | \alpha_a(\widehat{\Delta\tau}, \widehat{x}_1) \geq 0\}$$

denote the SU cooperation region and the aggregator cooperation region, respectively. The set \mathcal{A}^s represents all the charge/price pairs that incentivize the DER to never fall back to the Stackelberg Equilibrium and uphold its cooperation agreement with the aggregator. The same is true for the set \mathcal{A}^a with respect to the aggregator. The region where both players cooperate is denoted by $\mathcal{A} = \mathcal{A}^{\text{der}} \cap \mathcal{A}^a$. The sets \mathcal{A}^{der} , \mathcal{A}^a , and \mathcal{A} are illustrated in Fig. 4.3.

4.5 Profit split via Nash Bargaining

Lemma 1 shows that there are infinitely many strategies that ensure long-term cooperation (i.e., there are many cooperative equilibria). In practice, one of these equilibria is chosen. Knowing the equilibrium strategy is crucial to predicting the aggregator's market participation strategy. This section presents the Nash Bargaining Model [144] that predicts the long-term equilibrium.

Let $\mathcal{B}_i = \mathcal{X}_i^{\text{der}} \times \mathcal{X}_i^a$ denote the set of possible outcomes of a bargaining process between the aggregator and DER i . Denote the outcome as $(\widehat{\boldsymbol{x}}_i^*, \widehat{\boldsymbol{\tau}}_i^*) = \xi(\mathcal{B}_i)$ where function $\xi(\cdot)$

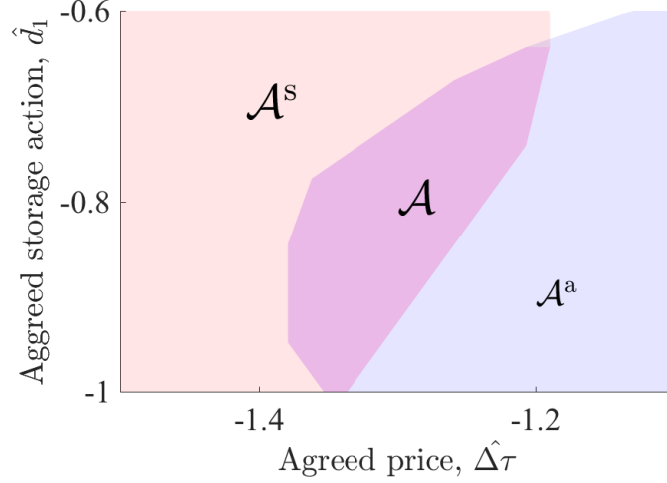


Figure 4.3: Cooperation regions. The x-axis shows the price set by the aggregator and the y-axis shows the charge amount. If the agreement is in the region \mathcal{A}^s , the SU never defects. If the agreement is in \mathcal{A}^a , the aggregator never defects. If the actions are in $\mathcal{A} = \mathcal{A}^s \cap \mathcal{A}^a$, both players cooperate indefinitely. **spelling mistake in plot. Fix the A regions too.**

maps a set of possible outcomes to the Nash Bargaining Solution [144]. Here, $\mathcal{X}_i^a = \{\tau_i | 0 \leq \tau_i \leq M\}$.

The Nash Bargaining Solution is a single point in a set of possible outcomes that satisfies the following axioms:

- *Pareto efficiency*: If $\mathbf{a}, \mathbf{b} \in \mathcal{B}_i$, $\pi^a(\mathbf{a}) > \pi^a(\mathbf{b})$, and $\pi_i^{\text{der}}(\mathbf{a}) > \pi_i^{\text{der}}(\mathbf{b})$ then $\mathbf{b} \neq \xi(\mathcal{B}_i)$.
- *Independence of irrelevant alternatives*: If $\tilde{\mathcal{B}}_i \subseteq \mathcal{B}_i$ and $\xi(\mathcal{B}_i) \in \tilde{\mathcal{B}}_i$, then $\xi(\tilde{\mathcal{B}}_i) = \xi(\mathcal{B}_i)$.

Lemma 2. *Assume that the aggregator engages in bilateral negotiations with each DER and that all players are risk neutral³. The aggregator and DERs split the maximum aggregate profit given by:*

$$\pi(\mathbf{x}^*) = \max_{\mathbf{x} \in \mathcal{X}^{\text{der}}} \left\{ \pi^a(\boldsymbol{\tau}; \mathbf{x}) + \sum_{i \in \mathcal{I}} \pi_i^{\text{der}}(\mathbf{x}_i; \tau_i) \right\}. \quad (4.7)$$

³As shown by [34], if one of the players is more risk averse than the other, its share of the profit decreases. Conversely, if a player is more risk-loving than the other, its share of the profit increases.

where $\mathcal{X}^{\text{der}} = \mathcal{X}_1^{\text{der}} \times \dots \times \mathcal{X}_n^{\text{der}}$. The Nash Bargaining Solution is given by:

$$\forall i : (\hat{\mathbf{x}}_i^*, \hat{\boldsymbol{\tau}}_i^*) = \arg \max_{\substack{0 \leq \boldsymbol{\tau}_i \leq M \\ \mathbf{x}_i = \mathbf{x}_i^* \\ (\boldsymbol{\tau}_i, \mathbf{x}_i) \in \mathcal{A}_i}} \left(\pi_i^{\text{der}} - \pi_i^{\text{der}'} \right) \left(\pi^{\text{a}} - \pi_i^{\text{a}'} \right) \quad (4.8)$$

where $\pi^{\text{a}} \equiv \pi^{\text{a}}(\{\boldsymbol{\tau}_i, \hat{\boldsymbol{\tau}}_{i-}^*\}; \{\mathbf{x}_i, \hat{\mathbf{x}}_{i-}^*\})$ and $\pi_i^{\text{der}} \equiv \pi_i^{\text{der}}(\mathbf{x}_i; \boldsymbol{\tau}_i)$. The set of agreed prices and storage actions that deliver profits in the cooperative equilibria is denoted by \mathcal{A}_i .

The proof of Lemma 2 is available in Appendix E.2. The result in Lemma 2 is important because for a few reasons. It predicts that the aggregator bids according to the Nash Bargaining Solution. This prediction allows us to replace the complex aggregator-DER model with an entity that bids \mathbf{x}^* . Notice from (4.7), that the DER actions from the bargaining solution \mathbf{x}^* deliver the maximum possible aggregate profit. Thus, \mathbf{x}^* is how the aggregator would operate the DERs if it had their full control. Thus, the Nash Bargaining Solution could be a theoretical justification of the existence of direct load control programs.

Example 3. This continues the previous example. Suppose that the aggregator engages in negotiations with the SU. By the Pareto-efficiency axiom, the aggregator and SU agree to $\hat{x}_1^* = x_1^* = -0.83$ which yield the maximum aggregate profit. Also by Pareto-efficiency, the agreed price schedule $\widehat{\Delta\tau}^*$ fosters long-term cooperation. From the previous example, long-term cooperation is possible when

$$\alpha_{\text{a}}(\widehat{\Delta\tau}, -0.83) \geq 0 \text{ and } \alpha_{\text{s}}(-0.83, \widehat{\Delta\tau}) \geq 0$$

or equivalently, when $-1.23 \leq \widehat{\Delta\tau} \leq -1.37$.

From reference [34], the bargaining outcome is the solution to the quadratic optimization problem

$$\max_{-1.23 \leq \widehat{\Delta\tau} \leq -1.37} \left(\pi^{\text{der}}(-0.83; \widehat{\Delta\tau}) - \pi^{\text{der}'} \right) \left(\pi^{\text{a}}(\widehat{\Delta\tau}; -0.83) - \pi^{\text{a}'} \right)$$

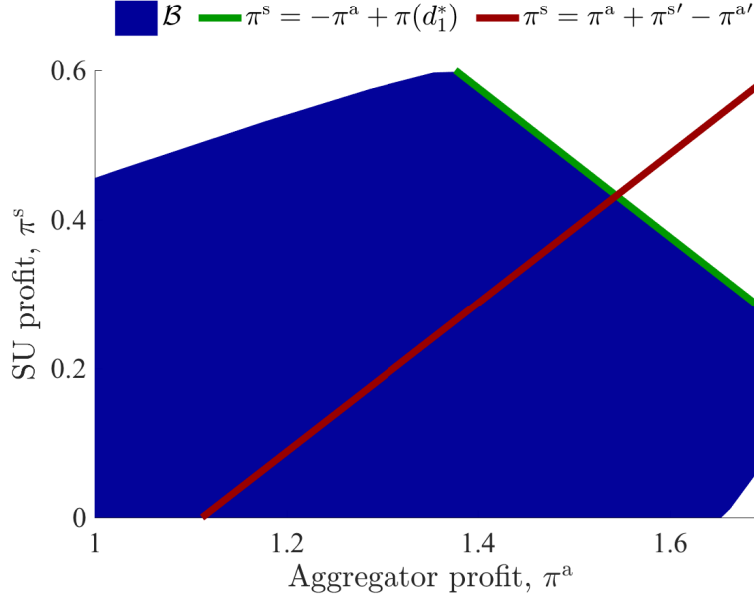


Figure 4.4: The symbol \mathcal{B} denotes the set of possible bargaining outcomes. Each point inside this area represents a realizable profit split between the aggregator and SU. The green line represents all possible Pareto-optimal profit allocations. The portion of \mathcal{B} that overlaps the green line represents the Pareto front. The red line is the line of symmetry. The intersection of these two lines is the bargaining solution.

which is $\widehat{\Delta\tau}^* = -1.31$.

Since $(\widehat{x}_1^*, \widehat{\Delta\tau}^*)$ lies on the interior of \mathcal{A} , the solution to the Nash Bargaining Problem is the solution to the system of equations $\pi^{\text{der}} = -\pi^a + \pi(x_1^*)$ and $\pi^{\text{der}} = \pi^a + \pi^{\text{der}'} - \pi^{a'}$ as shown in [144]. This concludes the example.

For larger aggregator defection equilibrium profits $\pi^{a'}$, the bargaining solution delivers a larger aggregator profit $\widehat{\pi}^{a*}$. Since $\pi^{a'}$ is the “outside option” profit of the aggregator (i.e., profit of the aggregator in case the negotiations fall apart), a larger outside option profit can be interpreted as the aggregator having greater bargaining power or “leverage.” The same can be said for the relationship between the DER profit $\widehat{\pi}^{\text{der}*}$ and the DER defection equilibrium profit $\pi^{\text{der}'}$.

4.6 *Summary*

In this chapter, we study the interactions between a distributed energy resources (DERs) aggregator, its DERs, and the wholesale electricity market. First, we model the aggregator-
DER interactions and show that while the short-term relationship can be Pareto-inefficient, long-term cooperative equilibria exist. Then, we use Nash Bargaining Theory to predict the cooperative equilibrium. The equilibrium, determined by the Nash Bargaining Solution, is Pareto-optimal. The Pareto-optimality of the equilibrium, allows us to simplify the relationship between the aggregator and its DERs by replacing it with an aggregate profit maximization problem. Moreover, our results serve as a theoretical justification for instances (e.g., direct-load control) in which aggregators cooperate with their constituents and vice versa.

Chapter 5

COORDINATION OF BUILDINGS AND ELECTRIC VEHICLES

5.1 Introduction

Integrating renewable energy sources (RESs) such as wind and solar to the power grid is challenging because of their variability and uncertainty [25]. Researchers and practitioners propose demand-side resources (DSRs) as means to accommodate the variability and uncertainty of renewable generation [29, 117, 174, 206, 219]. Two kinds of DSRs are of particular importance:

1. **Buildings** are responsible for over 70% of the total electricity consumption in the United States [9]. As building controls, sensors, and algorithms become more sophisticated; buildings are increasingly capable of providing services to the grid. For instance, the work in [97] studies the use of building-level demand response for frequency regulation in a microgrid. In [87] the authors propose a framework where a retailer controls thermal loads to minimize imbalance costs while considering the cost of user's discomfort. Reference [159] proposes an integrated model of the supply and demand sides of the electric grid to determine appropriate demand response actions.
2. The global **electric vehicle** (EV) stock is projected to increase from 180,000 units in 2012 to more than 20 million in 2020 [11]. The increasing number of EVs has two significant effects on the power grid. On the one hand, higher energy demand by EVs stresses the power system. On the other hand, EVs can help to integrate RESs by providing the necessary services to the grid [142, 156, 176, 205].

5.1.1 *Problem and proposed solution*

Buildings and EV charging stations often share infrastructure (e.g., a transformer) or may be coupled financially (e.g., by a tariff structure that penalizes aggregate peak load). Thus, common constraints couple the building and EV operation. In such cases, it is more useful to think of the building(s) and EVs as components of a larger system rather than two separate entities. For instance, individually scheduling load consumption may result in transformer overloads or an unnecessarily high peak load. Often, however, the building and EVs cannot be integrated into a single system due to software compatibility, privacy, cybersecurity, or other practical reasons.

We adopt the Dantzig-Wolfe Decomposition Algorithm (DWDA) to solve the building-EV demand scheduling problem in a decentralized fashion. The DWDA eliminates the need for sharing private data among the two entities. Our algorithm requires each entity to share only information essential to the coupling constraints.

5.1.2 *Previous works*

References [116, 147, 185, 225] study the joint optimization/scheduling of building loads and EVs. The authors of [185] study monetary incentives when used to induce desired behaviors of house appliances and EVs. The work in [147] studies the scheduling of residential loads and EVs considering the cost of energy and discomfort. In [225], the authors propose a model predictive control strategy for a home energy management system (EMS) that includes heating, ventilation, and air conditioning (HVAC) systems, EVs, and deferrable loads. Finally, [116] studies the use of HVAC systems and EVs in commercial buildings to provide ancillary services. The previously mentioned works assume central scheduling of the building appliances and EVs.

In practice, however, centrally scheduling building loads and EVs may not be possible. For instance, the building manager and EV aggregator may be unable to share the internal data (e.g., EV trip information, battery state-of-charge (SOC), building occupancy,

temperature preferences, among others) because of privacy or cybersecurity concerns [102]. Furthermore, even if internal data were allowed to be shared, centrally storing or maintaining it may be difficult [39]. This chapter proposes a privacy-friendly and distributed approach to solve the building-EV demand scheduling problem.

Distributed optimization is studied in both mathematics, e.g., [66], and power engineering, e.g., [23, 55, 188, 222]. In [66], the authors propose a decomposition principle for linear programs (LPs), now known as the Dantzig-Wolfe Decomposition. Dantzig's technique breaks down a LP into subproblems and reaches the global optimum in a decentralized fashion via column generation. The authors of [188] optimize interconnected subsystems using the DWDA. In [23], the authors use the DWDA to delegate the global task of energy management in a microgrid to local controllers. Lastly, the authors of [222] schedule appliances and batteries using Bender's Decomposition and Lagrangian relaxation.

5.1.3 Contributions

The main contributions of this chapter are:

- A decentralized and scalable approach for optimal scheduling of building loads and EV charging/discharging using a mixed-integer linear program (MILP) adaptation of the DWDA.
- Identification and modeling of three instances in which constraints couple the building and EV operation. The coupling constraints in each of the three instances are the product of:
 1. A shared demand limit.
 2. A demand charge to the aggregate building and EV peak demand.
 3. An itemized billing scheme¹.
- A demonstration of the effectiveness and scalability of the approach.
- An assessment of the impacts of the coupling constraints on the building operation,

¹Under an itemized billing scheme, the price of energy bought from the grid is different than the price of energy sold to the grid

EV operation, and the power grid.

5.2 Organization of this chapter

This chapter is organized as follows. Sections 5.3 and 5.4 describe the building model and EV aggregator model, respectively. Section 5.5 describes the building-EV demand scheduling problem and offers a high-level overview of the DWDA. Section 5.6 discusses three case studies and the scalability of the proposed method. Section 5.7 concludes and summarizes this chapter.

5.3 Building model

Similar to [185, 198], we consider a commercial building whose EMS minimizes electricity cost by operating various loads and actuators. Additionally, the EMS must enforce physical and comfort constraints. The model assumes that perfect parameter forecasts (e.g., for ambient temperature, electricity prices, zone occupancy, hot water demand) and perfect variable measurements (e.g., temperatures, light levels). While these parameters are stochastic, managing uncertainty is beyond the scope of this chapter. Refer to section 5.5 for further discussion of uncertainty.

5.3.1 Objective function

The EMS's objective is to minimize total cost of electricity over an optimization horizon \mathcal{T} . We express the objective as

$$\min \Delta t \cdot \sum_{t \in \mathcal{T}} \tau_t \cdot d_t^b$$

where τ_t is the electricity price. The total electricity demand of the building is given by

$$d_t^b = p_t^{\text{fix}} + p_t^{\text{hc}} + p_t^{\text{wh}} + \sum_{z \in \mathcal{Z}} p_{t,z}^{\text{light}} + p_t^{\text{dl}},$$

where p_t^{fix} represents the fixed load of the building; p_t^{hc} and p_t^{wh} represent the heating/cooling load and water heater load, respectively; $p_{t,z}^{\text{light}}$ represents the artificial lighting load of each zone; and p_t^{dl} is the total non-interruptible discrete load. The length of a time period t is Δt . The objective function of the EMS is subject to constraints (5.2) - (5.13).

5.3.2 Temperature dynamics

We model the temperature dynamics of a hot water tank via resistance-capacitance (RC) circuit analogy [134]

$$c \cdot \dot{\theta}^{\text{wh}} = q^{\text{wh}} - q^{\text{hwd}} + \frac{\theta^{\text{amb}} - \theta^{\text{wh}}}{r}, \quad (5.1)$$

where c is the thermal capacitance of the hot water tank; the symbols θ^{wh} and θ^{amb} represent the temperature of the water inside the tank and ambient temperature, respectively; the heat input from the water heater and the demand for hot water by the building occupants are denoted by q^{wh} and q^{hwd} , respectively; finally, the parameter r represents the thermal resistance of the hot water tank. Equation (5.1) is represented in discrete time as

$$\theta_{t+1}^{\text{wh}} = a \cdot \theta_t^{\text{wh}} + b \cdot q_t^{\text{wh}} + \epsilon_t^{\text{wh}} \quad \forall t \in \mathcal{T} \quad (5.2)$$

where $a = 1 - \frac{\Delta t}{r \cdot c}$, $b = \frac{\Delta t}{c}$, and $\epsilon_t^{\text{wh}} = \Delta t \cdot \left(\frac{\theta_t^{\text{amb}}}{r \cdot c} - \frac{q_t^{\text{hwd}}}{c} \right)$.

Similarly to (5.2), the temperature dynamics of the building zones are expressed as

$$\boldsymbol{\theta}_{t+1} = \mathbf{A}_t \boldsymbol{\theta}_t + \mathbf{B} \mathbf{q}_t^{\text{heat}} - \mathbf{C} \mathbf{q}_t^{\text{cool}} + \mathbf{D} \mathbf{p}_t^{\text{light}} + \mathbf{E}_t \mathbf{u}_t^{\text{b}} + \boldsymbol{\epsilon}_t \quad \forall t \in \mathcal{T} \quad (5.3)$$

where $\boldsymbol{\theta}_t$ is a vector of zone temperatures; the vector $\mathbf{q}_t^{\text{heat}}$ ($\mathbf{q}_t^{\text{cool}}$) denotes the heat input (heat removal) by the heating (cooling) system to (from) each zone; the vector $\mathbf{p}_t^{\text{light}}$ represents the artificial lighting power consumption; \mathbf{u}_t^{b} represents the position of the blinds in each zone; and vector $\boldsymbol{\epsilon}_t$ represents the disturbances to each zone's temperature and is a function of a number of parameters that include occupancy, exterior temperature, wall temperatures,

and electric equipment heat emissions. The matrices \mathbf{A}_t , \mathbf{B} , \mathbf{C} , \mathbf{D} , and \mathbf{E}_t in describe the thermal dynamics model of the building zones. The matrix \mathbf{A}_t relates the temperature of each zone to the other zones and is a function of zone thermal capacitance, air flows, and thermal insulation between zones. Matrices \mathbf{B} and \mathbf{C} are analogous to the term b from equation (5.2) and contain thermal capacitance and linear approximations of convective and radiative heat transfer coefficients. Matrix \mathbf{D} relates the artificial lighting power consumption in each zone to its heat input to the zone. The matrix \mathbf{E}_t relates the position of blinds in each zone to heat gains in the respective zones. It also contains data of solar irradiance as well as convective and radiative heat transfer coefficients. We refer to [159] for further details.

We ensure that all the energy used for heating or cooling is bought during the optimization horizon by enforcing

$$\boldsymbol{\theta}_0 = \boldsymbol{\theta}_{|\mathcal{T}|} \text{ and } \theta_0^{\text{wh}} = \theta_{|\mathcal{T}|}^{\text{wh}}. \quad (5.4)$$

Constraint (5.4) requires the temperatures of the hot water and each zone at the end of the optimization horizon to be the same as the initial temperatures.

5.3.3 Technical constraints

The power limits of the heating and cooling systems are described by

$$0 \leq \frac{1}{COP_t^j} \cdot \sum_{z \in \mathcal{Z}} q_{t,z}^j \leq \bar{p}^j \quad \forall t \in \mathcal{T}, j \in \{\text{cool}, \text{heat}\} \quad (5.5)$$

where COP_t^{heat} and COP_t^{cool} are the coefficients of performance (COP) of the heating and cooling systems, respectively. The power limit of the heating and cooling systems are \bar{p}^{heat} and \bar{p}^{cool} , respectively.

The artificial lighting power limits are enforced by

$$0 \leq p_{t,z}^{\text{light}} \leq \bar{p}_z^{\text{light}} \quad \forall t \in \mathcal{T}, z \in \mathcal{Z}, \quad (5.6)$$

where artificial lighting capacity each zone is denoted by \bar{p}_z^{light} .

The position of the blinds in each zone $u_{t,z}^b \in [0, 1]$ are expressed as the proportion of natural light that is let in (e.g., 0 if the blinds are completely shut and 1 if the blinds are open). Thus, the positions of the blinds in each zone are constrained between 0 and 1.

5.3.4 Comfort constraints

Arguably, the most crucial role of a building manager is to maintain a comfortable environment for the occupants. In our model, the comfort indices that must be within limits are air quality, ambient temperature, hot water temperature, and light levels [45, 227].

We assume that the operation of the ventilation system maintains acceptable air quality levels. We take the operation rules of the ventilation system from EnergyPlus simulations [70] and model the rest of the indices as decision variables.

The temperature limits in each zone are expressed by

$$\underline{\theta}_z \leq \theta_{t,z} \leq \bar{\theta}_z \quad \forall t \in \mathcal{T}_z^{\text{occ}}, z \in \mathcal{Z} \quad (5.7)$$

and enforce minimum and maximum temperatures for each zone when occupants are present. The symbols $\underline{\theta}_z$ and $\bar{\theta}_z$ represent minimum and maximum zone temperature limits. The set $\mathcal{T}_z^{\text{occ}}$ is the subset of elements in \mathcal{T} in which zone z has at least one occupant. Similarly, the constraints

$$\underline{\theta}^{\text{wh}} \leq \theta_t^{\text{wh}} \leq \bar{\theta}^{\text{wh}} \quad \forall t \in \mathcal{T}^{\text{occ}} \quad (5.8)$$

enforce minimum and maximum temperatures of the water in the tank during the subset of \mathcal{T} in which the building has at least one occupant \mathcal{T}^{occ} . The parameters $\underline{\theta}^{\text{wh}}$ and $\bar{\theta}^{\text{wh}}$ represent minimum and maximum water temperature limits, respectively.

The constraints

$$\underline{l} \leq \gamma_{t,z} \cdot u_{t,z}^b + \beta_z \cdot p_{t,z}^{\text{light}} \leq \bar{l} \quad \forall t \in \mathcal{T}_z^{\text{occ}}, z \in \mathcal{Z} \quad (5.9)$$

enforce minimum and maximum light levels in each zone when occupants are present. The minimum and maximum light levels in each zone are represented by \underline{l} and \bar{l} , respectively. The parameter $\gamma_{t,z}$, in lumens, is the natural light that is let in when the blinds are the fully open. The parameter β_z relates the electric power used by artificial lights in each zone to illumination.

The position of the blinds in each zone have a lower bound expressed by

$$\underline{u}_z^b \leq u_{t,z}^b \quad \forall t \in \mathcal{T}_z^{\text{occ}}, z \in \mathcal{Z}. \quad (5.10)$$

Constraints (5.10) reflect the fact that occupants might not be comfortable in a room with the blinds completely closed [37]. The blind position lower limit is denoted by \underline{u}_z^b .

Finally, occupants might feel discomfort if the window blinds and artificial lights continuously change positions and light levels. We reflect the preference for steady source of light via the constraint

$$-\overline{\Delta u}^b \leq u_{t+1,z}^b - u_{t,z}^b \leq \overline{\Delta u}^b \quad \forall t \in \mathcal{T}_z^{\text{occ}}, z \in \mathcal{Z} \quad (5.11)$$

$$-\overline{\Delta p}^{\text{light}} \leq p_{t+1,z}^{\text{light}} - p_{t,z}^{\text{light}} \leq \overline{\Delta p}^{\text{light}} \quad \forall t \in \mathcal{T}_z^{\text{occ}}, z \in \mathcal{Z} \quad (5.12)$$

where $\overline{\Delta u}^b$ and $\overline{\Delta p}^{\text{light}}$ are the maximum rates of change of blind position and artificial light levels, respectively.

5.3.5 Shiftable, non-interruptible discrete power loads

Shiftable, non-interruptible discrete power loads (e.g., dishwashers or computer batch processes) are modeled as in [185]. The constraints

$$\sum_{t \in \mathcal{T}_i} \delta_{t,i} = CT_i \quad \forall i \in \mathcal{I} \quad (5.13)$$

$$\delta_{t,i} \in \{0, 1\} \quad \forall t \in \mathcal{T}, i \in \mathcal{I} \quad (5.14)$$

ensure that discrete load i completes its duty cycle CT_i . The binary decision variable $\delta_{t,i}$ is 1 if the discrete power load i is on and 0 if it is off. The set of time periods discrete power load i is allowed to run is denoted by \mathcal{T}_i . The set of discrete loads is denoted by \mathcal{I} .

Constraint

$$\sum_{t'=t+1}^{t+CT_i} \delta_{t',i} \geq CT_i \cdot (\delta_{t+1,i} - \delta_{t,i}) \quad \forall t \in \mathcal{T}, i \in \mathcal{I} \quad (5.15)$$

ensures that the operation of discrete load i is not interrupted before its duty cycle is complete. The total power from the discrete loads at time t is defined by

$$p_t^{\text{dl}} = \sum_{i \in \mathcal{I}} P_i^r \cdot \delta_{t,i}$$

where P_i^r is the power rating of discrete power load i .

5.4 Electric vehicles

In this work, the EVs hand over control of the charge/discharge schedule to an aggregator. The primary goal of the aggregator is to satisfy each EV's transportation energy requirements. Additionally, the aggregator can discharge energy from the EV battery if doing so is viable.

We assume that EV arrival and departure times, initial SOC, and transportation energy

requirement are known with certainty. While these parameters are stochastic, managing uncertainty is beyond the scope of this work. Refer to Section 5.6 for further discussion on uncertainty.

5.4.1 Objective function

The objective of the EV aggregator is to

$$\text{minimize } \left\{ \Delta t \cdot \sum_{t \in \mathcal{T}} \tau_t \cdot d_t^{\text{ev}} + c^{\text{cyc}} \right\}$$

where $d_t^{\text{ev}} = \sum_{v \in \mathcal{V}} \{ p_{t,v}^{\text{chg}} - \eta_v^{\text{dsg}} \cdot p_{t,v}^{\text{dsg}} \}$ represents the electricity demand of the EVs. The constant η_v^{dsg} denotes the EV's discharging efficiency. The variables $p_{t,v}^{\text{chg}}$ and $p_{t,v}^{\text{dsg}}$ are the charging and discharging rates, respectively. The cost of cycling (degradation) for all EVs during the optimization horizon is denoted by c^{cyc} . The objective function of the EV aggregator is subject to Constraints (5.16) - (5.20).

5.4.2 Cycling costs

In this work, we approximate the cost of cycling using the linear function

$$c^{\text{cyc}} = \Delta t \cdot \phi \cdot C_v^{\text{B}} \cdot \sum_{t \in \mathcal{T}} \sum_{v \in \mathcal{V}} p_{t,v}^{\text{dsg}}$$

as proposed in [154]. The parameters ϕ and C^{B} are the slope of the linear approximation of the battery life as a function of the cycles² and the battery cost per unit energy, respectively.

²The parameter ϕ can be estimated using battery manufacture data sheets [154].

5.4.3 State-of-charge dynamics

The SOC of an EV battery is a measure of the amount of energy stored in a battery and is a function of the SOC at the previous time step and the energy inflows and outflows:

$$soc_{t+1,v} = soc_{t,v} + \Delta t \cdot \left(\eta_v^{\text{chg}} \cdot p_{t,v}^{\text{chg}} - p_{t,v}^{\text{dsg}} \right) - \frac{\xi_v \cdot S_{t,v}}{\sum_{t' \in \mathcal{T}} S_{t',v}} \quad \forall t \in \mathcal{T} \quad v \in \mathcal{V}. \quad (5.16)$$

The charging efficiency, the power obtained from the grid, and the power injected to the grid are denoted by η_v^{chg} , $p_{t,v}^{\text{chg}}$, and $p_{t,v}^{\text{dsg}}$, respectively. The total energy required for transportation is denoted by ξ_v while the motion schedule by $S_{t,v}$. The parameter $S_{t,v} = 1$ if the EV is in motion in period t , otherwise $S_{t,v} = 0$.

The constraints

$$soc_{|\mathcal{T}|,v} = soc_{0,v} \quad \forall v \in \mathcal{V} \quad (5.17)$$

ensure that the total energy available in the battery at the end of the time horizon is the same as it is at the beginning of the horizon. The constraints in (5.17) ensure that energy used is during the optimization horizon.

5.4.4 Power and energy limits

The charging and discharging behavior of the EVs needs to be within the maximum power \bar{p}_v , as denoted by the constraints

$$0 \leq p_{t,v}^{\text{chg}} \leq \alpha_{t,v} \cdot \bar{p}_v \quad \forall t \in \mathcal{T}, \quad v \in \mathcal{V} \quad (5.18)$$

$$0 \leq p_{t,v}^{\text{dsg}} \leq \alpha_{t,v} \cdot \bar{p}_v \quad \forall t \in \mathcal{T}, \quad v \in \mathcal{V}. \quad (5.19)$$

In addition, an EV can only charge or discharge if it is connected to a charging point. The availability is determined by the parameter $\alpha_{t,v}$ ($\alpha_{t,v} = 1$ if connected, $\alpha_{t,v} = 0$ otherwise). We assume that an EV is available as soon as it arrives in the building and before it leaves.

$$\begin{array}{c}
\min f(d_t^b, d_t^{ev}) \\
\boxed{\begin{array}{l} \mathbf{A}_b \mathbf{x}_b = \mathbf{b}_b \\ \mathbf{x}_b \geq \mathbf{0} \end{array}} \\
\boxed{\begin{array}{l} \mathbf{A}_{ev} \mathbf{x}_{ev} = \mathbf{b}_{ev} \\ \mathbf{x}_{ev} \geq \mathbf{0} \end{array}} \\
\boxed{g(d_t^b, d_t^{ev}) = 0}
\end{array}$$

Figure 5.1: Visual representation of the building-EV demand scheduling problem structure. The function $f(d_t^b, d_t^{ev})$ is the objective. Equations $\mathbf{A}_b \mathbf{x}_b = \mathbf{b}_b$ and $\mathbf{x}_b \geq \mathbf{0}$ represent the building constraints while $\mathbf{A}_{ev} \mathbf{x}_{ev} = \mathbf{b}_{ev}$ and $\mathbf{x}_{ev} \geq \mathbf{0}$ represent the EV constraints. The function $g(d_t^b, d_t^{ev}) = 0$ represents the coupling constraints.

Finally, the SOC must be within the minimum and maximum limits as expressed by

$$\underline{soc}_v \leq soc_{t,v} \leq \overline{soc}_v \quad \forall t \in \mathcal{T}, v \in \mathcal{V}. \quad (5.20)$$

5.5 The building-EV demand scheduling problem

There might be cases where the building EMS and EV problems are two parts of a larger scheduling problem, i.e., the building-EV demand scheduling problem. For instance, the building and EVs may be connected to the grid through the same transformer or substation that may impose power limits; or they may want to coordinate to reduce peak consumption. Fig. 5.1 shows a representation of the building-EV demand scheduling problem.

Solving the building-EV demand scheduling problem as a single problem, however, may not be possible. We propose a MILP adaptation of the DWDA to solve the problem without requiring each entity to disclose private information and with the software/algorithms of choice.

5.5.1 The Dantzig-Wolfe Decomposition Algorithm

The DWDA is a method to solve LPs in a decentralized manner at the cost of iterations [66]. The building manager and the EV aggregator handle their respective subproblems while the master problem solver handles the coupling constraints. Additionally, the master problem broadcasts the dual variables associated with the coupling constraints. The building EMS and EV aggregator use the dual variables to penalize the variables in the coupling constraints. A technical description of the algorithm is given in Appendix A. For further information refer to [55] and for implementation of the algorithm refer to [113].

While many decomposition algorithms (e.g., Bender’s decomposition, Lagrangian methods) are available, we choose to base our method on the DWDA for the following reasons

- The DWDA is well-suited for problems coupled by constraints. Other methods such as Bender’s decomposition are well-suited for problems linked by variables.
- The DWDA is a well-known technique that has been improved and enhanced over the years. For instance, some of the available enhancements and improvements are:
 - Computational enhancements proposed by references [80,98,101] improve the computational performance of the DWDA for some classes of LPs.
 - Privacy-related enhancements proposed by references [77,102] prevent sensitive information from being revealed.
 - A generalization of the DWDA to include MILPs was proposed by [208].
- Unlike the Lagrangian relaxation method, the DWDA provides a feasible primal solution at each iteration [106].

5.5.2 Information sharing

A major advantage of the DWDA is that it does not require sharing of private information among parties. The master problem solver only requires *aggregate data essential to the coupling constraints and integrality of the solution*. For instance, if the coupling constraint is a limit on aggregate demand, the master problem only needs the proposed EV and building

demands. Additionally, the master problem needs information on the integer variables to find an integer-feasible solution. Conveniently, sharing demand of individual loads or EVs is not needed. The master problem solver broadcasts values of the coupling and convexity constraints to the building EMS and the EV aggregator.

5.5.3 *Privacy of sensitive information*

The aggregate data shared with the master problem could still carry sensitive information. For instance, aggregate consumption of the EVs may encode information such as arrival and departure times and energy needs of EVs. However, communication and encoding protocols can prevent others from learning about internal (private) constraints and data. For instance, Hong et al. show that using a simple communication protocol, the privacy of internal data (i.e., constraints and cost functions of the subproblems) *can not be learned by solving the problem using the DWDA* [102]. The communication protocol in [102] does not add complexity because it uses simple linear transformations as encoding tools.

5.5.4 *Optimality and convergence properties*

The DWDA for LPs is guaranteed to converge in a finite number of iterations [66]. However, MILPs are hard to solve [33] in general and finding the optimal solution in polynomial time is not guaranteed. For both LPs and MILPs, a trade-off exists between optimality and computational effort [208].

5.6 *Case studies*

We test the proposed method with three case studies. All cases consider a typical small office building and 10 EVs under an aggregator. In the first case, the coupling constraint is an aggregate demand limit. In the second one, the coupling constraints are the result of a peak demand charge. In the third case, the coupling constraint arise from an itemized billing tariff where the buying energy price is different to the selling energy price.

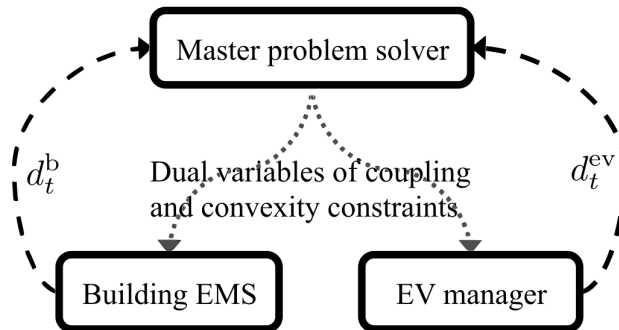


Figure 5.2: Visual representation of the DWDA implementation information flow.

Summary of data

We base the building model on data (e.g., building zone areas, wall areas, U-values, window areas, hot water tank capacity, COP, ventilation schedule, exterior lights schedules, airflow schedules, electrical equipment, weather parameters) from the U.S. Department of Energy Commercial Building Models small office building [70]. We simulate one typical cooling weekday in Seattle, WA, USA.

The EV aggregator model is based on [185]. The arrival, departure, and energy needed by the EVs for transportation purposes were generated using methodology from [199].

Sources of uncertainty

The demand scheduling problem contains stochastic parameters. In particular, the potential sources of uncertainty are

- **Building occupancy:** arrival, departure, and presence of occupants. Implicitly, this translates uncertain availability of EVs and occupant thermal disturbances.
- **Weather parameters:** ambient temperatures and solar irradiation.
- **EV transportation parameters:** initial SOC and transportation energy requirements.
- **Measurements:** we assume that the SOC of the EVs, water temperatures, light levels,

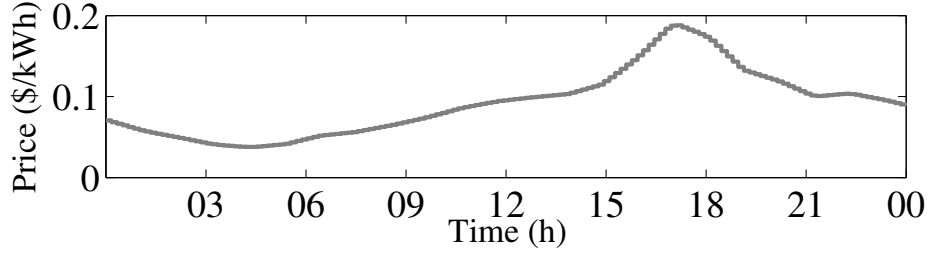


Figure 5.3: Southern California Edison hourly RTP schedule.

among other variables and parameters, can be measured accurately.

We assume that good predictions of uncertain parameters are available. As shown in [92, 221], good predictions allows a deterministic formulation to yield solutions that perform well against solutions obtained using stochastic approaches. Developing such predictions is beyond the scope of our work. However, more complex uncertainty models can be incorporated on top our framework as long as the subproblems remain tractable. We refer the interested reader to [132, 134, 152, 198, 211, 225] for tractable methods for uncertainty.

5.6.1 Coupling constraints: demand limits

In this case study, demand limits couple the building and EV aggregator problems. The limits could be imposed by transformer, circuit breaker, feeder or safety limits. Problem (5.21) describes the optimization problem where the building manager and EV aggregator minimize energy and cycling costs. We write the problem as

$$\min \left\{ \Delta t \cdot \sum_{t \in \mathcal{T}} \tau_t \cdot (d_t^b + d_t^{\text{ev}}) + c^{\text{cyc}} \right\} \quad (5.21a)$$

subject to :

$$\text{constraints (5.2) – (5.20)}$$

$$\underline{d} \leq d_t^b + d_t^{\text{ev}} \leq \bar{d} \quad \forall t \in \mathcal{T}. \quad (5.21b)$$

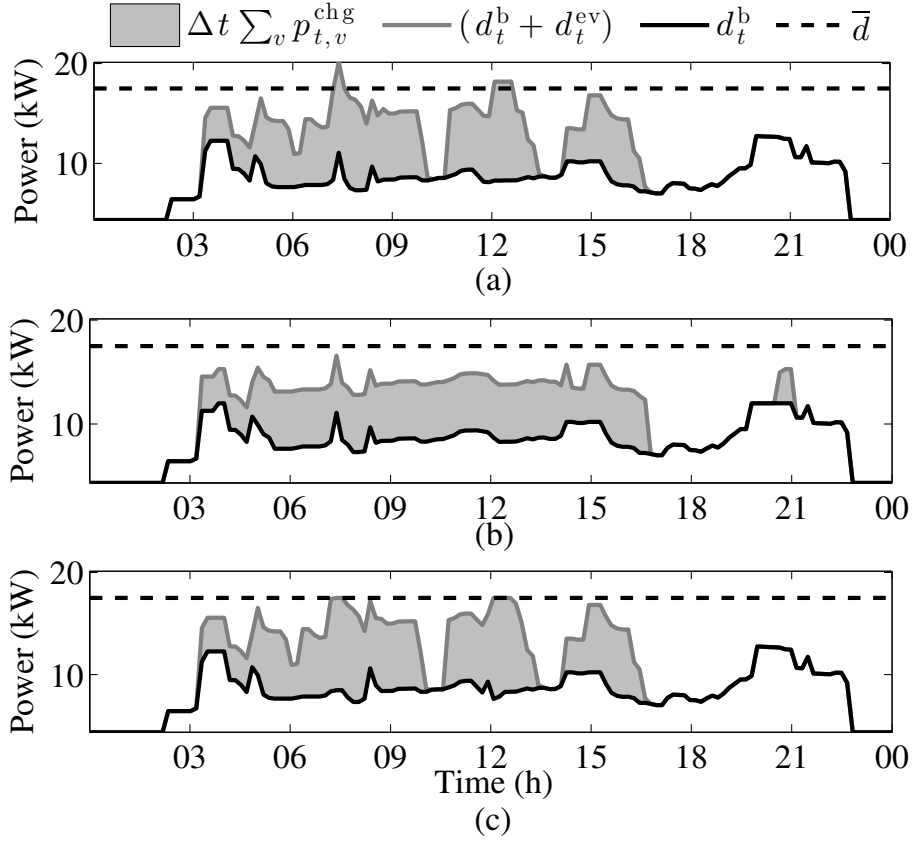


Figure 5.4: Case Study: demand limits. Aggregate building and EV demand for three different strategies: a) uncoordinated strategy, b) rule-based coordination, and c) optimal coordination.

The objective function (5.21a) represents the total energy cost. The price τ_t is the Southern California Edison hourly real-time price (RTP) schedule [13] shown in Fig. 5.3. Constraints (5.2) - (5.20) are the building and EV constraints. The coupling constraint (5.21b) limits the total demand to a maximum of $\bar{d} = 17.5$ kW and a minimum of $\underline{d} = -17.5$ kW.

Fig. 5.4 shows the aggregate demand three different strategies. The strategy in Fig. 5.4(a) is the uncoordinated strategy: the building and EV aggregator pursue their objective functions and ignore the coupling constraints. Naturally, the objective value of the uncoordinated strategy is “lower” than the optimal coordination objective because i) this problem is a re-

laxed version of (5.21) and ii) real costs associated with violating the coupling constraints are ignored (e.g., transformer damage costs).

Fig. 5.4(b) shows the aggregate demand for a rule-based coordination strategy in which each party pursues its objective independently but agree on ad hoc rules to satisfy the coupling constraints. In this particular case, the building manager agrees to restrict its demand to ± 12 kW and the EV aggregator to ± 5.5 kW. The limits allow both parties to find solutions that do not violate the coupling constraints without the need for further coordination. However, the rule-based solution is suboptimal.

Fig. 5.4(c) shows the optimal coordination strategy (using the DWDA). Compared to the non-optimal coordination strategy, optimal coordination allows the EV aggregator (and the building manager to a lesser extent) to shift its load to lower priced hours.

5.6.2 Coupling constraints: peak demand charge

In this case, a peak demand charge couples the building and EV aggregator problems Problem (5.22) describes an optimization problem where both parties minimize their power, energy, and cycling costs.

$$\min \left\{ \Delta t \cdot \sum_{t \in \mathcal{T}} \tau_t \cdot (d_t^b + d_t^{ev}) + \Omega \cdot d^{\max} + c^{\text{cyc}} \right\} \quad (5.22a)$$

subject to :

constraints (5.2) – (5.20)

$$d_t^b + d_t^{ev} \leq d^{\max} \quad \forall t \in \mathcal{T} \quad (5.22b)$$

The objective function (5.22a) has three components: the energy cost given (first term), a peak demand charge (second term), and the cycling costs. The demand charge in \$/kW is represented by Ω and the peak demand value by the variable d^{\max} . Constraint (5.22b) defines the peak demand.

The tariff used in this case study is as follows: an energy charge τ_t of 6.38 ¢ for each

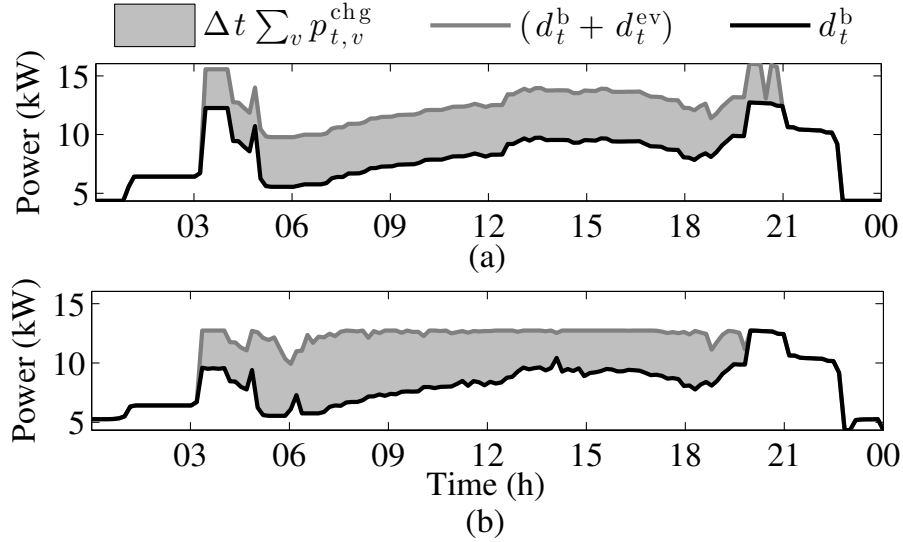


Figure 5.5: Case Study: peak demand charge. Aggregate building and EV demand for two different strategies: a) uncoordinated strategy b) optimal coordination.

kWh consumed during peak hours (between 0600 and 2200 h) and 4.32 ¢ for each kWh consumed at off-peak hours. Additionally, a 98 ¢ charge is levied for every kW of maximum demand [10].

We define the uncoordinated strategy for this case as follows: each entity minimizes its own cost of energy and penalizes its individual peak demand. Post-operation of the building and EVs, we calculate the peak demand charge by solving $d^{\text{max}} = \max_{t \in \mathcal{T}} (d_t^{\text{ev}} + d_t^{\text{b}})$. Fig. 5.5(a) shows the building and EV demand for the uncoordinated strategy.

Fig. 5.5(b) shows the coordinated strategy building and EV demand. In the uncoordinated case, both parties avoid high energy prices and reduce their peak demands independently. However, the total peak demand is suboptimal as energy could be shifted from peak times to the “valley” between the early morning and early evening peaks. On the other hand, when the parties coordinate, the EVs obtain energy without contributing to peak demand. Optimal coordination allows the building manager and the EV aggregator to reduce their peak demand by 3.3 kW.

5.6.3 Coupling constraints: itemized billing

In this final case, different buying and selling energy prices couple the building and EV aggregator problems. This phenomenon can happen when a utility bills the consumer a \$ per kWh charge that includes energy, demand, and fixed costs as described in [146]. However, the consumer only receives the energy portion when selling back to the grid. This tariff structure is referred to as *itemized billing*.

The building manager and EV aggregator seek to

$$\text{minimize } \left\{ \Delta t \cdot \sum_{t \in \mathcal{T}} ([\tau_t^e + \tau_t^{\text{other}}] \cdot d_t^+ - \tau_t^e \cdot d_t^-) \right\} \quad (5.23a)$$

subject to :

constraints (5.2) – (5.20)

$$d_t^b + d_t^{\text{ev}} = d_t^+ - d_t^- \quad \forall t \in \mathcal{T} \quad (5.23b)$$

$$d_t^- \geq 0 \quad \forall t \in \mathcal{T} \quad (5.23c)$$

$$d_t^+ \geq 0 \quad \forall t \in \mathcal{T} \quad (5.23d)$$

under itemized billing. We denote the energy component of the tariff as τ_t^e and the demand and customer related components of the tariff as τ_t^{other} . The energy bought and the energy sold is d_t^+ and d_t^- , respectively. In this case study, we neglect EV battery cycling costs³.

The energy buying price is the real-time price described in Subsection 5.6.1. We assume that the energy component of the tariff is 53% of the price [146].

Figs. 5.6(a) and 5.6(b) show the uncoordinated and coordinated strategies, respectively. In the uncoordinated strategy, the EV aggregator does not have a price incentive to sell energy to the grid (i.e., the buy-back price is too low). However, under a coordinated strategy, the EVs discharge to offset 19.3 kWh during high price hours.

³We do so because we wish to study the non-trivial case where the EVs perform Vehicle-to-Grid (V2G) or Vehicle-to-Building (V2B). The cost of cycling discourages V2B and V2G under this particular price schedule.

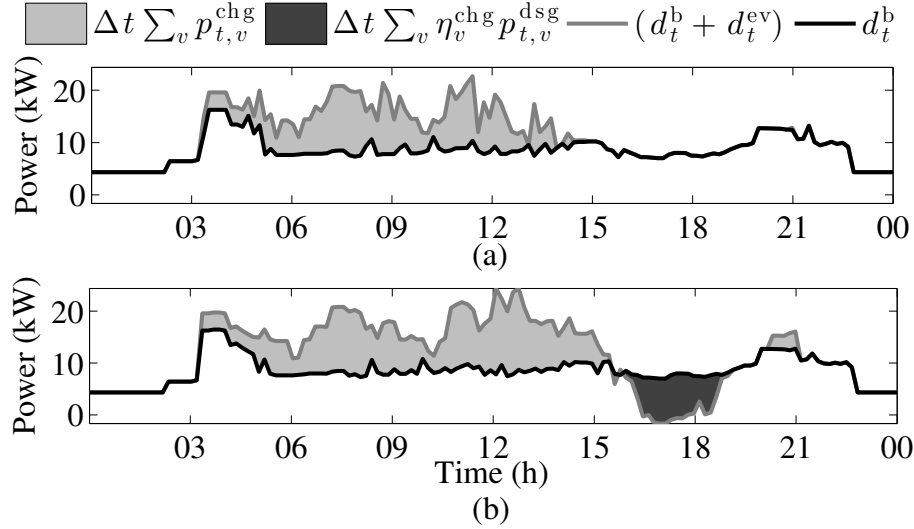


Figure 5.6: Case Study: itemized billing. Aggregate building and EV demand for two different strategies: a) uncoordinated strategy b) optimal coordination.

5.6.4 Computational analysis

The case studies were implemented on a desktop computer running on an Intel(R) Xeon(R) CPU E3-1220 v3 @ 3.10 GHz with 16 GB of RAM. The MILPs in the case studies (the building subproblem and the master problem) were modeled using GAMS and solved using CPLEX with an optimality tolerance of 1%. The LPs were modeled and solved using GAMS and CPLEX, respectively, and solved to optimality. The DWDA tolerance⁴ is 1%.

Figs. 5.7(a), 5.7(b), and 5.7(c) show the iteration number and total cost for case studies 5.6.1 (demand limit), 5.6.2 (peak demand charge), and 5.6.3 (itemized billing), respectively. In Fig. 5.7(a), the algorithm starts by searching for a feasible solution (known as phase I of DWDA) from iterations 1 through 3. Once a feasible solution is found, the algorithm switches to phase II where the master problem solver adjusts the dual values of the coupling constraints to reach the optimal solution. Because of the structure of the coupling constraints, phase I is only performed during the first iteration in cases 5.6.2 and 5.6.3. In

⁴See Appendix (A) for further details on termination of the DWDA.

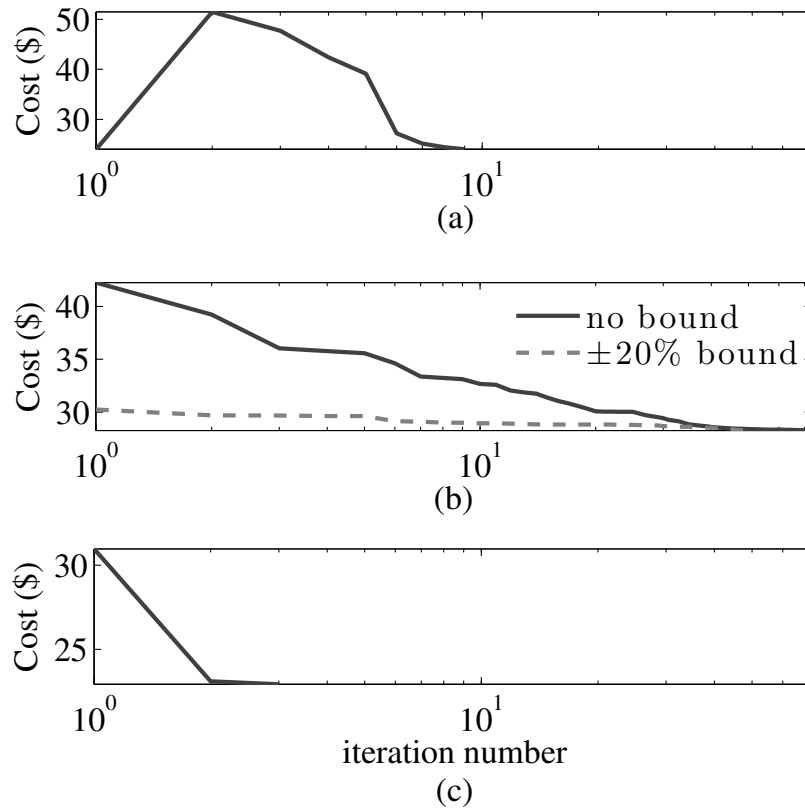


Figure 5.7: Objective function value vs number of iterations for each case study. Plots (a), (b), and (c) refer to cases 5.6.1, 5.6.2, and 5.6.3, respectively.

other words, it is trivial for the phase I master problem to find a feasible solution. See the Appendix for a detailed discussion of the Phase I/II Algorithm.

The convergence rate of the DWDA is closely related to the structure of the coupling constraints and their relationship with each subproblem. It has been reported that the DWDA can exhibit slow convergence due to unstable dual variable behavior (this phenomenon is known as the *tailing-off effect*) [129].

A simple way of improving the convergence rate is to bound the initial proposals. We bound the initial proposals of case study 5.6.2 to $\pm 20\%$ from the optimal values since it is the slowest one to converge. Bounding the initial proposals to $\pm 20\%$ is not unreasonable

Table 5.1: Computational performance for the three Case Studies.

Case	Avg. solve time of problem:			Total time	# iter.
	EV ⁱ	Building ^a	Master ^a		
(a)	0.03	6.56	0.06	53.16	8
(b)	0.03	3.19	0.07	238.63	73
(b) ⁱⁱ	0.03	2.53	0.07	127.3	49
(c)	0.04	7.47	0.06	22.61	3

ⁱSolve times are measured in CPU seconds

ⁱⁱ Using a $\pm 20\%$ forecast of EV and building demand

since it is equivalent to having a relatively inaccurate $\pm 20\%$ forecast. As shown in Table 5.1, the $\pm 20\%$ bounds on the initial proposals decreases the number of iterations required to 49 and cuts the solve time by almost half.

5.6.5 Scalability

We test the scalability of the proposed method by increasing i) the number of buildings and ii) the number of EV fleets. The coupling constraints are upper and lower demand limits as in test case 5.6.1 but scaled to the number of buildings and EV fleets. For instance, for one building and one EV fleet, the demand limits are ± 17.5 kW. For n buildings and n EV fleets, the demand limits are $\pm n \cdot 17.5$ kW.

The time devoted to solving the building subproblem is the most substantial portion of the total algorithm run time. As shown in Table 5.2, the average solve time for the EV subproblem grows approximately linearly with the number of EV fleets. The number of iterations to convergence is 8 for all cases. However, the building subproblem solve time increases faster than linear with the number of buildings.

The solve time of building subproblem can be sped up by solving each building in parallel. In fact, even a single building - and certainly the EV fleet - could be decomposed in several

Table 5.2: Computational performance for Case Study 1 with an increased number of buildings and EVs.

N ^a	Avg. solve time (CPU sec.) of problem			Total solve time (CPU sec.)		# iter.
	EV	Building ^b	Master	S ^b	P ^c	
1	0.03	6.56	0.06	53.16	53.16	8
2	0.04	21.67	0.03	173.6	56.56	8
5	0.10	104.9	0.06	840.2	57.28	8
10	0.21	326.8	0.07	2614	58.24	8
20	0.45	1067	0.06	7474	60.11	8

^aNumber of buildings and EV fleets

^b Simultaneous solving of the buildings subproblem

^c Parallel solving of the buildings subproblem

subsystems⁵ to further speed up the algorithm. As shown in Table 5.2, the sensitivity of the total solve time to the number of buildings and EV fleets is small when the building problems are parallelized.

5.7 Summary

This chapter presents a method to optimally schedule loads in a commercial building and the charging/discharging of an electric vehicle (EV) fleet in a decentralized fashion. The building and EV aggregator schedule their power consumption to meet a common goal (e.g., minimize the operation costs) while observing a set of constraints that are functions of both building and EV variables, i.e., the coupling constraints. We implement the proposed method via a MILP adaptation of the Dantzig-Wolfe Decomposition Algorithm in which only variables *essential* to the coupling constraints and the integrality of the solution are shared with the master problem solver.

We study three classes of constraints that couple the building and EV aggregator prob-

⁵This decomposition could be carried out internally to preserve privacy.

lems: i) demand limits, ii) a peak demand charge, and iii) itemized billing where the price of energy bought differs from the price of energy sold. For each of these cases, we show that the coordinated strategy optimally schedules building appliances and EV charging/discharging. Finally, we test the scalability of the proposed method by increasing the number of buildings and EV fleets.

Chapter 6

MARKET POWER

6.1 Introduction

Prior to the 1990s, the majority of electricity customers in the United States were served by vertically integrated monopolies that controlled every stage of the electric industry, from production all the way to billing [36]. During the 1990s and early 2000s, however, electric industries in places such as the United States, the United Kingdom, Argentina, and Chile underwent major restructuring or “liberalization.” Under this transformation, the generation, transmission, and delivery portions of the business were split, and vertical coordination was (in part) replaced by market-based mechanisms.

Despite the increased role of markets in the electricity industry, restructuring seldom means full deregulation [191]. For one, electricity is unlike any other commodity: its transportation (transmission) is dictated by the laws of physics, it is not easily traceable, its safe and reliable supply requires a number of intertwined products and services (e.g., energy, voltage support, reserves), storing it is hard, etc. Moreover, electricity is an indispensable product for which the public demands and expects extraordinarily high levels of reliability. These quirks of electricity require, for now, a coordinating entity (e.g., a system operator or “SO”) to manage power flows, coordinate grid services, ensure reliability and resource adequacy, etc. The presence of such an invasive coordinator inevitably interferes with purely free-market outcomes. Furthermore, the electricity industry deviates from ideal markets in more classical ways: high entry barriers and market concentration, inelastic demand, market segmentation, etc [67].

One of the most notable phenomena that can arise in non-ideal markets is *market power*. In the most general sense, refers to the practice (illegal under some circumstances) of devi-

ating from the fair pricing of goods and services for private gains at the expense of reduced social welfare. Market power can take on a few different forms. For instance, firms could *dump* products at below-cost prices to starve more fragile competitors and drive them out of the market for longterm gains [79]. Or, suppliers can withhold otherwise available capacity to increase prices and short-term profits (e.g., during the California energy crisis [44]). In this chapter, we consider the second form of market power: when firms bid strategically and alter market prices for short-term gains.

6.1.1 Problem statement and contributions

We consider a single profit-maximizing strategic bidder (the “firm”) under a perfect information setting. The firm can be a supplier, consumer, or both, e.g., a prosumer or an energy storage system (ESS). A market operator maximizes social welfare as revealed by the participants’ bids.

By definition, strategic bids by the firm increases (or at worst, does not decrease) its short-term profit with respect to the socially optimum¹. Also by definition, the social welfare under strategic bidding is lower than the optimum. The efficiency gap that results from strategic bids motivates the central contribution of this chapter: our market power mitigating price (MPMP), a pricing mechanism that induces the firm to bid the social optimum.

The MPMP has the following characteristics:

1. when the firm is exposed to it (e.g., in lieu of traditional marginal pricing) its profit-maximizing bid equals the social-welfare maximizing bid,
2. its formulation requires no private information about the firm,
3. it is firm-agnostic, i.e., it is applicable to firms that are producers, consumers, or prosumers, and
4. it allows the SO or regulator to regulate the firm’s profit.

In addition to the MPMP, the rest of the contributions of this chapter are:

¹In the social optimum, the firm bids according to its true cost or utility.

- An analysis of the social and private impacts of strategic bidding by an ESS.
- An analysis of the performance of the MPMP.

The analyses listed above are performed in the IEEE 24 bus reliability test system (RTS).

6.1.2 Literature review

Market power in practice

The Federal Energy Regulatory Commission (FERC), state regulators, and SOs perform market monitoring functions to detect, remedy, and prevent abuse of market power [190]. Detecting market power with *certainty* is virtually impossible because most drivers of bidding behavior (e.g., operating costs or equipment status) are opaque to regulators. However, regulators often use indices and heuristics designed to detect market power in a probabilistic fashion. For instance, California ISO (CAISO) uses the Residual Supply Index (RSI), which is correlated with above-competitive-rates-markup, to detect likely market power cases [190]. FERC, on the other hand, relies on the Herfindahl-Hirschman Index (HHI) as a measure of market concentration [67]. The aforementioned indices were developed when only large conventional generators could realistically exercise market power. Nowadays, however, it is increasingly unclear how to apply those metrics to atypical participants such as large-scale energy storage or aggregators controlling a heterogeneous mix of resources.

Several techniques to mitigate or prevent the effects of market power exist. For instance:

- FERC limits the market share of any single supplier to 20% [67]. Limiting market share reduces the likelihood of price-making capabilities by large suppliers.
- Another technique is to increase the connectivity of the electric network (e.g., with transmission infrastructure) to avoid market segmentation. A segmented electricity market (e.g., a system with a significant number of congested lines) may leave some nodes at the mercy of a few suppliers with price-making capabilities [67].
- Longterm contracts are also known to reduce market power as they reduce the amount of capacity that could be taken off-line during operation [114].

- There is evidence that demand-side bidding reduces the market power of suppliers, e.g., in [172, 223].
- And finally, a popular, but often criticized by free marketeers, technique to prevent market power are price caps [61].

The aforementioned market power mitigation and prevention techniques are *approximately* lead to more desirable market outcomes from society’s point of view. In contrast, our proposed MPMP is an *exact* technique to mitigate the market power, in the sense that it creates optimal, not just more desirable, market outcomes.

Market power in academic works

In the realm of academia, most works deal with the market power of generating units (e.g., see [114, 189]). The focus on generation is understandable since large-scale penetration of more diverse market participants is a relatively new phenomenon. Our MPMP, however, allows for it to be applied to generic market participants: whether these are suppliers, demand, or both.

References [137, 200] study the issue of market power by ESSs. However, the problem is seen from the perspective of the ESS. The social point of view is not fully addressed. Moreover, to the best of our knowledge, a market power mitigation mechanism for ESSs or generic firms is not yet available.

6.1.3 Where do distributed energy resources fit in the context of market power?

A commonly proposed way of allowing distributed energy resources (DERs) to participate in electricity markets is through aggregators [43]. Under this paradigm, aggregators gather enough capacity to participate in wholesale markets and bid on behalf of their constituent DERs.

While incorporating DERs into electricity markets unlocks their potential to provide system-wide benefits [43], some researchers have pointed out their potential to act strategically for private gains, e.g., in [58, 151, 178]. Notably, our work in Chapter 4 shows how a

strong DER-aggregator coalition can arise even from selfish agents and bid as a single block. Thus, at least in theory, an aggregator could potentially amass enough DERs to rival the size of any single large-scale power plant and exercise unacceptable levels of market power.

As previously mentioned, most practical and academic work on market power detection and mitigation has been focused on traditional suppliers (e.g., large power plants). It is unclear how regulators would apply market concentration indices like the HHI to large ensembles of heterogeneous DERs, or cost-based indices like the PCMI to non-suppliers. Similarly, it is unclear how traditional market power mitigation approaches could be adapted to DER aggregators. In contrast to traditional approaches, our MPMP is firm-agnostic and is applicable to ensembles of producers, consumers, prosumers, or a combination of thereof.

6.1.4 Organization of this chapter

This chapter is organized as follows. Sections 6.2 and 6.3 describes the strategic firm and the market model, respectively. Section 6.4 identifies the two market outcomes that we consider: the social optimum and the outcome under strategic bidding by the firm. Section 6.5 presents the MPMP, Section 6.6 presents a case study on the IEEE 24 bus RTS, and Section 6.7 concludes the chapter.

6.2 Strategic participant model

We consider a single strategic player participating in an electricity market and assume that all other market participants are non-strategic. Non-strategic participants reveal their true preferences through their bids², i.e., they bid their true cost or utility function. The strategic player can be a consumer, producer, or prosumer and participate by offering or bidding at any number of nodes of a power system. Hereinafter we refer to the strategic player as *the firm*.

²The truthfulness assumption of the rest of the market participants can be relaxed without loss of generality, i.e., they are not required to reveal true preferences. However, the crucial assumption here is that they do not modify their bids in response to the strategic player.

The firm is characterized by a concave utility function $\tilde{u} : \mathbb{R}^{|\mathcal{T}| \cdot |\mathcal{N}|} \rightarrow \mathbb{R}$ and can represent a consumer, producer, or prosumer. For consumers, the function \tilde{u} takes on positive values maps consumption at each time period $t \in \mathcal{T}$ and node $n \in \mathcal{N}$ to utility. For the case of producers, \tilde{u} takes on negative values and represents a disutility or cost. Prosumers can act as net producers of electricity during some time periods and at some nodes and act as net consumers during other periods and nodes [170].

Additionally, the firm is characterized by a convex set $\mathcal{X} \subset \mathbb{R}^{|\mathcal{T}| \cdot |\mathcal{N}|}$ that defines admissible consumption/production schedules $\mathbf{x} = \{\mathbf{x}_t\}_{t \in \mathcal{T}}$. The symbol \mathbf{x}_t denotes nodal consumption (when negative) or production (when positive) of the firm at time t and \mathbf{x} is simply the collection of all \mathbf{x}_t 's. To simplify notation, we embed \mathcal{X} in the firms utility function as follows

$$u(\mathbf{x}) = \begin{cases} \tilde{u}(\mathbf{x}) & \text{if } \mathbf{x} \in \mathcal{X} \\ -\infty & \text{otherwise} \end{cases} .$$

6.2.1 Market participation

The firm participates in a day-ahead market by submitting inverse supply and/or demand curves, $\mathbf{s}_t^{-1} : \mathbb{R}_+^{|\mathcal{N}|} \rightarrow \mathbb{R}^{|\mathcal{N}|}$ and/or $\mathbf{d}_t^{-1} : \mathbb{R}_+^{|\mathcal{N}|} \rightarrow \mathbb{R}^{|\mathcal{N}|}$. The function \mathbf{s}_t^{-1} maps the supply quantity during period t at each of the $|\mathcal{N}|$ nodes to prices and is required to be non-decreasing. Similarly, the inverse demand curve \mathbf{d}_t^{-1} is required to be non-increasing and maps energy demanded at each node to nodal prices.

6.3 Market model

We consider a market in which the market operator receives supply/demand bids from the firm, supply bids from the rest of the players, and covers a fixed demand by the load. Then, the market operator clears the market by maximizing the social welfare as revealed by the collection of bids from all players. The following definitions introduce the precise meaning of social welfare and details the market clearing mechanism.

Definition 2. Let $\mathbf{f} = \{\mathbf{f}_t = \mathbf{d}_t^{-1} - \mathbf{s}_t^{-1}\}_{t \in \mathcal{T}}$. Given a set inverse supply $\{\mathbf{s}_t^{-1}\}_{t \in \mathcal{T}}$ and demand curves $\{\mathbf{d}_t^{-1}\}_{t \in \mathcal{T}}$, of the system welfare is defined as

$$\text{SW}(\mathbf{f}) = u(\mathbf{x}(\mathbf{f})) - \sum_{t \in \mathcal{T}} \mathbf{1}^\top \mathbf{c}_t^{\text{gen}}(\mathbf{g}_t(\mathbf{f})) \quad (6.1)$$

where $\mathbf{c}_t^{\text{gen}} : \mathbb{R}_+^{|\mathcal{N}|} \rightarrow \mathbb{R}_+^{|\mathcal{N}|}$ is a function that maps hourly generation (by generators not owned by the firm) at each node to generation cost at each node. The dispatch of the generators at time t is denoted by \mathbf{g}_t . The n^{th} entry of vector \mathbf{g}_t represents generation from node n at time t . We write \mathbf{g}_t as a function of \mathbf{f} to emphasize the bid's impact on the generation dispatch. The dispatch of the firm is denoted by \mathbf{x} and is a function of the firm's bids.

The dispatch values of $\mathbf{g}_t(\mathbf{f})$ and $\mathbf{x}(\mathbf{f})$, denoted by $\mathbf{g}_t^*(\mathbf{f})$ and $\mathbf{x}^*(\mathbf{f})$, are determined by the market clearing process, which maximizes the ‘‘apparent’’ social welfare as revealed by the bids. The following definition formalizes the market-clearing process.

Definition 3. The dispatch values $\mathbf{g}_t^*(\mathbf{f})$ and $\mathbf{x}^*(\mathbf{f})$ are a product of the market clearing problem given by

$$\{\mathbf{g}_t^*(\mathbf{f}), \mathbf{x}^*(\mathbf{f})\} = \arg \max_{\mathbf{g}_t, \mathbf{x}_t} \sum_{t \in \mathcal{T}} \int_0^{\mathbf{x}_t} \mathbf{f}(\mathbf{y}) d\mathbf{y} - \sum_{t \in \mathcal{T}} \mathbf{1}^\top \mathbf{c}_t^{\text{gen}}(\mathbf{g}_t(\mathbf{f})) \quad (6.2a)$$

s.t.

$$\mathbf{1}^\top \mathbf{g}_t + \mathbf{1}^\top \mathbf{x} = \mathbf{1}^\top \mathbf{q}_t \quad \forall t \in \mathcal{T} \quad (6.2b)$$

$$\mathbf{H}(\mathbf{g}_t + \mathbf{x}_t - \mathbf{q}_t) \leq \bar{\mathbf{l}} \quad \forall t \in \mathcal{T} \quad (6.2c)$$

$$\mathbf{x} = \{\mathbf{x}_t\}_{t \in \mathcal{T}} \quad (6.2d)$$

where the objective (6.2a) is to maximize the social welfare as revealed by the firm's and other player's bids during \mathcal{T} . The nodal demand at time t are given by \mathbf{q}_t . Equations (6.2b), (6.2c), represent the system power balance constraints and represent the system transmission constraints, respectively. The symbol \mathbf{H} represents the transmission shift factor matrix and $\bar{\mathbf{l}}$ represents line limits.

The dispatch quantities are crucial in calculating the social welfare, a measure of efficiency. Additionally, the market clearing mechanism determines the prices of electricity at which the firm and the rest of the market participants transact. A common pricing mechanism is locational marginal pricing [118]. Under locational marginal pricing, the price of electricity (potentially) fluctuates both in time and location.

Definition 4. *The locational marginal prices (LMP) at time t are defined as the gradient of the Lagrangian of problem (6.2) with respect to the nodal demands at time t : $\lambda_t(\mathbf{f}) = \nabla_{\mathbf{q}_t} \mathcal{L}$ [118].*

Throughout this chapter, we illustrate relevant models and results via simple and easy-to-follow numerical examples.

Example 4. *Consider a firm that owns generation and operates in a uni-node and uni-period electricity market. The firm is characterized by the quadratic cost function $\tilde{u}(x) = -\frac{1}{2}x^2$ generation limits given by $\mathcal{X} = \{x | 0 \leq x \leq 10\}$. Then, $u(x) = \tilde{u}(x)$ if $x \in \mathcal{X}$ and $u(x) = -\infty$ otherwise. The market is characterized by a demand of 10, the supply from the firm, and a cost function for the rest of the generation in the system given by $c^{\text{gen}}(g) = \frac{1}{2}g^2$. The demand derives 5 units of utility per unit energy consumed.*

Suppose that the SO accepts bids by the firm in the form $f(y, a) = -a \cdot y$. Then, the market clears by solving the problem

$$\max_{x,g} \int_0^x f(y, a) dy - c^{\text{gen}}(g) + 5 \cdot 10 \quad (6.3a)$$

s.t.

$$x + g = 10. \quad (6.3b)$$

The first term of the objective represents the firm's reported generation costs, the second represents the cost of generation for the rest of the market participants, and the last one the utility derived by the load. The price of electricity is given by the dual variable of the power balance constraint.

6.4 Market outcomes

In this section, we introduce two market outcomes. The first one is the *strategic bidding* outcome. In this case, the firm formulates bids \mathbf{f} to maximize its profit. In the second outcome, the *socially optimal* case, the bids maximize social welfare. The first case models a situation where the firm has the potential to exercise market power, that is, the firm is a *price maker*. The second case models an ideal scenario that would arise if the firm is controlled by a social welfare-maximizing entity, e.g., the state, if the market is perfectly competitive, or if the firm's strategy is to reveal its true preferences to the SO.

6.4.1 Strategic bidding

For the strategic bidding case, we assume that

1. the firm maximizes short-term profits,
2. the market operator determines dispatch values and prices by solving Problem (6.2),
3. the rest of the market participants bid truthfully, and
4. a perfect information setting where the firm knows the parameters of Problem (6.2).

Under the aforementioned assumptions, the firm formulates bids \mathbf{f}^* by solving

$$\mathbf{f}^* = \arg \max_{\mathbf{f}} u(\mathbf{x}(\mathbf{f})) + \sum_{t \in \mathcal{T}} \boldsymbol{\lambda}_t(\mathbf{f})^\top \mathbf{x}_t(\mathbf{f}). \quad (6.4)$$

The value of \mathbf{x} and $\boldsymbol{\lambda}_t$ are determined by the market clearing process, that is, by the solution to Problem (6.2) and by Definition 4. Note that we model strategic bidding by the firm as a *Stackelberg Game* where the firm moves first by submitting bids to the SO and the SO responds by clearing the market.

Example 5. *This continues the previous example. Under strategic bidding, the firm chooses the value of $a \in \mathbb{R}_+$ in its bid $f(y, a) = -a \cdot y$ that delivers the highest profit. That is, it chooses a by solving*

$$a^* = \arg \max_{a \in \mathbb{R}_+} u(x) + x \cdot \lambda$$

where both x and λ are implicit functions of a and result of the market clearing process described in the previous example. Analyzing the Karush-Kuhn-Tucker (KKT) conditions of Problem (6.3), we find that x and λ as functions of a are

$$x = \frac{10}{a+1} \text{ and } \lambda = \frac{a \cdot 10}{a+1}.$$

Then, the profit maximizing bid, dispatch values, and market-clearing price are given by

$$a^* = 2, \quad x^* = \frac{10}{3}, \text{ and } \lambda^* = \frac{20}{3}$$

and the optimal profit by

$$u(x^*) + x^* \cdot \lambda^* = \frac{50}{3} \approx 16.33.$$

continue here

6.4.2 Social optimum

While the social optimum may be hard to realize in practice, we are interested in it because it is an outcome to “strive” for. Also, the social optimum can serve as a benchmark to compare non-ideal outcomes against. We define socially optimal bids $\mathbf{f}^{\text{social}}$ as those that maximize social welfare:

$$\mathbf{f}^{\text{social}} = \arg \max_{\mathbf{f}} \text{SW}(\mathbf{f}). \quad (6.5)$$

By definition, $\text{SW}(\mathbf{f}^{\text{social}}) \geq \text{SW}(\mathbf{f}^*)$. The magnitude of the difference, however, is dependent on the market characteristics that include the size and spatial dispersion of the firm, the composition of the supply, and the demand’s elasticity.

An important goal of regulators (including FERC in the United States) market efficiency, i.e., outcomes close to $\text{SW}(\mathbf{f}^{\text{social}})$. In the next section, we propose a pricing mechanism that

a regulator or system operator (SO) could implement if she deems the gap between the optimum and the actual outcome is too large to bear.

Example 6. *This continues the previous example. The socially optimal is, from the KKT conditions to of Problem (6.3), given by*

$$a^{\text{social}} = \frac{10}{x^{\text{social}}} - 1$$

where x^{social} is given by the solution to

$$\max_{x,g} u(x) - c^{\text{gen}}(g) + 5 \cdot 10 \quad (6.6a)$$

s.t.

$$x + g = 10. \quad (6.6b)$$

Problem (6.6) is similar to (6.3) except that the stated preferences of the firm, i.e., its bids, are replaced by its true preferences, i.e., its utility function. Thus, the socially optimal bid is $a^{\text{social}} = 1$. In this case, the social welfare is

$$\text{SW}^{\text{social}} = u(x^{\text{social}}) - c^{\text{gen}}(g^{\text{social}}) + 5 \cdot 10 = 25.$$

In the strategic bid case, on the other hand, the social welfare is

$$\text{SW}^* = u(x^*) - c^{\text{gen}}(g^*) + 5 \cdot 10 \approx 22.22. \quad (6.7)$$

Strategic bidding represents a social welfare loss of ≈ 2.77 or about 11%. The load is notoriously affected as their payments increase by ≈ 16.6 units. Table 6.1 shows the profits and welfare for each of the two market outcomes. A curious result is that the rest of the generators in the system benefit from the firm's strategic bid even more than the firm itself. The reason for this is that the rest of the generators enjoy the higher price and higher dispatch.

Table 6.1: Welfare and profits for each market outcome: strategic bid and social optimum.

market outcome	firm profit	generator profits ¹	Load payments	SW
strategic bid	16.33	22.22	66	22.22
social optimum	12.5	12.5	50	25
difference	3.83	9.72	-16	-2.78

¹For participants other than the firm

6.5 Market power mitigation

As shown in the previous example, social welfare and consumers can suffer the consequence of the firm's strategic bids. This section proposes a non-uniform pricing mechanism designed to mitigate the adverse effects of strategic bidding.

6.5.1 Market clearing with market power mitigating price

If the SO or regulator could expose a firm that exercises market power to the market power mitigating price (MPMP) proposed in the following theorem The MPMP aligns the profit-seeking behavior of the firm with the goal of maximizing social welfare. That is, under the MPMP, the firm bids the social optimum.

Theorem 1. *If the firm is exposed to the MPMP given by*

$$\mathbf{p}_t(\mathbf{f}) = -\text{diag}(\mathbf{x}_t(\mathbf{f}))^{-1} \cdot (\mathbf{c}_t^{\text{gen}}(\mathbf{g}_t(\mathbf{f})) - \boldsymbol{\gamma}_t) \quad t \in \mathcal{T}$$

the market clears at the social optimum. The function $\text{diag}(\mathbf{a})$ takes the vector $\mathbf{a} \in \mathbb{R}^N$ and outputs a $N \times N$ diagonal matrix whose (i, i) entry is the i^{th} element of \mathbf{a} . The constant vector $\boldsymbol{\gamma}_t$ can be set arbitrarily and used to regulate the firm's profit. The dispatch values $\mathbf{x}_t(\mathbf{f})$ and $\mathbf{g}_t(\mathbf{f})$ are product of the market clearing.

The proof of Theorem 1 can be found in Appendix E. The proposed MPMP has three key properties. First, it is compatible with both rational behavior of the firm and the regulator's desire to maximize social welfare: by maximizing profits, the firm bids the social optimum.

Second, the terms γ_t allows for regulation of the firm's profit. Third, it is firm-agnostic: it is applicable to producers, consumers, or prosumers. And finally, its formulation requires no private information: the characteristics (i.e., operating constraints and cost functions) of the firm do not need to be disclosed.

6.5.2 Regulated profit of the firm

The proposed MPMP allows for the regulation of the firm's profit by selecting constants γ_t such that it receives a desired (and arbitrary) amount of profit. The profit must come from charges to other players in the system. The profit allocation decision is a problem to be solved by the regulator, the SO, market operator, and/or other stakeholders. This, however, is a decision that is system, market structure, and regulatory environment-dependent and is outside the scope of this dissertation.

The amount of regulated profit does not affect the short-term operation of the firm as the γ_t 's are constants in the objective of the firm's profit maximization problem. However, selecting a proper amount of regulated profit is crucial. Assigning too much or too little profit to the firm may induce an undesirable long-term evolution of the system.

Example 7. *This continues the previous example. As previously noted, the clearing price as a function of the bid parameter a is*

$$\lambda = \frac{a \cdot 10}{a + 1}.$$

Also as previously discussed, under λ , the firm has the ability to bid strategically to increase its profits at the expense of the load's welfare. However, if the firm is exposed to the MPMP of the form

$$p = \frac{-c^{\text{gen}}(g) + \gamma}{x}$$

the it's profit maximization problem becomes

$$\max_{a \in \mathbb{R}_+} u(x) + x \cdot p = u(x) - c^{\text{gen}}(g) + \gamma. \quad (6.8)$$

As with traditional pricing, x and g are products of the market clearing process and implicitly functions of a . Notice that the profit maximization problem (6.8) under MPMP and the social welfare maximization problem (6.7).

6.5.3 How does the MPMP fit in current market designs?

The MPMP has three major features that relate to the design of modern electricity markets. First, it encourages a monopolist to bid the social optimum. Second, through its γ_t constants, it allows the regulator to assign the firm an arbitrary amount of profit. Last, as consequence of the profit regulation property, the MPMP could serve as a welfare allocation tool to accomplish regulatory goals, subsidize, or tax certain technologies in the power system. These three properties are compatible with current market designs and practices as discussed in the rest of this section.

Market power mitigation

One of the responsibilities of the FERC is to oversee wholesale electricity markets. FERC Order 888 [78] states that

“The Commission’s goal is to remove impediments to competition in the wholesale bulk power marketplace and to bring more efficient, lower cost power to the Nation’s electricity consumers.”

Aligned to FERC Order 888, Independent System Operators throughout the country (e.g., CAISO, NE-ISO) have established departments dedicated to monitoring market activity and countering abuses of market power. Understandably, in both academia and in practice, such efforts have typically been focused on the market power of generators. Nevertheless, the

proposed MPMP is in line with the goal of fomenting market efficiency and discouraging monopolistic behaviors.

Profit regulation

The MPMP also has the ability to regulate the profit of the monopolist firm. Regulating profits of monopolies is a fairly common practice in many sectors of the economy, including the electricity sector. In fact, one of the most prominent examples of this is the profit regulation of electric and gas utilities [201]. A common way of regulating the profit of electric utilities is through *cost-plus* schemes where the utilities are allowed to cover their costs plus an administratively designated rate of return.

Welfare allocation

The MPMP can also play alongside and assist features of modern electricity markets. For instance, some systems use uplift payments to mitigate market failures [100]. The MPMP could serve as an additional tool to collect and deliver uplift payments. Additionally, the MPMP could be used as a collection mechanism to subsidize desirable technologies in the power system (e.g., energy storage, flexible resources, or clean generation) and penalize undesirable ones (e.g., dirty generation). The question of whether a welfare allocation is good or evil is outside the scope of this work.

6.5.4 Limitations and practicality of the MPMP

Under our assumptions, the MPMP is a *perfect* solution to market power. The pricing scheme is easy to formulate, transparent, requires no private information, and delivers the social optimum. However, some of the assumptions may not hold in practice.

A perfect information setting is the first assumption that is unlikely to hold in reality. Empiric studies such as the one in [103] show that observed behaviors do not fully match the theory. Furthermore, assuming that the firm has *full* knowledge of the market clearing

problem is likely unreasonable. Firms that formulate strategic bids are likely to use simpler models, e.g., residual-demand based ones [210]. Thus, a practical implementation of the MPMP should probably be based on bidding models that are observed in practice.

The second assumption that may not hold in practice is the unique strategic bidder assumption. In some cases, more than one firm may act strategically - each one potentially with different levels of sophistication. As discussed in references [138, 139, 168], markets with multiple strategic players can be analyzed as equilibrium problems with equilibrium constraints (EPECs). Thus, when appropriate the MPMP should be adapted to accommodate multiple strategic players.

A potential difficulty of implementing of the MPMP is the sensitivity of the outcomes of interest (e.g., prices, social welfare, or welfare distribution) to the mismatch between models and reality (e.g., the difference between the bidding model and actual strategy, network model and actual network, etc.). It would be undesirable if normal levels of model misspecification lead to severely bad outcomes. Thus, an implementation of the MPMP should be robust to differences between models and assumptions and their reality. Ideally, an implementation of the MPMP should guarantee outcomes that are not worse than the status quo pricing mechanism.

Finally, the longterm implications of profit regulation and welfare redistribution (via selecting the constants γ_t and arranging side-payment schemes) must be explored. It is well-known how perfectly competitive markets not only deliver efficient short-term allocation of resources but also incentivize efficient allocation of production capacity and longterm consumption patterns. The MPMP allows the regulator, to some extent, to determine welfare allocation throughout the system - an admittedly difficult task.

6.6 Case study: the market power of an ESS in the IEEE 24 bus RTS

In this section, we study the effects of market power and the MPMP on a larger instance. We analyze the welfare and performance of the participants in a multi-period, multi-node market. Furthermore, compared to the previous numerical examples, we consider a more

complex firm: an ESS operator. This case study is based on on [56].

We consider the two entities that participate actively: *i*) the SO, who is responsible for maximizing social welfare while observing the power system constraints of the IEEE 24 bus RTS; and *ii*) the ESS operator who strives to maximize profits derived from energy arbitrage. Additionally, we consider three passive market participants and stakeholders: the load, the generation, and the transmission system.

6.6.1 Power system model

We consider a setting where the SO has perfect forecasts of demand, generation, and transmission availability. The network is modeled using DC power flows.

The SO ensures that four technical limits are observed. The first one is related to each generator: the power output of each generator, $g_{i,t}$, must be within the operating limits. \underline{g}_i and \bar{g}_i , as shown by constraints (6.9a). The rest of the technical limits concern the entire power system: the power produced must equal the demand (6.9b); each line flow must be within limits, $-\bar{l}_k$ and \bar{l}_k , at all times as expressed by equations (6.9c); and the bus voltage angles, $\theta_{n,t}$ must be within stability limits, as expressed by equations (6.9d). The following equations state these constraints:

$$\underline{g}_i \leq g_{i,t} \leq \bar{g}_i, \quad \forall i \in \mathcal{I}, \quad \forall t \in \mathcal{T} \quad (6.9a)$$

$$g_{n,t}^{\text{bus}} + x_{n,t}^{\text{bus}} = q_{n,t} + \sum_{l \in L} m_{k,n}^L \frac{\theta_{s^{(k)},t} - \theta_{e^{(k)},t}}{X_k}, \quad \forall n \in \mathcal{N}, \quad \forall t \in \mathcal{T} \quad (6.9b)$$

$$-\bar{l}_k \leq \frac{\theta_{s^{(k)},t} - \theta_{e^{(k)},t}}{X_k} \leq \bar{l}_k, \quad \forall k \in \mathcal{K}, \quad \forall t \in \mathcal{T} \quad (6.9c)$$

$$-\pi \leq \theta_{n,t} \leq \pi, \quad \forall n \in \mathcal{N}, \quad \forall t \in \mathcal{T} \quad (6.9d)$$

$$\theta_{n,t} = 0, \quad n = \text{ref}, \quad \forall t \in \mathcal{T} \quad (6.9e)$$

where the set of all generators, buses, energy storage units, lines, and time periods are denoted by \mathcal{I} , \mathcal{N} , \mathcal{H} , \mathcal{K} , and \mathcal{T} , respectively.

The power injected (when positive) or extracted (when negative) at time t by the storage

units connected to bus b is denoted by $x_{n,t}^{\text{bus}} = \sum_{h \in \mathcal{H}} m_{h,n}^{ES} (x_{h,t}^d - x_{h,t}^c)$ where rate of charge and discharge of storage unit h at time t are denoted by $x_{h,t}^c$ and $x_{h,t}^d$, respectively. The power injected at time t by generators connected to bus n is denoted by $g_{n,t}^{\text{bus}} = \sum_{i \in \mathcal{I}} m_{i,n}^G g_{i,t}$. The parameters $m_{i,n}^G$ and $m_{h,n}^{ES}$ are elements of the generator and ESS incidence matrices, respectively. The constant $m_{i,n}^G/m_{h,n}^{ES}$ is 1 if generator i / storage unit h is connected to bus b and 0 otherwise. The load at bus b at time t is denoted by $q_{n,t}$. The constant $m_{k,n}^L$ is an element of the line map matrix and its value is 1 if line l starts at node n , -1 if it ends at node n , and 0 otherwise. The power flow on a line from bus $s(k)$ to bus $e(k)$ is a function of the difference between the voltage angle at bus $s(k)$ and the voltage angle at bus $e(k)$, and the line reactance X_k [197]. Finally, the voltage angle at the reference bus is set by constraints (6.9e).

Constraints (6.9a)-(6.9e) define the feasible set of the power system. Now we characterize the feasible operating regimes of the ESS.

6.6.2 Energy storage system

In this case study, we focus on when the ESS is used for *energy arbitrage*. Energy arbitrage is an important revenue stream for an energy storage system and can help justify investment costs [68].

The ESS operator owns and operates a set of storage units distributed throughout the grid. The rate of charge, $x_{h,t}^c$, and discharge, $x_{h,t}^d$, must be within bounds, \bar{x}_h^c and \bar{x}_h^d , as expressed by constraints (6.10a) and (6.10b), respectively. The amount of stored energy, $SoC_{h,t}$, must be within bounds, \underline{SoC}_h and \overline{SoC}_h , at all times as expressed by constraints (6.10c). Constraints (6.10d) describe the state-of-charge (SOC) dynamics. The SOC of storage unit h at time t , $SoC_{h,t}$, is equals its SOC at $t-1$ plus the energy inflows, $\Delta x_{h,t-1}^c \eta_h^c$ and outflows $\Delta x_{h,t-1}^d / \eta_h^d$ at $t-1$. The length of each time step is denoted by Δ . The charging and discharging efficiencies are characterized by $\eta_h^c \in (0, 1]$ and $\eta_h^d \in (0, 1]$, respectively. Additionally, the initial energy stored by each storage unit must equal their final energy stored as expressed by constraint (6.10e). This ensures that energy sold during the time

horizon is paid for during the time horizon. The following equations describe technical limits of the ESS:

$$0 \leq x_{h,t}^c \leq \bar{x}_h^c, \forall h \in \mathcal{H}, \forall t \in \mathcal{T} \quad (6.10a)$$

$$0 \leq x_{h,t}^d \leq \bar{x}_h^d, \forall h \in \mathcal{H}, \forall t \in \mathcal{T} \quad (6.10b)$$

$$\underline{SoC}_h \leq SoC_{h,t} \leq \overline{SoC}_h, \forall h \in \mathcal{H}, \forall t \in \mathcal{T} \quad (6.10c)$$

$$SoC_{h,t} = SoC_{h,t-1} + \Delta x_{h,t-1}^c \eta_h^c - \Delta q_{h,t-1}^d / \eta_h^d, \forall h \in \mathcal{H}, \forall t \in \mathcal{T} \quad (6.10d)$$

$$SoC_{h,|T|} = SoC_{h,0}, \forall h \in \mathcal{H}. \quad (6.10e)$$

Finally, it is known that charging/discharging affects the useful lifetime of chemistry-based ESSs [155]. The cost of utilizing the ESS is characterized by the linear cost function

$$C^{ES} = \sum_{h \in \mathcal{H}, t \in \mathcal{T}} \alpha_h \Delta (x_{h,t}^d + x_{h,t}^c).$$

where the coefficient α_h is related to the degradation and operation costs of unit h .

The aforementioned constraints characterize the feasible set of ESS operating regimes. The following section introduces the problem that the ESS solves to maximize its profit. Rather than bidding according to its true cost, the ESS determines profit-maximizing bids.

6.6.3 Bidding strategy

In this section, we introduce the market setting in which the ESS operates and formulates its profit maximization problem. If the ESS is large enough, its bids might significantly affect the market clearing prices. In this case, the ESS's best strategy is to treat the market clearing prices as endogenous to its profit maximization problem. The problem of ESS profit maximization under endogenous prices is typically modeled as a *bilevel optimization* problem where the upper-level objective is to maximize the ESS's profit subject to the market clearing process in the lower level [137, 158, 215].

Price-quantity bids from the ESS

We consider a market setting that allows the ESS to submit price-quantity demand bids (for energy purchases) and price-quantity supply bids (for energy sells) as in [215]. For each storage unit and time period, it bids $\Delta x_{h,t}^{\text{supply}}$ units of energy (for injection) at the price $\rho_{h,t}^{\text{supply}}$ or bids for $\Delta x_{h,t}^{\text{demand}}$ units of energy (for extraction) at the price $\rho_{h,t}^{\text{demand}}$. The objective of the ESS operator is to formulate supply and demand bids such that its profit, given by

$$J^{ESS}(\mathbf{y}, \boldsymbol{\lambda}) = \sum_{n \in \mathcal{N}, t \in \mathcal{T}} \lambda_{n,t} \Delta x_{n,t}^{\text{bus}} - C^{ES},$$

is maximized. The price paid to (when selling) or paid for (when buying) by the ESS operator for withdrawals/injection at bus n is the LMP, $\lambda_{n,t}$. The ESS-exclusive variables are denoted by $\mathbf{y} = \left\{ x_{h,t}^c, x_{h,t}^d, SoC_{h,t}, \rho_{h,t}^{\text{supply}}, \rho_{h,t}^{\text{demand}} \right\}_{h \in \mathcal{H}, y \in \mathcal{T}}$. The set of all LMPs is denoted by $\boldsymbol{\lambda} = \{ \lambda_{n,t} \}_{n \in \mathcal{N}, t \in \mathcal{T}}$. The LMPs $\boldsymbol{\lambda}$ are the dual variables of the nodal power balance constraints (6.9b) obtained from the market clearing process.

Market clearing

The ESS determines its bids while assuming that the load bids its true utility and that the generators bid their true cost. The market clearing process is modeled as an optimization problem in which the SO maximizes the social welfare as revealed by the participant's bids. The SO maximizes

$$J^{SO, \text{bid}}(\mathbf{x}, \mathbf{z}) = \sum_{h \in \mathcal{H}, t \in \mathcal{T}} (\rho_{h,t}^c \Delta x_{h,t}^c - \rho_{h,t}^d \Delta x_{h,t}^d) - \sum_{i \in \mathcal{I}, t \in \mathcal{T}} c_i^{\text{gen}}(g_{i,t}),$$

where the function $c_i^{\text{gen}}(\cdot)$ represents the piece-wise linear price-quantity bid (and true cost) of generator i . The clearing charging/discharging quantities $\Delta x_{h,t}^c / \Delta x_{h,t}^d$ should be smaller than or equal to the bid quantities $\Delta x_{h,t}^{\text{demand}} / \Delta x_{h,t}^{\text{supply}}$. It is assumed that the load price bid is high enough for all its quantity to be cleared. This last assumption allows ignoring the

load's utility term in the SO's objective function.

Bilevel optimization model of strategic bidding

The prices paid by/for the ESS derive from the social welfare maximization problem. Thus, bidding problem of the ESS operator can be formulated as the following bilevel optimization problem:

$$\max_{\mathbf{x}, \mathbf{z}, \boldsymbol{\lambda}} J^{ESS}(\mathbf{y}, \boldsymbol{\lambda}) \quad (6.11a)$$

$$\text{s.t. } \mathbf{y} \in \mathcal{Y}^{ESS} \quad (6.11b)$$

$$\{\mathbf{z}, \boldsymbol{\lambda}\} \in \arg \max_{\mathbf{z} \in \mathcal{Z}^{SO}} J^{SO, \text{bid}}(\mathbf{z}, \mathbf{y}) \quad (6.11c)$$

where the power system-exclusive variables are denoted by

$$\mathbf{z} = \{ \{g_{i,t}\}_{i \in \mathcal{I}}, \{\theta_{b,t}\}_{n \in \mathcal{N}} \}_{t \in \mathcal{T}}.$$

The feasible operating region of the electric network described by equations (6.9a)-(6.9e) is denoted by \mathcal{Z}^{SO} . Similarly, the feasible operating region of the ESS described by equations (6.10a) - (6.10e) is denoted by \mathcal{Y}^{ESS} . Here, the upper-level objective, (6.11a), is to maximize the ESS profit subject to the ESS constraints (6.11b) and the market clearing process (6.11c). In the upper level, the ESS determines its supply/demand price-quantity bids. In the lower level, the SO schedules generation and charging/discharging of the ESS in order to maximize the social welfare.

Solution approach

The bilevel problem described by equations (6.11) is recast as a single-level optimization problem by replacing the lower level problem (6.11c) with its KKT optimality conditions. The resulting single-level problem, however, is hard to solve as it is non-linear (the upper-level objective, J^{ESS} , is a product of variables) and non-convex (the lower-level complementary

slackness conditions are equalities and product of variables). However, the upper-level objective is linearized by invoking the strong duality theorem on the convex lower-level problem. The lower-level complementary slackness conditions are linearized using the Fortuny-Amat and McCarl transformations. The resulting problem is a mixed-integer linear program that can be efficiently solved using commercial solvers (e.g., CPLEX). We skip the detailed description and refer interested readers to [73, 215].

6.6.4 Social welfare

In this section we define *i)* how the welfare/profits are allocated among participants and *ii)* the problem that the SO solves in the ideal case. Ideally, each participant would bid according to its true cost/utility. In this case, the market clearing process maximizes the *true* social welfare of the system.

Social welfare distribution

In order to know who “wins” and who “looses” due to the ESS strategic bid, it is useful to define how the social welfare is allocated among four actors in the system: *i)* the producers and *ii)* ESS whose welfare is their profit, *iii)* the load whose welfare is the utility derived from consuming electricity minus electricity payments, and *iv)* the transmission system owner whose welfare is the transmission surplus. All in all, the system welfare is given by the following definition.

Definition 5. *The social welfare, SW, of the system is equivalently defined as i) the sum of the welfare of the four aforementioned actors or ii) the benefit that the load derives from*

consuming electricity minus the cost of operating the power system and the ESS:

$$\begin{aligned} SW &= J^G + J^{ESS} + J^D + J^{TS} \\ &= \sum_{n \in \mathcal{N}, t \in \mathcal{T}} U \Delta d_t - \sum_{i \in \mathcal{I}, t \in \mathcal{T}} c_i^{\text{gen}}(g_{i,t}) - C^{ES} \end{aligned} \quad (6.12)$$

$$(6.13)$$

where

$$\begin{aligned} J^G &= \sum_{i \in \mathcal{I}, t \in \mathcal{T}} [\lambda_{n(i),t} \Delta g_{i,t} - c_i^{\text{gen}}(p_{i,t})], \\ J^D &= \sum_{n \in \mathcal{N}, t \in \mathcal{T}} (U - \lambda_{n,t}) \Delta q_{n,t} \\ J^{TS} &= \sum_{n \in \mathcal{N}, t \in \mathcal{T}} \lambda_{n,t} \Delta (q_{n,t} - x_{n,t}^{\text{bus}} - g_{n,t}^{\text{bus}}). \end{aligned}$$

The load's benefit per MWh is denoted by U . The symbol J^D denotes the load's surplus. The producer's profit is denoted by J^G and $\lambda_{n(i),t}$, is the locational marginal price (LMP) at time t at the bus generator i is connected to. The bus that generator i is connected to is denoted by $n(i)$. The transmission surplus as defined in [99] is denoted by J^{TS} .

Social optimum

Ideally, the SO would operate the system by maximizing the social welfare as defined by (6.12) while observing all technical constraints. Then, the socially optimal operation of the system is given by the following definition.

Definition 6. *The solution to the problem*

$$\max_{\mathbf{z}, \mathbf{y}} SW \quad (6.14a)$$

$$s.t. \{\mathbf{z}, \mathbf{y}\} \in \mathcal{Z}^{SO} \quad (6.14b)$$

$$\mathbf{y} \in \mathcal{Y}^{ESS}, \quad (6.14c)$$

denoted by \mathbf{z}^* and \mathbf{y}^* , defines the socially optimal operation of the system.

6.6.5 Simulation results

Numerical simulations are performed using the one area IEEE 24 bus RTS found in [5]. The system is composed of 37 generators, 38 transmission lines, and load at 17 buses. The ESS owner operates five energy storage units at buses 114, 119, 117, 120, and 123. The power and energy capacities of the ESS are varied throughout the simulations but always at a constant $\frac{SoC_h}{\bar{x}_h^c} = \frac{200}{3}$. The system is modeled using GAMS and solved using CPLEX.

Effects of strategic bidding on the social welfare

By definition, strategic bidding decreases the social welfare with respect to the social optimum. The magnitude of such decrease depends on a number of factors including load shape and magnitude, the location and size of the storage units, topology of the transmission system, market set-up, among others. In this work we use the simulations to draw *qualitative* insights and conclusions.

For instance, as shown in Fig. 6.1, the number of piece-wise linear segments used to model the generator's cost curve has a significant impact on the estimation of welfare loss. The loss of welfare with respect to the social optimum is largest when modeling the generator cost curves using 5 segments. Even though the magnitude of the loss of welfare is modest (it tops at roughly \$600 per day, which amounts to roughly 0.75% of the system cost) it is not possible to conclude that the welfare loss will be as small for a generic power system. In

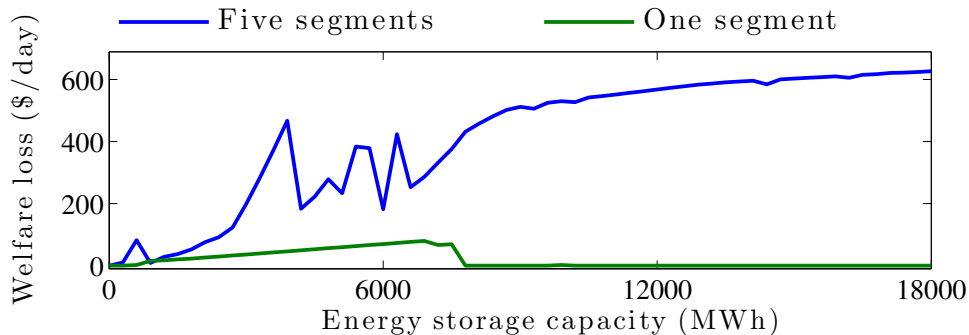


Figure 6.1: Social cost increase (with respect to the social optimum) due to strategic bidding of the ESS.

the rest of this section, we model the generator costs using 5 piece-wise segments.

It is important to note that even though strategic bidding has an adverse effect on social welfare, results suggest that it is better to have an ESS bidding strategically than no energy storage at all. As shown in Table 6.2, the social cost with no storage is $\$90.3 \times 10^3$ while the cost under strategic bidding is $\$86.8 \times 10^3$.

Social welfare distribution

As shown in Fig. 6.1, there is always a non-negative welfare loss due to the strategic bid by the ESS. In other words, the system as a whole is never better-off compared to the social optimum. However, some players do benefit from the bidding behavior of the ESS. Naturally, the ESS benefits from its own profit-maximizing behavior but as shown in Fig. 6.2 the other players benefit at some energy storage penetration levels and suffer at other levels.

Interestingly, the only other participant who provides arbitrage besides the ESS, the transmission system (who arbitrages energy in space), experiences profit gains that are remarkably similar to those of the ESS (see Fig. 6.1). The load and generation, on the other hand, experience losses and gains, respectively, that mirror each other.

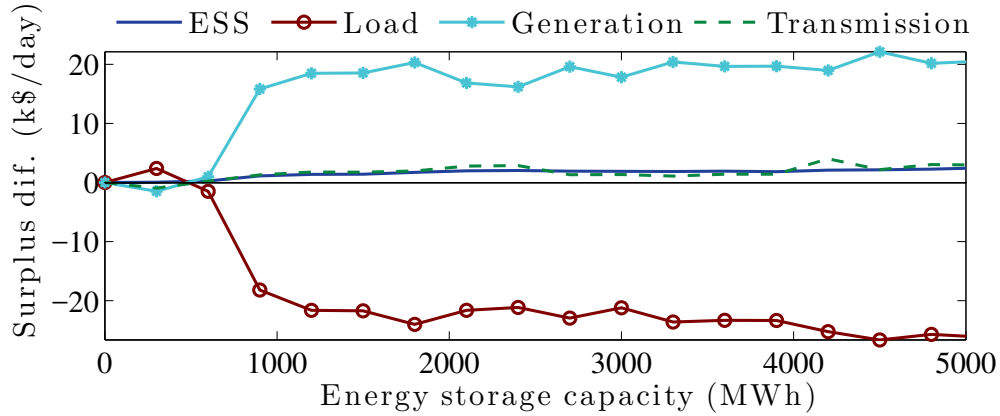


Figure 6.2: Surplus difference (with respect to the social optimum) due to the ESS’s strategic bid for each power system actors. Positive differences denote gains while negative differences denote losses with respect to the social optimum.

6.6.6 Profit regulation and side payments

In this section, we study the welfare/profit allocation among the participants. The question of whether a welfare/profit allocation is good or evil is outside the scope of this work.

Suppose that the system has an energy storage penetration of 3,900 MWh and that the SO deems the welfare distribution given by the social optimum as a desirable distribution of the social welfare. Then the SO could set the profit regulation constants such that the ESS has a profit of $\$1.82 \times 10^3$ per day and transfer $\$17 \times 10^3$ per day to the load. These funds would have to come from the generation and transmission who, compared to the social optimum, are better off with the τ pricing scheme (see Table 6.2 for details).

If the SO deems that a fair distribution of the welfare is such that everyone is at least as well-off as in the strategic bidding case. In that case, the SO could set up a side-payment scheme that redistributes the welfare such that everyone is better-off compared to the strategic bidding case. Note that since the social welfare is $\$500$ per day higher using the MPMP scheme, it is possible to make every player strictly better-off compared to the strategic bidding case.

Table 6.2: Surplus distribution among the four power system actors and social cost for four cases: no energy storage case, social optimum, strategic bidding case, and market clearing under MPMP .

Model	Surplus (k\$)				Social cost (k\$)
	ESS	Gen.	Trans.	Load	
No energy storage	0	193	10.7	807	90.3
Social optimum	1.82	178	7.06	829	86.3
Strategic bid	3.63	197	8.46	805	86.8
MPMP	reg.	181	14.34	820	86.3

For the last 3 cases, the energy storage penetration is 3,900 MWh.

6.7 Summary

In this chapter, we study the adverse effects of the market power of a single strategic firm on the social welfare. We propose a pricing mechanism, the MPMP, that incentivizes the firm to bid according to the social optimum. Additionally, the formulation of the MPMP does not require private information from any party and provides an instrument for profit regulation of the firm. We showcase the performance of the MPMP via small numerical examples and a larger study on the IEEE 24 bus RTS.

Chapter 7

NON-WIRE ALTERNATIVES TO CAPACITY EXPANSION

7.1 Introduction

Electric utility distribution systems are typically designed for the peak load, which happens a small number of hours per year. When the load reaches capacity, the traditional solution is to install more wires or reinforce existing ones [187]. While decades of experience makes this “wires” solution reliable and safe, it often carries enormous capital costs, results in hostile public opinion, and can experience time-consuming legal issues (e.g., eminent domain questions) [196].

Lately, planners have shown increased interest in distributed energy resources (DERs) such as energy storage (ES), energy efficiency (EE), demand response (DR), and distributed generation (DG) as alternatives to the traditional “wires” solution. For example, the I-5 corridor project in the Pacific Northwest of the United States [112] explores alternatives to transmission capacity and the Brooklyn-Queens Demand Management Program in New York [53] focuses on distribution-level capacity issues. In the planning community, DER-based approaches to long-term planning problems are often referred to as *non-wire alternatives (NWAs)*. The basic premise is that NWAs can manage load to avoid or at least delay the need for capacity expansion.

The values of delaying investment are two-fold. Economically, the reason for deferring is the time-value of money, which states that a dollar spent now is more valuable than a dollar spent later [124]. Policy-wise, the benefits of delaying capital-intensive projects are reducing the risk of the expected load not materializing and avoiding politically unpopular projects [196]. In this chapter, we focus on the economic question and ask: is delaying traditional expansion investments worth the costs of NWAs?

The answer to the this question is not trivial. For one, the cost and benefits of NWAs are not only a function of their installed capacities but also of their operations. Thus, one must co-optimize investment and operation of NWAs. This co-optimization leads to a large problem that can be computationally difficult to solve, especially if we consider uncertainty from renewable resources such as wind and solar. Furthermore, considering the time-value of delaying investments introduces non-linearities that result in a non-convex problem even when integer variables are not present.

7.1.1 Contributions

In this work, we tackle the resulting large-scale non-convex problem. Specifically, we make the following contributions:

1. A *formulation* of the NWAs planning problem that determines 1) the investment, 2) the operation of NWAs and 3) the timing of the capacity expansion. We manage load, solar generation, and EE performance uncertainty via robust optimization [32, 104].
2. *Tractable algorithms* for the NWAs planning problem. This problem contains (on the order of) millions of variables because the modeling of the operation of the NWAs over a decades-long investment horizon. The variables and constraints that model the timing of capacity expansion introduce the non-convexities. We present two solution techniques. The first technique is through the *Dantzig-Wolfe Decomposition Algorithm (DWDA)*. We deal with the scale of the NWAs planning problem by decomposing it into smaller subproblems. The non-convexities end up confined to a small master problem (in the order of tens to hundreds of variables). We deal with the non-convexities of the master problem by decomposing it and solving a small number of linear programs. In the second technique, *we fix the timing of capacity expansion to eliminate the problem's non-convexities*. We sequentially solve the convex problem one time for each year in the optimization horizon and pick the solution that produces the minimum objective value.

Both techniques have pros and cons. The DWDA is scalable because of its decom-

position properties. However, sometimes it can exhibit slow convergence rates¹. The second technique can provide faster convergence but has limited scalability. In practice, a utility can choose their preferred solution method according to the specific planning problem at hand.

3. A *case study* where NWAs may be used to defer substation and feeder upgrades at the University of Washington Seattle Campus using real data. We estimate the performance of the NWAs planning solution via Monte Carlo simulations.

7.1.2 Related works

The idea of delaying infrastructure investment by curbing load was first introduced in [125]. The work in [125] quantifies the effects of load reduction on avoided infrastructure costs but does not find the optimal amount of reduction or the appropriate technologies to do so. On a similar note, the authors of [84] and [162] quantify the value of capacity deferral by explicitly modeling DR as the mechanism to reduce net load. However, they also do not address the problem of finding optimal DG investment nor consider other types of DERs. In [180], the authors determine optimal investments in DG considering the value of network investment deferral. However, their non-linear mixed-integer formulation is intractable for large systems. In contrast, we consider a broader set of NWAs and tackle the problem by solving a series of smaller convex problems.

Beyond the above cited works, there is relatively little literature on holistic DER planning. Most consider a narrow definition of the term DER that only includes DG, e.g., [21, 226], or only ES and DR [72]. Instead, we consider a generic definition of DERs and present a case that considers solar photovoltaic (PV) generation, DR, EE, and ES.

¹In practice, slow convergence rates are a minor issue because the planning problem only has to be solved a limited number of times in an off-line setting.

7.1.3 Chapter organization

This chapter is organized as follows. Section 7.2 states the capacity expansion problem and formulates it as an optimization problem. Section 7.3 formulates a generic NWA model and four specific technologies: EE, PV, DR, and ES. Section 7.4 describes the NWAs planning problem and uncertainty modeling. Section 5.5.1 provides two solution techniques for the planning problem. Section 7.6 presents a case study of load-growth at the University of Washington. Section 7.7 concludes the chapter.

7.2 The capacity expansion problem

System planners typically like to expand capacity at the *latest* possible time that meets the expected load growth [193]. The main economical reason to delay capacity expansion as much as possible is the time-value of money: we would like to spend a dollar later rather than now. Let l_a^p denote expected peak load² during year a and the pre-expansion capacity as \bar{l} . The vector of expected peaks in the planning horizon is denoted as \mathbf{l}^p . After expansion, we assume that any reasonable load can be accommodated during the planning horizon. Then, the decision rule for choosing a year to expand capacity is

$$\text{CapEx}(\mathbf{l}^p) = a \mid l_{a+1}^p > \bar{l}, l_k^p \leq \bar{l} \forall k \leq a. \quad (7.1)$$

The decision rule CapEx states that the planner expands capacity at a future year a immediately before the limit \bar{l} is *first* reached by the load. In this chapter, we analyze capacity expansion at a single point in a radial system (e.g., a feeder or substation) and assume that the downstream network is non-congested. Since most distribution systems are (approximately) radial, if a point in the downstream network is congested, the same technique in this chapter can be applied to the subnetwork.

Let I denote the inflation-adjusted cost of capacity expansion. Here, we assume that the

²The expected peak load \mathbf{l}^p is typically forecasted using a variety of inputs such as population growth projections, planned construction projects, weather forecasts, gross domestic product, etc [187].

inflation-adjusted cost of capacity expansion is constant throughout the planning horizon. Then, if system capacity is expanded at year $\text{CapEx}(\mathbf{l}^P)$, the present cost of the investment is

$$\tilde{I}(\mathbf{l}^P) = \frac{I}{(1 + \rho)^{\text{CapEx}(\mathbf{l}^P)}} \quad (7.2)$$

where ρ is the annual discount rate, a quantity closely related to the interest rate [124,187].

Our goal would be to minimize $\tilde{I}(\mathbf{l}^P)$ via the variable $\text{CapEx}(\mathbf{l}^P)$. However, since $\text{CapEx}(\mathbf{l}^P)$ itself is given by a decision rule in (7.1), it is more convenient to write the present cost $\tilde{I}(\mathbf{l}^P)$ itself as an minimization problem:

Lemma 3. *Let the planning horizon be denoted as \mathcal{A} . The function \tilde{I} from (7.2) can be reformulated as the optimization problem*

$$\tilde{I}(\mathbf{l}^P) = \min_{\delta} \frac{I}{(1 + \rho)^\delta} \quad (7.3a)$$

$$\text{s.t. } 0 \leq \delta \leq |\mathcal{A}| \quad (7.3b)$$

$$l_a^P \leq \bar{l} \forall a < \delta. \quad (7.3c)$$

The reformulation of \tilde{I} allows us to embed it in an optimization problem without the need of including conditionals in (7.1). The proof of Lemma 3 is found in Appendix E.4.

Note that for any given set of yearly peak loads \mathbf{l}^P , (7.3) is convex. However, if we treat the peak load as a function of NWAs operation, and therefore as an optimization variable, (7.3) becomes non-convex.

While it is unfortunate that (7.3) is non-convex in \mathbf{l}^P , Section 5.5.1 shows how to handle its non-convexities by solving at most $|\mathcal{A}|$ small-scale linear problems. This is because the length of the planning horizon, $|\mathcal{A}|$, is in the order tens of years. These small problems can be reliably solved using off-the-shelf solvers (e.g., Gurobi). In the next section, we introduce the generic models of an NWA and instantiate it.

7.3 Non-wire alternatives

Let the index i denote an NWA technology. A generic NWA is characterized by six elements:

1. investment (or sizing) decision variables ϕ_i ,
 - e.g., the energy capacity of an ES system;
2. operating decision variables \mathbf{x}_i ,
 - e.g., ES hourly charging and discharging decisions;
3. a set of feasible investment decisions Φ_i ,
 - e.g., the set of ES systems that physically fit in a site;
4. a set of feasible operating regimes $\mathcal{X}_i(\phi_i)$,
 - e.g., the set of hourly charging and discharging decisions that comply with charge, discharge, and state-of-charge limits;
5. a set of functions $l_{a,t}^i(x_i)$ that map operating decisions onto load at time t of year a ,
 - e.g., for an ES system at time a, t the load is defined as charge minus discharge;
 - and
6. an investment cost function $I_i^{\text{NW}}(\phi_i)$,
 - e.g., the investment cost of an ES system is the energy capacity times the per kWh cost of storage.

While investment decisions are made once in the planning horizon, operating decisions are made frequently on significantly shorter horizons. In this work, the operating decision time intervals length is Δt hours and \mathcal{T} denotes the set of operating intervals in one year.

We assume that Φ_i and $\mathcal{X}_i(\phi_i)$ are convex, $I_i^{\text{NW}}(\phi_i)$ is a convex function, and that the load functions $l_{a,t}^i(x_i)$ are linear in \mathbf{x}_i . These assumptions allow us to guarantee the algorithms proposed in Section 5.5.1 converge. Now, we describe each of the six elements that characterizes a NWA for the four technologies that we consider in this work: EE, PV, DR, and ES.

Energy Efficiency (EE) For EE, the investment decision is to choose a percentage base load reduction that translates into a $r_{a,t}^{\text{EE}}$ reduction at every time period. We model the investment cost, $I_{\text{EE}}^{\text{NW}}$, as a convex piece-wise linear function of load reduction [41]. The slope of each of the B^{EE} segments, C_b^{EE} , represents the marginal cost of load reduction. The six parameters that define DR as a NWA are

$$\begin{aligned}
\phi_{\text{EE}} &= \{\epsilon_b^{\text{EE}}\}_{b=1,\dots,B^{\text{EE}}} \\
\mathbf{x}_{\text{EE}} &= \{r_{a,t}^{\text{EE}}\}_{a \in \mathcal{A}, t \in \mathcal{T}} \\
\Phi_{\text{EE}} &= \{\epsilon_b^{\text{EE}} \mid \epsilon_b^{\text{EE}} \in [0, \bar{\epsilon}_b^{\text{EE}}] \ \forall b = 1 \dots, B^{\text{EE}}\} \\
\mathcal{X}_{\text{EE}}(\phi_{\text{EE}}) &= \left\{ r_{a,t}^{\text{EE}} \mid r_{a,t}^{\text{EE}} = \alpha_{a,t}^{\text{EE}} \cdot l_{0,t}^{\text{b}} \cdot \sum_{b=1}^{B^{\text{EE}}} \epsilon_b^{\text{EE}} \ \forall a \in \mathcal{A}, t \in \mathcal{T} \right\} \\
l_{a,t}^{\text{EE}}(\mathbf{x}_{\text{EE}}) &= -r_{a,t}^{\text{EE}} \\
I_{\text{EE}}^{\text{NW}}(\phi_{\text{EE}}) &= \sum_{b=1}^{B^{\text{EE}}} C_b^{\text{EE}} \cdot \epsilon_b^{\text{EE}}
\end{aligned}$$

where ϵ_b^{EE} is the projected percentage reduction for each piece-wise linear segment of $I_{\text{EE}}^{\text{NW}}$, $\bar{\epsilon}_b^{\text{EE}}$ is the size of each segment, and $l_{0,t}^{\text{base}}$ is the base load (i.e., the pre-EE load). The parameter $\alpha_{a,t}^{\text{EE}}$ represents error on the projected load reduction. For instance, $\alpha_{a,t}^{\text{EE}} = 1$ represents no error while $\alpha_{a,t}^{\text{EE}} = 0.9$ represents a 10% underestimation.

Solar photovoltaic generation (PP) The PV investment decision is the installed capacity $g_{\text{CAP}}^{\text{PV}}$. The solar energy generation at time t , a is $g_{a,t}^{\text{PV}} = \alpha_{a,t}^{\text{PV}} \cdot g_{\text{CAP}}^{\text{PV}}$ where $\alpha_{a,t}^{\text{PV}} \in [0, 1]$ is solar generation per unit of PV installed capacity and is related to solar irradiation. For instance, at night, when solar irradiation is zero, $\alpha_{a,t}^{\text{PV}} = 0$ and if the PV system is outputting

its capacity, $\alpha_{a,t}^{\text{PV}} = 1$. The parameters that define solar PV as a NWA are

$$\begin{aligned}
\phi_{\text{PV}} &= g_{\text{CAP}}^{\text{PV}} \\
\mathbf{x}_{\text{PV}} &= \{g_{a,t}^{\text{PV}}\}_{a \in \mathcal{A}, t \in \mathcal{T}} \\
\Phi_{\text{PV}} &= \{g_{\text{CAP}}^{\text{PV}} \mid g_{\text{CAP}}^{\text{PV}} \in [0, \bar{g}_{\text{CAP}}^{\text{PV}}]\} \\
\mathcal{X}_{\text{PV}}(\phi_{\text{PV}}) &= \{g_{a,t}^{\text{PV}} \mid g_{a,t}^{\text{PV}} = \alpha_{a,t}^{\text{PV}} \cdot g_{\text{CAP}}^{\text{PV}} \forall a \in \mathcal{A}, t \in \mathcal{T}\} \\
l_{a,t}^{\text{PV}}(\mathbf{x}_{\text{PV}}) &= -g_{a,t}^{\text{PV}} \\
I_{\text{PV}}^{\text{NW}}(\phi_{\text{PV}}) &= C^{\text{PV}} \cdot g_{\text{CAP}}^{\text{PV}}
\end{aligned}$$

where C^{PV} is the per-unit PV capacity cost and $\bar{g}_{\text{CAP}}^{\text{PV}}$ is the PV capacity limit.

Demand response (DR) We consider investments in DR communication and control infrastructure that enable shifting a portion of the load. The investment decision is the amount DR-enabled load $r_{\text{CAP}}^{\text{DR}}$ which limits the demand reduction $r_{a,t}^{\text{DR}}$ deployed during year a , operating period t . A load reduction $r_{a,t}^{\text{DR}}$ causes a demand rebound of $\alpha^{\text{DR}} \cdot r_{a,t}^{\text{DR}}$ during time period $t + 1$. The coefficient α^{DR} is a number ≥ 1 and is related to efficiency losses caused by DR deployment [131]. More sophisticated rebound models such as the ones in [131] are admissible in our framework. The parameters that define DR are

$$\begin{aligned}
\phi_{\text{DR}} &= r_{\text{CAP}}^{\text{DR}} \\
\mathbf{x}_{\text{DR}} &= \{r_{a,t}^{\text{DR}}\}_{a \in \mathcal{A}, t \in \mathcal{T}} \\
\Phi_{\text{DR}} &= \{r_{\text{CAP}}^{\text{DR}} \mid r_{\text{CAP}}^{\text{DR}} \in [0, \bar{r}_{\text{CAP}}^{\text{DR}}]\} \\
\mathcal{X}_{\text{DR}}(\phi_{\text{DR}}) &= \{r_{a,t}^{\text{DR}} \mid r_{a,t}^{\text{DR}} \in [0, r_{\text{CAP}}^{\text{DR}}] \forall a \in \mathcal{A}, t \in \mathcal{T}\} \\
l_{a,t}^{\text{DR}}(\mathbf{x}_{\text{DR}}) &= \alpha^{\text{DR}} r_{a,t-1}^{\text{DR}} - r_{a,t}^{\text{DR}} \\
I_{\text{DR}}^{\text{NW}}(\phi_{\text{DR}}) &= C^{\text{DR}} r_{\text{CAP}}^{\text{DR}}
\end{aligned}$$

where C^{DR} is the per-unit cost of DR. In our work, we ignore binary variables that arise from fixed DR costs or customer enrollment costs.

Lithium-ion energy storage The ES investment decision is the initial (e.g., name-plate capacity) energy capacity s_0^{max} of the storage system. The operating variables are the charge $c_{a,t}$, discharge $d_{a,t}$ and the state-of-charge $s_{a,t}$. In addition, we consider energy capacity as an operating variable since s_a^{max} may be different than s_0^{max} because we model battery degradation. The feasible operating region of the ES system is defined by (7.7c)-(7.7f) and include the usual charge, discharge, and state-of-charge limits [184]. Additionally, as expressed in (7.7e), the storage capacity degrades by β^{ESD} per-unit charge/discharge [184]. The parameters that define ES are

$$\phi_{\text{ES}} = s_0^{\text{max}}, \mathbf{x}_{\text{ES}} = \{c_{a,t}, d_{a,t}, s_{a,t}, s_a^{\text{max}}\}_{a \in \mathcal{A}, t \in \mathcal{T}} \quad (7.7a)$$

$$\Phi_{\text{ES}} = \{s_0^{\text{max}} \mid s_0^{\text{max}} \in [0, \bar{s}_0^{\text{max}}]\} \quad (7.7b)$$

$$\mathcal{X}_{\text{ES}}(\phi_{\text{ES}}) = \left\{ c_{a,t}, d_{a,t}, s_{a,t}, s_a^{\text{max}} \mid \right. \quad (7.7c)$$

$$s_{a,t+1} = s_{a,t} + \Delta t \cdot \left(\eta_c \cdot c_{a,t} - \frac{d_{a,t}}{\eta_d} \right) \forall a \in \mathcal{A}, t \in \mathcal{T} \quad (7.7d)$$

$$s_a^{\text{max}} = s_0^{\text{max}} - \beta^{\text{ESD}} \cdot \sum_{k=1}^{a-1} \sum_{t \in \mathcal{T}} (c_{k,t} + d_{k,t}) \forall a \in \mathcal{A} \quad (7.7e)$$

$$s_{a,t} \in [0, s_a^{\text{max}}], c_{a,t}, d_{a,t} \in \left[0, \frac{s_a^{\text{max}}}{\alpha^{\text{EPR}}} \right] \forall a \in \mathcal{A}, t \in \mathcal{T} \quad (7.7f)$$

$$I_{a,t}^{\text{ES}}(\mathbf{x}_{\text{ES}}) = c_{a,t} - d_{a,t} \quad (7.7g)$$

$$I_{\text{ES}}^{\text{NW}}(\phi_{\text{ES}}) = C^{\text{ES}} \cdot s_0^{\text{max}} \quad (7.7h)$$

where η_c (η_d) is the charge (discharge) efficiency, α^{EPR} is the energy-to-power ratio of the ES system, and C^{ES} is the dollar per-unit energy cost of ES capacity. We consider investments in lithium-ion ES in this work because of their ubiquity although other chemistries are compatible with the proposed framework.

Our framework allows for other NWAs to be included, for example, electric vehicles, diverse range of storage technologies, dispatchable DG, etc. In this work, we limit our consideration to the four technologies described above because they are the most mature and readily deployable in an urban environment, which fits our case study about the University of Washington.

7.3.1 The capacity expansion problem revisited

Let the total load including a set \mathcal{N} of NWAs be denoted by $l_{a,t}(\mathbf{x}) = l_{a,t}^b + \sum_{i \in \mathcal{N}} l_{a,t}^i(\mathbf{x}_i)$ where $\mathbf{x} = \{\mathbf{x}_i\}_{i \in \mathcal{N}}$. Then, the yearly peak load as a function of NWA operation is $l_a^p(\mathbf{x}) = \max_{t \in \mathcal{T}} \{l_{a,t}(\mathbf{x})\}$ where \mathbf{x} denote the operating decisions of all the NWAs.

The only decision to be made in the traditional capacity expansion problem is when to expand capacity. With NWAs, however, the present cost of expansion

$$\tilde{I}(l^p(\mathbf{x})) \tag{7.8}$$

is a function of the NWAs operation and gives the planner the opportunity to invest in and operate a set of NWAs that minimizes (7.8). However, a good plan should consider additional NWAs costs and benefits (e.g., demand charge reductions, DR rebound costs, etc.). In the next Section, we present a holistic NWAs planning problem that decides the investment and operation of NWAs, and the timing of capacity expansion.

7.4 The non-wire alternatives planning problem

7.4.1 Deterministic formulation

The NWA planning problem in (7.9) minimizes 1) operating costs $\sum_{i \in \mathcal{N}} C_i^O(\mathbf{x}_i)$, 2) NWA investment costs $\sum_{i \in \mathcal{N}} I_i^{\text{NW}}(\phi_i)$, 3) a peak demand charge $C^D(l^p(\mathbf{x}))$, and 4) the present

cost of capacity expansion $\tilde{I}(\mathbf{l}^P(\mathbf{x}))$:

$$\min_{\substack{\phi_i \in \Phi_i \\ \mathbf{x}_i \in \mathcal{X}_i(\phi_i)}} \left\{ \sum_{i \in \mathcal{N}} [C_i^O(\mathbf{x}_i) + I_i^{\text{NW}}(\phi_i)] + C^D(\mathbf{l}^P(\mathbf{x})) + \tilde{I}(\mathbf{l}^P(\mathbf{x})) \right\}. \quad (7.9)$$

From (7.2), \tilde{I} contains the condition-based function CapEx. The presence of CapEx makes incorporating \tilde{I} in large-scale optimization problems difficult and (7.9) intractable. Using Lemma 3, Theorem 2 shows a more convenient formulation of the planning problem.

Theorem 2. *The problem in (7.9) is equivalent to*

$$\min \sum_{i \in \mathcal{N}} [C_i^O(\mathbf{x}_i) + I_i^{\text{NW}}(\phi_i)] + C^D(\mathbf{l}^P) + \frac{I}{(1+\rho)^\delta} \quad (7.10a)$$

$$\text{s.t. } \phi_i \in \Phi_i \quad \forall i \in \mathcal{N} \quad (7.10b)$$

$$\mathbf{x}_i \in \mathcal{X}_i(\phi_i) \quad \forall i \in \mathcal{N} \quad (7.10c)$$

$$l_{a,t}^b + \sum_{i \in \mathcal{N}} l_{a,t}^i(\mathbf{x}_i) \leq l_a^p \quad \forall a \in \mathcal{A}, t \in \mathcal{T} \quad (7.10d)$$

$$l_a^p \leq \bar{l} \quad \forall a < \delta \quad (7.10e)$$

$$0 \leq \delta \leq |\mathcal{A}| \quad (7.10f)$$

$$\mathbf{l}^P = \{l_a^p\}_{a \in \mathcal{A}}. \quad (7.10g)$$

The proof of Theorem 2 is given in the Appendix. The objective of (7.10) is convex because we assume that $C_i^O(x_i)$, $I_i^{\text{NW}}(\phi_i)$ and $C^D(\mathbf{l}^P)$ are convex, and $\frac{I}{(1+\rho)^\delta}$ is also convex. Constraint (7.10e), however, introduces non-convexities to the feasible solution space. Section 5.5.1 shows how we decompose (7.10) and deal with the large-scale and non-convex nature of the problem. In the rest of this section, we present how uncertainties are treated in the planning problem.

7.4.2 Uncertainty modeling

In this work we consider three major sources of uncertainty: solar irradiation ($\alpha_{a,t}^{\text{PV}}$), base load ($l_{a,t}^{\text{b}}$), and projected load reduction from EE measures ($\alpha_{a,t}^{\text{EE}}$). We formulate the NWAs planning problem as a robust problem because it is less computationally-intensive than its stochastic counterpart and it does not require the underlying density function of the uncertain parameters (we only need the maximum and minimum possible values) [32,104]. Furthermore and perhaps most importantly, utility planning practices typically focus on the worst-case realization. Thus, a robust approach to NWAs planning is likely more attractive to engineers at utilities.

We write Problem 7.10 in compact form as

$$\min_x c^\top x \tag{7.11a}$$

$$\text{s.t. } Ax \leq b. \tag{7.11b}$$

In Problem 7.10, A and b contain the uncertain parameters. We implement uncertainty in b by replacing the inequality with $\tilde{A}\tilde{x} \leq 0$ where $\tilde{A} = [A, -b]$, $\tilde{x} = [x, y]^\top$, and $y = 1$.

Let $a_{i,j}$ denote the i, j element of A . Suppose that $a_{i,j}$ is a randomly distributed parameter with an unknown distribution that takes on values in $[\bar{a}_{ij} - \hat{a}_{ij}, \bar{a}_{ij} + \hat{a}_{ij}]$. Then, as detailed

in [32], the robust counterpart of (7.11) is

$$\begin{aligned}
& \min_{\substack{x, p_{i,j} \\ z_i, y_j}} c^\top x \\
& \text{s.t.} \quad \sum_j a_{i,j} x_j + z_i \cdot \Gamma_i + p_{i,j} \leq b_i \quad \forall i \\
& \quad \quad z_i + p_{i,j} \geq \hat{a}_{i,j} \cdot y_j \quad \forall i, j \in J_i \\
& \quad \quad -y_j \leq x_j \leq y_j \quad \forall j \\
& \quad \quad p_{i,j} \geq 0 \quad \forall i, j \in J_i \\
& \quad \quad y_j \geq 0 \quad \forall j \\
& \quad \quad z_i \geq 0 \quad \forall i.
\end{aligned}$$

Here, the set $J_i = \{j | \hat{a}_{i,j} > 0\}$ and Γ_i is allowed to take on values in $[0, |J_i|]$. The parameter Γ_i adjusts the robustness of the solution and is known as the protection level of the i^{th} constraint ($\Gamma_i = |J_i|$ produces the most robust solution).

Although our robust formulation does not need scenarios of uncertain parameters, we use them for two reasons. First, the scenarios allow us to estimate the maximum and minimum values of an uncertain parameter $a_{i,j}$ that are required to formulate the robust NWAs planning problem. And second, it allows us to evaluate the performance of a NWAs planning solution (e.g., via Monte Carlo simulation as in the case study in this chapter).

We adopt the scenario generation technique introduced in [49] to produce load and solar irradiation scenarios. The technique relies on Generative Adversarial Networks (GANs), a machine learning-based generative model [88]. We base the GANs on a game theory setup between two deep neural networks, the *generator* and the *discriminator*. The generator G transforms input from a known distribution \mathbb{P}_Z (e.g., Gaussian) to an output distribution \mathbb{P}_G . On the other hand, the discriminator D discerns historical data \mathbb{P}_X from the output distribution \mathbb{P}_G . In the case study, we use UW campus load data and solar data from NREL [149].

7.5 Solution techniques

The non-convexity and high-dimensionality of (7.10) present computational challenges that existing solvers cannot directly handle. Consider that for a time step length of 1 hour and a planning horizon of 20 years, the dimensionality of the sets $\mathcal{X}_i(\phi_i)$ ranges from roughly 175,000 for the simplest cases (e.g., solar PV or EE) to more than half a million for the more complex ES case. Considering all four NWAs and the robust formulation, the problem in (7.10) has roughly 2,000,000 variables and constraints.

We decompose (7.10) into $|\mathcal{N}|$ subproblems using the Dantzig-Wolfe Decomposition Algorithm to handle the dimensionality issue. Each NWA falls into a subproblem while a low-dimensional master problem handles the demand charge and the present cost of capacity expansion.

In our case studies, every subproblem is tractable. However, subproblem tractability is not necessarily true for more complex NWAs. Bender's decomposition is a suitable technique to solve non-tractable subproblems since it is designed for problems coupled by variables [55]. For a NWAs subproblem, the investment variables ϕ_i would be the couple the problems defined by the operation variables and constraints during a sufficiently small time horizon (e.g., a year or a month).

The master problem inherits the non-convexities of (7.10). We decompose the master problem and find its solution by solving a small number of small-scale linear programs.

7.5.1 Technique 1: Dantzig-Wolfe Decomposition

The NWA subproblems are given by

$$\min_{\substack{\phi_i \in \Phi_i \\ \mathbf{x}_i \in \mathcal{X}_i(\phi_i)}} C_i^O(\mathbf{x}_i) + I_i^{\text{NW}}(\phi_i) + \underbrace{\sum_{a \in \mathcal{A}} \sum_{t \in \mathcal{T}} \pi_{a,t}^1 \cdot l_{a,t}^i(\mathbf{x}_i)}_{\text{penalty term}}$$

for all $i \in \mathcal{N}$. The objective of subproblem i is composed of the operation cost $C_i^O(\mathbf{x}_i)$, investment cost $I_i^{\text{NW}}(\phi_i)$, and a term that penalizes the load $l_{a,t}^i(\mathbf{x}_i)$ by $\pi_{a,t}^1$. The penalty coefficients $\pi_{a,t}^1$ are the dual variables of the coupling constraints (7.13b) in the master problem. The operating and investment decisions must be in their respective set of feasible solutions.

We write the master problem as

$$\min_{\delta, \mathbf{l}^P, \lambda_k} \left\{ \sum_{k=1}^K \lambda_k \cdot C_{(k)}^{\text{prop}} + C^D(\mathbf{l}^P) + \frac{I}{(1+\rho)^\delta} \right\} \quad (7.13a)$$

$$\text{s.t. } l_{a,t}^b + \sum_{k=1}^K \lambda_k \cdot l_{a,t,(k)}^{\text{prop}} \leq l_a^P \quad (\pi_{a,t}^1) \quad \forall a \in \mathcal{A}, t \in \mathcal{T} \quad (7.13b)$$

$$l_a^P \leq \bar{l} \quad \forall a \in \mathcal{A} \quad (7.13c)$$

$$0 \leq \delta \leq |\mathcal{A}| \quad (7.13d)$$

$$\mathbf{l}^P = \{l_a^P\}_{a \in \mathcal{A}} \quad (7.13e)$$

$$\sum_{k=1}^K \lambda_k = 1 \quad (\pi^2) \quad (7.13f)$$

$$\lambda_k \geq 0 \quad \forall k = 1, \dots, K \quad (7.13g)$$

$$(7.13h)$$

and its objective is to minimize the sum of three terms: a convex combination of K cost proposals, peak demand charges, and the present cost of capacity expansion. The k^{th} cost proposal is

$$C_{(k)}^{\text{prop}} = \sum_{i \in \mathcal{N}} C_i^O(\mathbf{x}_{i,(k)}) + I_i^{\text{NW}}(\phi_{i,(k)})$$

where $x_{i,(k)}$ and $\phi_{i,(k)}$ represent optimal operating and investment decisions, respectively, for the k^{th} iteration. The positive variables λ_k are the weights of each cost proposal. The coupling constraints are (7.13b). We define the load proposals as

$$l_{a,t,(k)}^{\text{prop}} = \sum_{i \in \mathcal{N}} l_{a,t}^i(x_{i,(k)}).$$

Constraints (7.13c), (7.13d), and (7.13e) originate from (7.10e), (7.10f), and (7.10g), respectively. Finally, (7.13f) and (7.13g) ensure that the sum of all λ_k 's equals one and that they are all non-negative. We skip the detailed description of the well-known Dantzig-Wolfe Decomposition. The interested reader is referred to [55] for an in-depth description and an implementation of the DWDA.

When decomposing (7.10), the non-convex Constraint (7.10e) lies in master problem. We solve the master problem by solving at most $|\mathcal{A}| + 1$ linear problems. Let $P(j)$ represent a function that sets $\delta = j$ in (7.13) and solves for \mathbf{l}^P and λ_k . A concrete interpretation of $P(j)$ is that capacity expansion happens at year j and the peak load limit \bar{l} is enforced from year 1 through j . Note that the function P involves solving a small-scale linear problem. The number of variables in P is $K + |\mathcal{A}|$ where K is in the order of a few hundred and $|\mathcal{A}|$ is close to 20.

The master problem-solving algorithm is as follows. We solve $P(j)$ for starting with $j = 0$ and increasing j by one after each iteration. If $P(j) > P(j - 1)$, $P(j)$ is the optimal solution to the master problem³. If $P(j)$ is infeasible, i.e., capacity expansion cannot be delayed further than year $j - 1$, $P(j - 1)$ is the optimal solution. Algorithm 1 describes the master problem-solving algorithm.

7.5.2 Technique 2

The standard implementation of the DWDA may exhibit slow convergence rates due to a phenomenon called the “tailing-off effect” [129]. In practice, the slow convergence of a long-term planning problem is not an issue. In contrast, a fast convergence of control and short-term planning problems is critical since the delivery of solutions is time-sensitive. Therefore, we provide an alternative solution technique that may converge faster than the DWDA in some instances. Technique 2 is applicable only if (7.10) is tractable when we we fix $\delta = j$.

Technique 2 consists of replacing P in Algorithm 1 with the NWAs planning prob-

³Since the master objective is convex, if $P(j) > P(j - 1)$, then $P(j + a) > P(j) \forall a \in \mathbb{Z}_+$.

```

Input:  $P, |\mathcal{A}|$ 
Output: objective value
 $j \leftarrow 0$ 
while  $j \leq |\mathcal{A}|$  and objective value =  $\emptyset$  do
  if  $P(j)$  is feasible then
    if  $j > 0$  and  $P(j) < P(j - 1)$  then
      | objective value  $\leftarrow P(j - 1)$ 
    end
    else if  $j = |\mathcal{A}|$  then
      | objective value  $\leftarrow P(j)$ 
    end
  end
  else
    | objective value  $\leftarrow P(j - 1)$ 
  end
   $j \leftarrow j + 1$ 
end

```

Algorithm 1: Master-problem solving algorithm.

lem (7.10). Similar to the master problem-solving algorithm, we fix $\delta = j$ to convexify (7.10). While this alternative may converge faster, it is not as scalable as the DWDA approach. Technique 1 handles each NWA separately while technique 2 solves a large-scale linear problem.

7.6 Case study: non-wire alternatives for the University of Washington

The University of Washington (UW) expects to add 6 million square feet of new buildings (e.g., labs, classrooms, office space) to its Seattle Campus during the next ten years [17]. The additional load from new buildings will likely require an expansion of the capacity to serve the campus.

Seattle City Light (SCL) and the UW are considering several traditional solutions to manage the expected load increase. The traditional solutions include building a new feeder to campus or increasing the service voltage to sub-transmission levels. However, these solutions are hard to implement in Seattle's dense urban environment and come at an estimated cost in the order of \$100 million. Moreover, there is an increasing appetite by SCL, the Washington

Table 7.1: Non-wire alternatives parameters

Parameter	Value	Source
Energy Efficiency		
Investment cost function	piece-wise linear	[41] ⁴
Demand response		
Investment cost	\$200/kW	[163]
Efficiency coefficient	1.1	modeling assumption
Energy Storage		
Investment cost	\$250/kWh	[110]
Ch./dis. efficiency	0.97/0.95	[184]
Degradation coefficient	0.028 kWh/kW	[184]
Energy-to-power ratio	4	[15]
Solar photovoltaics		
Investment cost	\$2/W	[81]
Production profile	-	[149]

State government, and the UW to explore novel approaches such as NWAs.

7.6.1 Data

Table 7.1 summarizes the main parameters of the NWAs. We assume that the cost of substation upgrades is \$100 million and adhere to a standard SCL planning horizon of 20 years. We assume a yearly discount rate of 7% and rates based on the high-demand customer rates for the City of Seattle [10].

We use National Renewable Energy Lab (NREL) PV output data from a site near Seattle to generate PV scenarios [149]. Seattle City Light (SCL) campus load data from the years 2011 to 2016 to generate load scenarios. Furthermore, we incorporate SCL’s projected load growth of 1.5% to 3.5% with respect to 2016 load to the scenario-generation algorithm.

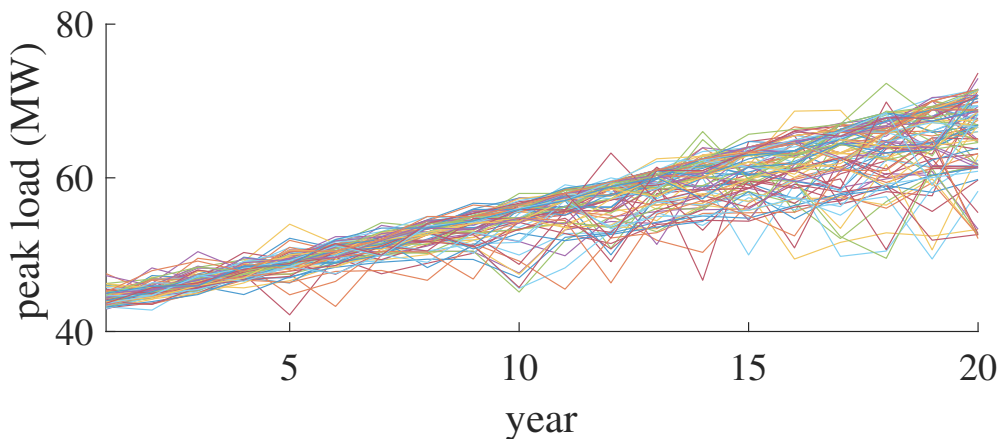


Figure 7.1: Campus peak load scenarios.

Fig. 7.1 shows the yearly peak load of each scenario. We solve this case study using Algorithm 2.

7.6.2 Long-term planning results

The main “knob” available to tune the results of the NWAs planning problem is the uncertainty protection level Γ_i . In this case study, we vary a single protection parameter $\Gamma \in [0, 1]$ and set all Γ_i 's equals to it, i.e., $\Gamma = \Gamma_i \forall i$.

We interpret Γ as follows. Suppose that we expect the load at point in time to be within 50 ± 5 MW. Then, with a protection level of Γ , we optimize for the worst-case realization in the range $50 \pm 5 \cdot \Gamma$ MW. For instance, with a protection level of 0.5, the optimization problem considers load realizations within 50 ± 2.5 MW. With higher Γ 's we consider a broader range of possibilities and thus produce more robust solutions.

However, more robust solutions represent higher costs. As shown in Fig. 7.2, higher values of Γ produce more expensive solutions to the NWAs planning problem. The solutions are more expensive in part because, as shown in Fig.7.3, expanding capacity earlier (at a higher present cost) produces more robust solutions.

The level of protection also impacts the optimal mix of NWAs. As shown in Fig. 7.4,

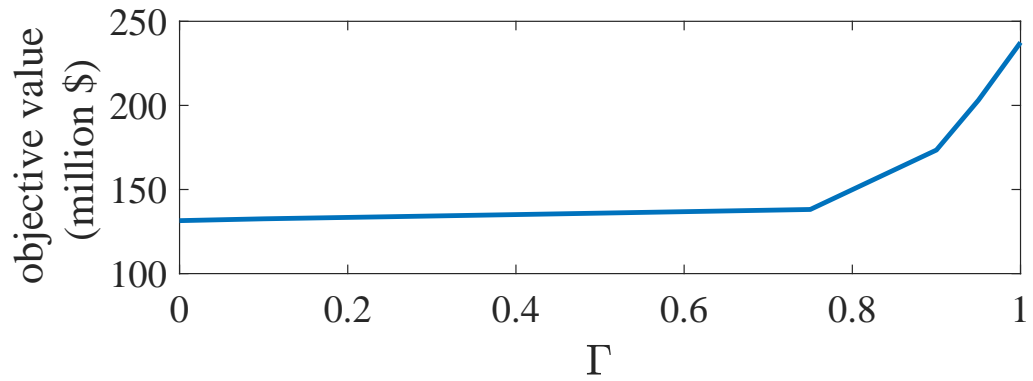


Figure 7.2: NWAs planning problem objective value as a function of the protection level Γ .

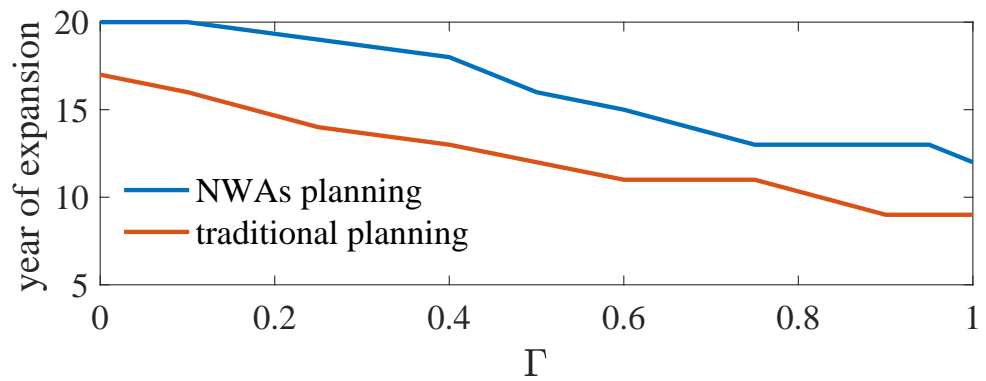


Figure 7.3: Year of expansion for traditional and NWAs-base planning as a function of the protection level Γ .

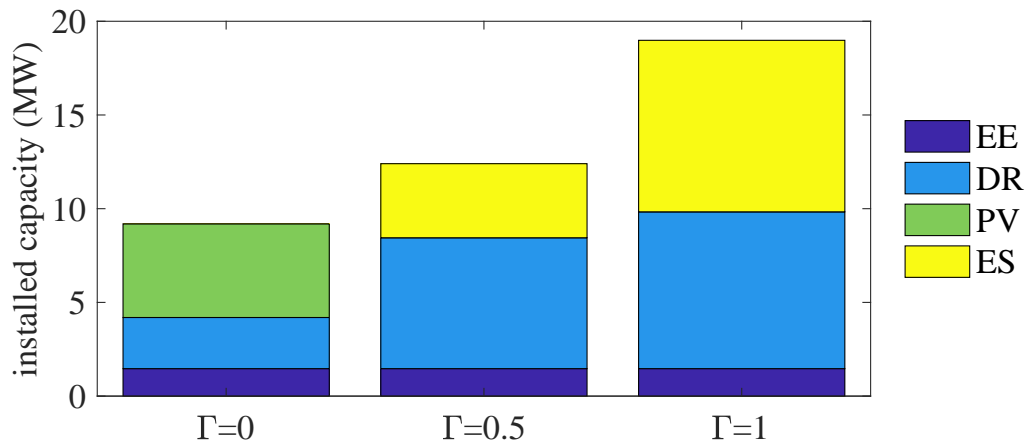


Figure 7.4: Installed NWAs capacities for three values of Γ : 0, 0.5, and 1.

solutions under large Γ favor dependable technologies such as DR and ES. Conversely, small $\Gamma = 1$ ignores risks associated with uncertain PV production and thus favors the installation of solar PV.

7.6.3 NWAs solution assessment via Monte Carlo simulations

Whether we plan with a large or small protection level does not impact the realization of the uncertain parameters in the real-time. We perform Monte Carlo simulations on the possible realization of load and solar scenarios to assess the performance of the NWAs planning solution.

Perhaps the most dreaded consequence of planning a system without enough spare capacity, i.e., a non-robust system, is load-shedding. Fig. 7.5 shows the probability density of shedding load as a function of the protection level of the NWAs planning problem solution. For the most part and as expected, load shedding decreases with Γ .

Load-shedding at U.S. university campuses such as the University of Washington is undesirable. Thus, the UW campus should plan for NWAs with a Γ guarantees no load shedding. That is, the planning problem should be solved with Γ equal or close to 1.

However, not every load requires such a high level of reliability. The maximum price

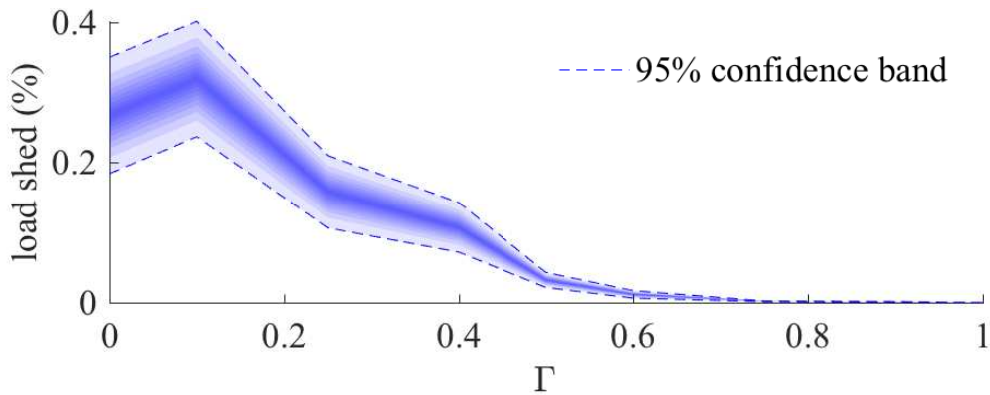


Figure 7.5: Load shed (as percentage of total load) as a function of Γ .

a load would be willing to pay not to be disconnected is known as the value of lost load (VOLL). For instance, the study in [123] estimates that residential loads in Northern Ireland are willing to pay up to 18€/kWh⁵ to avoid load disconnections.

7.6.4 How to select the level of protection?

Although Γ can be intuitively interpreted as in Section 7.6.2, we believe Γ is too abstract to be readily determined by practitioners. Alternatively, a particular load could select a level of robustness that corresponds to its VOLL. Thus, we propose that for a given VOLL, we select the value of Γ that minimizes the sum of

1. investment costs (NWAs and capacity expansion),
2. expected energy costs,
3. expected peak demand charges,
4. and the expected cost of lost load

over the optimization horizon.

For instance Fig. 7.6 shows the total costs for two different VOLL. The left-hand plot shows the probability density of the total cost for VOLL = 10/kWh and its expected value

⁵In 2007 €.

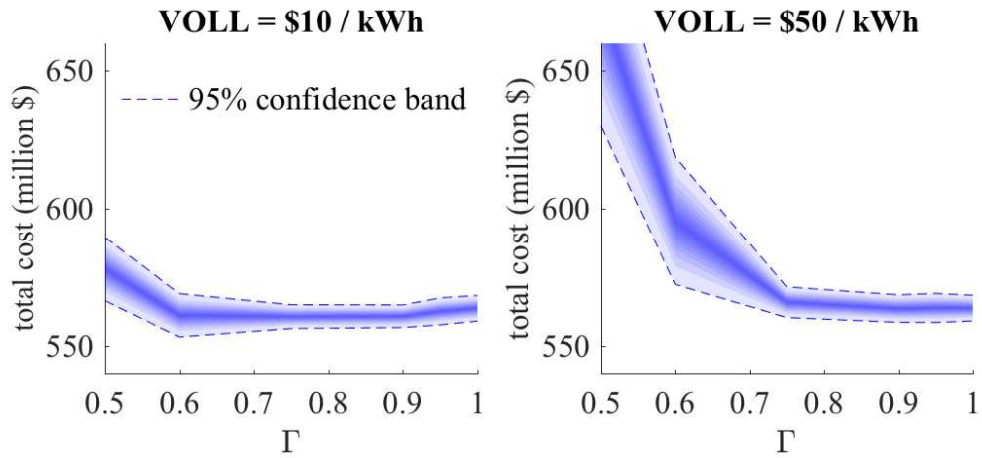


Figure 7.6: Total as a function of Γ for two different values of lost load.

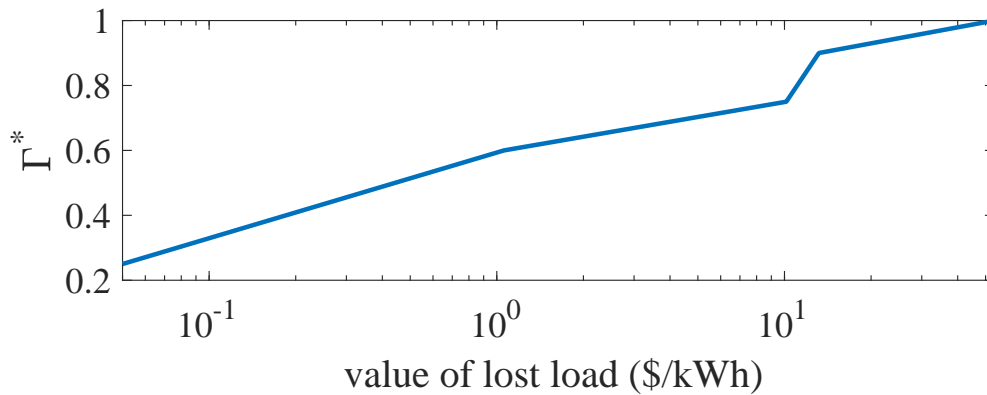


Figure 7.7: Optimal protection level as a function of VOLL. We define the optimal protection level Γ^* for a given VOLL as the Γ that minimizes the expected total cost.

reaches a minimum at $\Gamma \approx 0.6$. The right-hand plot, on the other hand, shows the probability density of the total cost for $\text{VOLL} = 50/\text{kWh}$ and its expected value reaches a minimum at a Γ closer to 1. Thus, a customer whose VOLL is $= 10/\text{kWh}$ would plan using $\Gamma \approx 0.6$ while a customer with a VOLL of $= 10/\text{kWh}$ would plan using $\Gamma \approx 1$. We plot the value of Γ that minimizes the expected total cost, Γ^* , as a function of VOLL in Fig. 7.6. Then, one can graphically map its VOLL to the appropriate Γ to use in the NWAs planning problem.

One might ask, why not use the VOLL and minimize the expected total cost via stochastic optimization? That would be a good approach except for the fact that stochastic optimization is computationally more expensive than our robust optimization approach⁶. Thus, the approach outlined in this chapter is friendly to limited computing resources.

7.7 Conclusion

We present a planning problem that determines investment and operation of distributed energy resources (DERs) and timing of capacity expansion. Considering the timing of capacity expansion has two interesting implications. First, it allows DERs to manage load and act as non-wire alternatives to capital-intensive capacity expansion. Second, it makes investments in DERs more attractive by explicitly accounting for the benefit of delaying capacity expansion investment. We formulate the problem as a large-scale non-convex robust optimization problem. We tackle with the size of the problem by decomposing it using the Dantzig-Wolfe Decomposition Algorithm. We deal with its non-convexity by further decomposing the master problem into a small number of linear programs. Additionally, we present a case study that considers solar photovoltaic generation, energy efficiency, energy storage, and demand response as alternatives to substation/feeder upgrades at the University of Washington.

⁶The computational cost of an stochastic optimization problem increases with the number of scenarios. On the other hand, the size of robust optimization problems remains constant with the number of scenarios.

Chapter 8

CONCLUSION AND SUGGESTIONS FOR FUTURE WORK

This dissertation addresses five of the many challenges of distributed energy resources (DERs) integration. The first one is the need for models of demand-side flexibility suitable to typical power system optimization and control frameworks. In Chapter 3, we propose a data-driven, mathematically and computationally simple (thus compatible in many power system applications), and statistically robust (i.e., predictions are feasible during operation with a degree of confidence). The main alternative to our model is the resistance-capacitance (RC) model of thermal dynamics which may or may not be data-driven, is simple, but is not robust. Robustness is an essential characteristic for system operators (SOs) as non-robust models may lead to control signals that are not attainable during operation and could introduce uncertainty to the system operation.

The second challenge is the need for models of an aggregator's relationship with its constituent DERs. The relationship model is essential to predict the aggregator's behavior in electricity markets. In Chapter 4, we argue that it is reasonable to assume that the players will settle on a long-term, Pareto-efficient, and cooperative equilibrium determined by Nash Bargaining Theory. This result is significant because it justifies reducing a model composed of many autonomous agents to a simpler one in which all DERs act as if they were owned and operated by a single entity.

The third challenge is the need for DER coordination schemes. DERs often interact with each other, e.g., in microgrids. In such cases, coordination between is needed to achieve optimal decisions (e.g., reduce peak demand) or observe shared constraints (e.g., distribution system constraints). Ideally, a group of interacting DERs would follow instructions from a central decision-maker. However, centralized control may not be possible due to pri-

vacy of data and software/data incompatibilities. In Chapter 5, we present a mixed-integer adaptation of the Dantzig-Wolfe Decomposition Algorithm (DWDA) for privacy-friendly coordination of a building and a fleet of electric vehicles (EVs). We show three instances where our coordination algorithm is useful and delivers optimal decisions.

Chapter 6 addresses the problem of market power, an issue not exclusive to DERs nor even to the electric power industry. However, market power could, in theory, arise from an aggregator controlling large amounts of DERs¹. We propose a pricing scheme that incentivizes a generic firm (i.e., the firm can be a producer, consumer, or a prosumer) to participate in a market in accordance to the social optimum. Additionally, our pricing scheme does not require private information and provides a transparent instrument for the regulation of the firm's profit.

The fifth and final challenge addressed by this dissertation is the non-wire alternatives (NWAs) planning problem whose objective is to select DER investment and operation decisions that minimize DER investment costs, operating costs, and the present cost of capacity expansion. Typically, DER planning focuses on the first two costs while our NWA approach accounts for the third cost as an additional value stream. Incorporating the present cost of capacity expansion introduces non-convexities to an already high-dimensional problem. We tackle the dimensionality issue by decomposing the problem along each DER using the DWDA. Then, we decompose the non-convex but small master problem into a small number of easy-to-solve linear problems.

Suggestions for future work

We are long ways from developing the algorithms, technologies, and processes needed to incorporate as many DERs of as many kinds as we would like. Here we provide possible extensions to the work presented in this dissertation.

As a general observation, I would encourage researchers to focus on practical application.

¹Recall that, as shown in Chapter 4, even autonomous and self-interested DERs may settle at an equilibrium that is equivalent to them being owned and controlled by a single entity.

While theoretical results are and will continue to be valuable, I believe there is a more imperative need for research and innovation that is closer to real-world applications.

Chapter 3: Modeling the Flexibility of Buildings

One of the obvious shortcomings of Chapter 3 is that we restrict ourselves to heating, ventilation, and air conditioning (HVAC) systems. SOs would benefit from generalizing the kind of data-driven modeling that we present to other types of flexible loads, e.g., database processes and washing machines, chemistry-based energy storage, etc. Researchers could expand on our work by validating and adapting the models with data from real buildings².

Chapter 4: Modeling an Aggregator

The work in Chapter 4 could be expanded by refining the aggregator-DER model to better reflect reality. Refinements could be towards an increase in generality of the model, e.g., the effect of market price uncertainty, imperfect information, competition among several aggregators, or an expanded strategy space for the repeated game model. Alternatively, the refinements could reflect specific instances of the problem, e.g., the effect of particular regulations, the composition of the DERs population, or a specific business model. Another valuable (but challenging) research direction is to validate the DER-aggregator relationship model against empirical data.

Chapter 5: Coordination of Buildings and Electric Vehicles

In Chapter 5, we consider buildings and EVs that, although unwilling or unable to share data, provide truthful information to the master problem. An interesting research direction is to examine what happens when one or more of the players (or the communication channels) are not reliable or cannot be trusted.

²In our work, we use EnergyPlus simulated data instead of real data.

Chapter 6: Market Power

The market power model of Chapter 6 could be enhanced to make the strategic bidding model better reflect reality. As it stands, Chapter 6 assumes a “controlled” environment, e.g., the firm acts on *perfect* information, the regulator can properly set the profit-regulation constants, etc. It is unclear how the market power mitigation price (MPMP) would perform under incomplete information. Furthermore, the long-term impacts of the MPMP are unclear and not guaranteed to be better than the presence of market power. Nonetheless, we believe that the idea of a pricing mechanism that equates a situation of market power abuse to the social optimum is a compelling idea that could be used to design incentives in other (potentially very different) settings.

Chapter 7: non-wire alternatives to capacity expansion

One of the reasons why traditional capacity expansion is beloved by system planners is that its performance is *certain* and, in a good way, “*boring*.” Absent a loss of distribution system infrastructure we can be sure that the capacity of a feeder or substation is available. The certainty of availability is not the case (or is not perceived to be the case) for NWAs. Thus, a research direction is to further explore the uncertainty of the NWAs planning problem, both at the investment stage and at the operation stage. I believe system planners would be glad to embrace NWAs once their performance is as predictable and boring as the traditional capacity expansion solutions.

BIBLIOGRAPHY

- [1] Centrica. <https://www.centrica.com/>. Accessed: 2018-04-27.
- [2] Drift. <https://www.joindrift.com>. Accessed: 2018-04-27.
- [3] Electric Vehicles: Tax Credits and Other Incentives. <https://www.energy.gov/eere/electricvehicles/electric-vehicles-tax-credits-and-other-incentives>. Accessed: 2018-04-27.
- [4] EnerNOC. <https://www.enernoc.com>. Accessed: 2018-04-27.
- [5] REAL Lab Library. <http://www.ee.washington.edu/research/real/library.html>.
- [6] Tesla Powerwall. <https://www.tesla.com/powerwall>. Accessed: 2018-04-27.
- [7] Tesla Solar Panels. <https://www.tesla.com/solarpanels>. Accessed: 2018-04-27.
- [8] Benefits of demand response in electricity markets and recommendations for achieving them. Technical report, U.S. Department of Energy, 2006.
- [9] *2011 Buildings Energy Data Book*. U.S. Dept. of Energy, Office of Energy Efficiency and Renewable Energy, 2012.
- [10] High Demand General Service: City. Electric Rates and Provisions, City of Seattle - City Light Department, 2012.
- [11] Global EV outlook. Technical report, Clean Energy Ministerial Secretariat, 2013.
- [12] A Review of Distributed Energy Resources. Technical report, New York Independent System Operator, prepared by DNV GL, September 2014.
- [13] Southern California Edison: Tariffs, 2015.
- [14] How Energy Storage Can Participate in New England's Wholesale Electricity Markets. http://www.iso-ne.com/static-assets/documents/2016/01/final_storage_letter_cover_paper.pdf, March 2016.

- [15] Levelized cost of storage - version 2.0, 2016.
- [16] Smart home, seamless life unlocking a culture of convenience. <https://www.pwc.com/us/en/industry/entertainment-media/publications/consumer-intelligence-series/assets/pwc-consumer-intelligence-series-iot-connected-home.pdf>, January 2017. Accessed: 2018-05-02.
- [17] University of Washington 2018 Seattle Campus Master Plan. Online, July 2017.
- [18] C. D. Ahrens. Transition to very high share of renewables in germany. *CSEE Journal of Power and Energy Systems*, 3(1):17–25, March 2017.
- [19] Mudathir Funsho Akorede, Hashim Hizam, and Edris Pouresmaeil. Distributed energy resources and benefits to the environment. *Renewable and Sustainable Energy Reviews*, 14(2):724 – 734, 2010.
- [20] M. J. E. Alam, K. M. Muttaqi, and D. Sutanto. A novel approach for ramp-rate control of solar pv using energy storage to mitigate output fluctuations caused by cloud passing. *IEEE Transactions on Energy Conversion*, 29(2):507–518, June 2014.
- [21] A. Alarcon-Rodriguez, E. Haesen, G. Ault, J. Driesen, and R. Belmans. Multi-objective planning framework for stochastic and controllable distributed energy resources. *IET Renewable Power Generation*, 3(2):227–238, June 2009.
- [22] M.H. Albadi and E.F. El-Saadany. A summary of demand response in electricity markets. *Electric Power Systems Research*, 78(11):1989 – 1996, 2008.
- [23] C. Altay and H. Delic. Distributed energy management of microgrids with Dantzig-Wolfe decomposition. In *IEEE PES Innovative Smart Grid Technologies, Europe*, pages 1–5, Oct 2014.
- [24] Maria Carmela Aprile, Vincenzina Caputo, and Rodolfo M. Nayga Jr. Consumers preferences and attitudes toward local food products. *Journal of Food Products Marketing*, 22(1):19–42, 2016.
- [25] Jay Apt. The spectrum of power from wind turbines. *Journal of Power Sources*, 169(2):369–374, 2007.
- [26] G. V. S. Babu and V. Ganesh. Power quality enhancement in distributed energy resources by four leg voltage source converter. In *2017 International Conference on Innovative Mechanisms for Industry Applications (ICIMIA)*, pages 327–331, Feb 2017.

- [27] Peder Bacher and Henrik Madsen. Identifying suitable models for the heat dynamics of buildings. *Energy and Buildings*, 43(7):1511 – 1522, 2011.
- [28] Galen Barbose, Naïm Darghouth, Samantha Weaver, and Ryan Wiser. Tracking the sun vi: An historical summary of the installed price of photovoltaics in the united states from 1998 to 2012. Technical report, Ernest Orlando Lawrence Berkeley National Laboratory, Berkeley, CA (US), 2013.
- [29] J. P. Barton and D. G. Infield. Energy storage and its use with intermittent renewable energy. *IEEE Transactions on Energy Conversion*, 19(2):441–448, June 2004.
- [30] Jovan Bebić, Gene Hinkle, Slobodan Matić, and William Schmitt. Grid of the future: Quantification of benefits from flexible energy resources in scenarios with extra-high penetration of renewable energy. Technical report, General Electric, Fairfield, CT, 2015.
- [31] A. S. Talhar Belge and S. B. Bodkhe. Use of solar energy for green building reduction in the electricity bill of residential consumer. In *2017 IEEE Region 10 Symposium (TENSymp)*, pages 1–6, July 2017.
- [32] Dimitris Bertsimas and Melvyn Sim. Robust discrete optimization and network flows. *Mathematical programming*, 98(1-3):49–71, 2003.
- [33] Dimitris Bertsimas and John Tsitsiklis. *Introduction to Linear Optimization*. Athena Scientific, 1st edition, 1997.
- [34] Ken Binmore, Ariel Rubinstein, and Asher Wolinsky. The nash bargaining solution in economic modelling. *The RAND Journal of Economics*, 17(2):176–188, 1986.
- [35] Milorad Boji, Novak Nikoli, Danijela Nikoli, Jasmina Skerli, and Ivan Mileti. A simulation appraisal of performance of different HVAC systems in an office building. *Energy and Buildings*, 43(6):1207 – 1215, 2011.
- [36] Severin Borenstein and James Bushnell. The US electricity industry after 20 years of restructuring. *Annual Review of Economics*, 7(1):437–463, 2015.
- [37] Mohamed Boubekri, Robert B. Hulliv, and Lester L. Boyer. Impact of window size and sunlight penetration in office worker’s mood and satisfaction. *Environment and Behavior*, 23(3), July 1991.
- [38] Franois Bouffard and Daniel S. Kirschen. Centralised and distributed electricity systems. *Energy Policy*, 36(12):4504 – 4508, 2008. Foresight Sustainable Energy Management and the Built Environment Project.

- [39] Stephen Boyd, Neal Parikh, Eric Chu, Borja Peleato, and Jonathan Eckstein. Distributed optimization and statistical learning via the alternating direction method of multipliers. *Foundations and Trends® in Machine Learning*, 3(1):1–122, 2011.
- [40] Stephen Boyd and Lieven Vandenberghe. *Convex optimization*. Cambridge university press, 2004.
- [41] Rich Brown, Sam Borgeson, Jon Koomey, and Peter Biermayer. Us building-sector energy efficiency potential. 2008.
- [42] W. A. Bukhsh, C. Zhang, and P. Pinson. An integrated multiperiod opf model with demand response and renewable generation uncertainty. *IEEE Transactions on Smart Grid*, 7(3):1495–1503, May 2016.
- [43] Scott Burger, Jose Pablo Chaves-Ávila, Carlos Batlle, and Ignacio J Pérez-Arriaga. The value of aggregators in electricity systems. Technical report, MIT Center for Energy and Environmental Policy Research, 2016.
- [44] Lus Cabral. The california energy crisis. *Japan and the World Economy*, 14(3):335 – 339, 2002. Production Technology and Productivity Growth.
- [45] Maria Castilla, Jose Domingo Alvarez, Francisco Rodriguez Diaz, and Manuel Berenguel. *Comfort in Buildings*. Advances in Industrial Control. Springer London, 2014.
- [46] Dimitris I. Chatzigiannis, Grigoris A. Dourbois, Pandelis N. Biskas, and Anastasios G. Bakirtzis. European day-ahead electricity market clearing model. *Electric Power Systems Research*, 140(Supplement C):225 – 239, 2016.
- [47] C. Chen, J. Wang, and S. Kishore. A distributed direct load control approach for large-scale residential demand response. *IEEE Transactions on Power Systems*, 29(5):2219–2228, Sept 2014.
- [48] Y. Chen, Y. Shi, and B. Zhang. Modeling and optimization of complex building energy systems with deep neural networks. In *Asilomar Conference on Signals, Systems and Computers*, 2017.
- [49] Yize Chen, Yishen Wang, Daniel Kirschen, and Baosen Zhang. Model-free renewable scenario generation using generative adversarial networks. *IEEE Transactions on Power Systems*, 33(3):3265–3275, 2018.

- [50] V Chvatal. *Linear Programming*. Series of Books in the Mathematical Sciences. W. H. Freeman, 1983.
- [51] Jon Coaffee. Risk, resilience, and environmentally sustainable cities. *Energy Policy*, 36(12):4633 – 4638, 2008. Foresight Sustainable Energy Management and the Built Environment Project.
- [52] Jaquelin Cochran, Mackay Miller, Owen Zinaman, Michael Milligan, Doug Arent, Bryan Palmintier, Mark O’Malley, Simon Mueller, Eamonn Lannoye, Aidan Tuohy, et al. Flexibility in 21st century power systems. Technical Report TP-6A20-61721, National Renewable Energy Laboratory (NREL), Golden, CO., May 2014.
- [53] M. Coddington, D. Sciano, and J. Fuller. Change in Brooklyn and Queens: How New York’s Reforming the Energy Vision Program and Con Edison Are Reshaping Electric Distribution Planning. *IEEE Power and Energy Magazine*, 15(2):40–47, March 2017.
- [54] New York Public Service Commission et al. Reforming the energy vision: Nys department of public service staff report and proposal. Technical report, Case 14-M-0101, April 24, 2014.
- [55] Antonio J Conejo et al. *Decomposition techniques in mathematical programming: engineering and science applications*. Springer Science & Business Media, 2006.
- [56] J. E. Contreras-Ocaña, Y. Wang, M. A. Ortega-Vazquez, and B. Zhang. Energy storage: Market power and social welfare. In *2017 IEEE Power Energy Society General Meeting*, pages 1–5, July 2017.
- [57] Jesus E. Contreras-Ocaña, Miguel A. Ortega-Vazquez, Daniel S. Kirschen, and Baosen Zhang. Tractable and robust modeling of building flexibility using coarse data. *to appear in IEEE Transaction on Power Systems*, 2018.
- [58] Jesus E. Contreras-Ocaña, Miguel A. Ortega-Vazquez, and Baosen Zhang. Participation of an energy storage aggregator in electricity markets. *to appear in IEEE Transactions on Smart Grid*, 2018.
- [59] Jesus E. Contreras-Ocaña, Mushfiqur R. Sarker, and Miguel A. Ortega-Vazquez. Decentralized coordination of a building manager and an electric vehicle aggregator. *IEEE Transactions on Smart Grid*, 9(4):2625–2637, July 2018.
- [60] Jesus E. Contreras-Ocaña, Uzma Siddiqi, and Baosen Zhang. Non-wire alternatives to capacity expansion. *to appear in the proceedings of the 2018 IEEE Power and Energy General Meeting*, Aug 2018.

- [61] C. Le Coq and H. Orzen. Price caps and fluctuating demands in electricity markets: Experimental evidence of competitive bidding. In *2012 9th International Conference on the European Energy Market*, pages 1–4, May 2012.
- [62] Steve Corneli, Steve Kihm, and Lisa Schwartz. Electric industry structure and regulatory responses in a high distributed energy resources future. Technical report, Lawrence Berkeley National Laboratory (LBNL), Berkeley, CA (United States), 2015.
- [63] Kenneth W. Costello and Ross C. Hemphill. Electric utilities death spiral: Hyperbole or reality? *The Electricity Journal*, 27(10):7 – 26, 2014.
- [64] Drury B Crawley, Linda K Lawrie, Frederick C Winkelmann, Walter F Buhl, Y Joe Huang, Curtis O Pedersen, Richard K Strand, Richard J Liesen, Daniel E Fisher, Michael J Witte, et al. Energyplus: creating a new-generation building energy simulation program. *Energy and Buildings*, 33(4):319–331, 2001.
- [65] J. Cruz. Leader-follower strategies for multilevel systems. *IEEE Transactions on Automatic Control*, 23(2):244–255, Apr 1978.
- [66] Goerge B. Dantzig and Philip Wolfe. Decomposition Principle for Linear Programs. *Operations Research*, 8, February 1960.
- [67] A. Kumar David and Fushuan Wen. Market power in electricity supply. *IEEE Transactions on Energy Conversion*, 16(4):352–360, Dec 2001.
- [68] Paul Denholm, Erik Ela, Brendan Kirby, and Michael Milligan. The role of energy storage with renewable electricity generation. Technical Report TP-6A2-47187, National Renewable Energy Laboratory, 2010.
- [69] Paul Denholm, Jennie Jorgenson, Marissa Hummon, Thomas Jenkin, David Palchak, Brendan Kirby, Ookie Ma, and Mark OMalley. The value of energy storage for grid applications. *Contract*, 303:275–3000, 2013.
- [70] Michael Deru, Kristin Field, Daniel Studer, Kyle Benne, Brent Griffith, Paul Torcellini, et al. U.S. Department of Energy commercial reference building models of the National Building Stock. Technical report, National Renewable Energy Laboratory, 2011.
- [71] Iain Dunning, Joey Huchette, and Miles Lubin. Jump: A modeling language for mathematical optimization. *SIAM Review*, 59(2):295–320, 2017.
- [72] Yury Dvorkin. Can merchant demand response affect investments in merchant energy storage? *to appear in IEEE Transactions on Power Systems*, 2018.

- [73] Yury Dvorkin, Ricardo Fernandez-Blanco, Daniel S. Kirschen, Hrvoje Pandzic, J. P. Watson, and Cesar A. Silva-Monroy. Ensuring profitability of energy storage. *IEEE Transactions on Power Systems*, 32(1):611–623, Jan 2017.
- [74] Cherrelle Eid, Javier Reneses Guilln, Pablo Frasn Marn, and Rudi Hakvoort. The economic effect of electricity net-metering with solar pv: Consequences for network cost recovery, cross subsidies and policy objectives. *Energy Policy*, 75:244 – 254, 2014.
- [75] Gregory Elcock. Brooklyn Queens demand management program: Implementation and outreach plan, 2016.
- [76] Jonathan Farland. Zonal and regional load forecasting in the new england wholesale electricity market: A semiparametric regression approach. Master’s thesis, University of Massachusetts Amherst, 2013.
- [77] Brion Feinberg. Coercion functions and decentralized linear programming. *Mathematics of Operations Research*, 14(1), 2009.
- [78] FERC Order No 888. Promotion of wholesale competition through open access non-discriminatory transmission services by public utilities and recovery of stranded costs by public utilities and transmitting utilities. April 1996.
- [79] Organization for Economic Co-operation and Development. Glossary of Industrial Organisation Economics and Competition Law, 1993.
- [80] Antonio Frangioni and Bernard Gendron. A stabilized structured dantzig–wolfe decomposition method. *Mathematical Programming*, 140(1):45–76, 2013.
- [81] Ran Fu, David Feldman, Robert Margolis, Kristen Ardani, and Mike Woodhouse. NREL US Solar Photovoltaic System Cost Benchmark Q1 2016 Report. Technical Report TP-6A20-66532, NREL, Golden, CO, September 2016.
- [82] Wei Fu and Patrick O Perry. Estimating the number of clusters using cross-validation. *arXiv preprint arXiv:1702.02658*, 2017.
- [83] Cary Funk and Brian Kennedy. The politics of climate. October 2016.
- [84] H. A. Gil and G. Joos. On the quantification of the network capacity deferral value of distributed generation. *IEEE Transactions on Power Systems*, 21(4):1592–1599, Nov 2006.

- [85] H. A. Gil and G. Joos. Customer-owned back-up generators for energy management by distribution utilities. *IEEE Transactions on Power Systems*, 22(3):1044–1050, Aug 2007.
- [86] T. Gonen and I. J. Ramirez-Rosado. Optimal multi-stage planning of power distribution systems. *IEEE Transactions on Power Delivery*, 2(2):512–519, April 1987.
- [87] N. Good, E. Karangelos, A. Navarro-Espinosa, and P. Mancarella. Optimization under uncertainty of thermal storage-based flexible demand response with quantification of residential users discomfort. *IEEE Transactions on Smart Grid*, 6(5):2333–2342, Sept 2015.
- [88] Ian Goodfellow, Jean Pouget-Abadie, Mehdi Mirza, Bing Xu, David Warde-Farley, Sherjil Ozair, Aaron Courville, and Yoshua Bengio. Generative adversarial nets. In *Advances in neural information processing systems*, pages 2672–2680, 2014.
- [89] M.M. Gouda, S. Danaher, and C.P. Underwood. Building thermal model reduction using nonlinear constrained optimization. *Building and Environment*, 37(12):1255 – 1265, 2002.
- [90] Solne Goy and Donal Finn. Estimating demand response potential in building clusters. *Energy Procedia*, 78:3391 – 3396, 2015.
- [91] S. Goyal, C. Liao, and P. Barooah. Identification of multi-zone building thermal interaction model from data. In *50th IEEE CDC and ECC*, pages 181–186, Dec 2011.
- [92] X. Guan, Z. Xu, and Q. S. Jia. Energy-efficient buildings facilitated by microgrid. *IEEE Transactions on Smart Grid*, 1(3):243–252, Dec 2010.
- [93] Burak Gunay, Weiming Shen, and Guy Newsham. Inverse blackbox modeling of the heating and cooling load in office buildings. *Energy and Buildings*, 142:200 – 210, 2017.
- [94] Gurobi Optimization Inc. Gurobi Optimizer Reference Manual. <http://www.gurobi.com>.
- [95] H. Hao, C. D. Corbin, K. Kalsi, and R. G. Pratt. Transactive control of commercial buildings for demand response. *IEEE Transactions on Power Systems*, 32(1):774–783, Jan 2017.
- [96] H. Hao, B. M. Sanandaji, K. Poolla, and T. L. Vincent. Aggregate flexibility of thermostatically controlled loads. *IEEE Transactions on Power Systems*, 30(1):189–198, Jan 2015.

- [97] Dawei He, Jie Mei, R. Harley, and T. Habeter. Utilizing building-level demand response in frequency regulation of actual microgrids. In *Industrial Electronics Society, IECON 2013 - 39th Annual Conference of the IEEE*, pages 2205–2210, Nov 2013.
- [98] James K. Ho and Etienne Loute. An advanced implementation of the dantzig—wolfe decomposition algorithm for linear programming. *Mathematical Programming*, 20(1):303–326, 1981.
- [99] William Hogan. Transmission benefits and cost allocation. Harvard University, May 2011.
- [100] William W Hogan and Brendan J Ring. On minimum-uplift pricing for electricity markets. *Electricity Policy Group*, 2003.
- [101] K. Holmberg and K. Jonsten. A simple modification of dantzig-wolfe decomposition. *Optimization*, 34(2):129–145, 1995.
- [102] Yuan Hong, Jaideep Vaidya, and Haibing Lu. Secure and efficient distributed linear programming. *Journal of Computer Security*, 20(5):583–634, 2012.
- [103] Ali Hortacsu and Steven L Puller. Understanding strategic bidding in restructured electricity markets: a case study of ERCOT. Technical report, National Bureau of Economic Research, 2005.
- [104] Michal Houda. Comparison of approximations in stochastic and robust optimization programs. In *Prague stochastics*, pages 418–425, 2006.
- [105] J. T. Hughes, A. D. Domnguez-Garca, and K. Poolla. Identification of virtual battery models for flexible loads. *IEEE Transactions on Power Systems*, 31(6):4660–4669, Nov 2016.
- [106] Dennis Huisman, Raf Jans, Marc Peeters, and Albert P.M. Wagelmans. *Combining Column Generation and Lagrangian Relaxation*, pages 247–270. Springer US, Boston, MA, 2005.
- [107] Jeffrey Inaba and Benedict Clouette. The life of buildings design for adaptation in tokyo, 2014. <http://www.columbia.edu/cu/arch/courses/facsyl/20143>.
- [108] Electric Motor Werks Inc. JuiceBox. <https://emotorwerks.com/>, 2018. [Online; accessed 21-February-2018].

- [109] ICF International. Integrated distribution planning. Technical report, U.S. Department of Energy, 2016.
- [110] IRENA. Electricity Storage and Renewables: Costs and Markets to 2030, October 2017.
- [111] Jeff St. John. California’s New Building Code: A Grid-Smart Thermostat in Every Facility. <https://www.greentechmedia.com/articles/read/californias-title-24-a-grid-smart-thermostat-in-every-building#gs.NUtXuGw>, Apr 2014.
- [112] Jeff St. John. In the Pacific Northwest, Non-Wires Transmission Alternative ‘Reflects a Shift’ in Grid Planning. <https://www.greentechmedia.com/articles/read/a-non-wires-transmission-alternative-reflects-a-shift-in-grid-planning>, May 2017.
- [113] Erwin Kalvelagen. Dantzig-Wolfe Decomposition with GAMS. Technical report, Amsterdam Optimization Modeling Group LLC.
- [114] R. Kelman, L. A. N. Barroso, and M. V. F. Pereira. Market power assessment and mitigation in hydrothermal systems. *IEEE Transactions on Power Systems*, 16(3):354–359, Aug 2001.
- [115] R. J. Kerestes, G. F. Reed, and A. R. Sparacino. Economic analysis of grid level energy storage for the application of load leveling. In *2012 IEEE Power and Energy Society General Meeting*, pages 1–9, July 2012.
- [116] Y. J. Kim, D. H. Blum, N. Xu, L. Su, and L. K. Norford. Technologies and magnitude of ancillary services provided by commercial buildings. *Proceedings of the IEEE*, 104(4):758–779, April 2016.
- [117] M. Kintner-Meyer, C. Jin, P. Balducci, M. Elizondo, X. Guo, T. Nguyen, F. Tuffner, and V. Viswanathan. Energy storage for variable renewable energy resource integration - A regional assessment for the Northwest Power Pool (NWPP). In *Power Systems Conference and Exposition (PSCE), 2011 IEEE/PES*, pages 1–7, March 2011.
- [118] Daniel Kirschen and G Strbac. *Fundamentals of Power System Economics*. United Kingdom. John Wiley & Sons, Ltd, 2004.
- [119] Ian Paul Knight. Assessing electrical energy use in HVAC systems. *REHVA Journal (European Journal of Heating, Ventilating and Air Conditioning Technology)*, 49(1):6–11, 2012.

- [120] Vijay Krishna and Roberto Serrano. Multilateral bargaining. *The Review of Economic Studies*, 63(1):61–80, 1996.
- [121] Lorenzo Kristov and Paul De Martini. 21st century electric distribution system operations. pages 1–11, 2014.
- [122] A. Kwasinski, V. Krishnamurthy, J. Song, and R. Sharma. Availability evaluation of micro-grids for resistant power supply during natural disasters. *IEEE Transactions on Smart Grid*, 3(4):2007–2018, Dec 2012.
- [123] Eimear Leahy and Richard S.J. Tol. An estimate of the value of lost load for ireland. *Energy Policy*, 39(3):1514 – 1520, 2011.
- [124] Haim Levy and Marshall Sarnat. *Capital investment and financial decisions*. Pearson Education, 1994.
- [125] Xin Li and G. K. Zielke. One-year deferral method for estimating avoided transmission and distribution costs. *IEEE Transactions on Power Systems*, 20(3):1408–1413, Aug 2005.
- [126] H. Liang, J. Su, and S. Liu. Reliability evaluation of distribution system containing microgrid. In *CICED 2010 Proceedings*, pages 1–7, Sept 2010.
- [127] Wei-Yin Loh. Classification and regression trees. *Wiley Interdisciplinary Reviews: Data Mining and Knowledge Discovery*, 1(1):14–23, 2011.
- [128] Rui Amaral Lopes, Adriana Chambel, Joo Neves, Daniel Aelenei, and Joo Martins. A literature review of methodologies used to assess the energy flexibility of buildings. *Energy Procedia*, 91:1053 – 1058, 2016.
- [129] Marco E Lübbecke. Column generation. *Wiley Encyclopedia of Operations Research and Management Science*.
- [130] Peter D. Lund, Juuso Lindgren, Jani Mikkola, and Jyri Salpakari. Review of energy system flexibility measures to enable high levels of variable renewable electricity. *Renewable and Sustainable Energy Reviews*, 45:785 – 807, 2015.
- [131] Philipp Lütolf. Impact of the rebound effect of demand response on secondary frequency control. Master’s thesis, ETH Zürich, 2016.
- [132] Y. Ma, F. Borrelli, B. Hancey, B. Coffey, S. Bengea, and P. Haves. Model predictive control for the operation of building cooling systems. *IEEE Transactions on Control Systems Technology*, 20(3):796–803, May 2012.

- [133] Y. Ma, A. Kelman, A. Daly, and F. Borrelli. Predictive control for energy efficient buildings with thermal storage: Modeling, stimulation, and experiments. *IEEE Control Systems*, 32(1):44–64, Feb 2012.
- [134] Yudong Ma, Anthony Kelman, Allan Daly, and Francesco Borrelli. Predictive control for energy efficient buildings with thermal storage. *IEEE Control System Magazine*, 32(1):44–64, 2012.
- [135] J. MacQueen. Some methods for classification and analysis of multivariate observations. In *Proceedings of the Fifth Berkeley Symposium on Mathematical Statistics and Probability, Volume 1: Statistics*, pages 281–297, Berkeley, Calif., 1967. University of California Press.
- [136] Eric Martinot, Lorenzo Kristov, and J. David Erickson. Distribution system planning and innovation for distributed energy futures. *Current Sustainable/Renewable Energy Reports*, 2(2):47–54, Jun 2015.
- [137] H. Mohsenian-Rad. Coordinated price-maker operation of large energy storage units in nodal energy markets. *IEEE Transactions on Power Systems*, 31(1):786–797, Jan 2016.
- [138] E. Moiseeva and M. R. Hesamzadeh. Bayesian and robust nash equilibria in hydrodominated systems under uncertainty. *IEEE Transactions on Sustainable Energy*, 9(2):818–830, April 2018.
- [139] E. Moiseeva, M. R. Hesamzadeh, and D. R. Biggar. Exercise of market power on ramp rate in wind-integrated power systems. *IEEE Transactions on Power Systems*, 30(3):1614–1623, May 2015.
- [140] I. Momber, S. Wogrin, and T. Gomez San Roman. Retail Pricing: A Bilevel Program for PEV Aggregator Decisions Using Indirect Load Control. *IEEE Transactions on Power Systems*, 31(1):464–473, Jan 2016.
- [141] Fabio Moret and Pierre Pinson. Energy collectives: a community and fairness based approach to future electricity markets. *to appear in IEEE Transactions on Power Systems*, 2018.
- [142] Stephanie Morse and Karen Glitman. Electric vehicles as grid resources in ISO-NE and Vermont. Technical report, Vermont Energy Investment Corporation, May 2014.
- [143] F. L. Mller, O. Sundstrm, J. Szab, and J. Lygeros. Aggregation of energetic flexibility using zonotopes. In *54th IEEE CDC*, pages 6564–6569, Dec 2015.

- [144] John F. Nash. The bargaining problem. *Econometrica*, 18(2):155–162, 1950.
- [145] A. I. Negash, T. W. Haring, and D. S. Kirschen. Allocating the cost of demand response compensation in wholesale energy markets. *IEEE Transactions on Power Systems*, 30(3):1528–1535, May 2015.
- [146] Ahlmahz I. Negash and Daniel S. Kirschen. Combined optimal retail rate restructuring and value of solar tariff. In *2015 IEEE Power Energy Society General Meeting*, pages 1–5, July 2015.
- [147] D. T. Nguyen and L. B. Le. Joint optimization of electric vehicle and home energy scheduling considering user comfort preference. *IEEE Transactions on Smart Grid*, 5(1):188–199, Jan 2014.
- [148] H. K. Nguyen, H. Mohsenian-Rad, A. Khodaei, and Z. Han. Decentralized reactive power compensation using nash bargaining solution. *IEEE Transactions on Smart Grid*, PP(99):1–10, 2015.
- [149] NREL. Solar Integration National Dataset Toolkit. <https://www.nrel.gov/grid/sind-toolkit.html>.
- [150] Barack Obama. The irreversible momentum of clean energy. *Science*, 355(6321):126–129, 2017.
- [151] Y. Okajima, K. Hirata, T. Murao, T. Hatanaka, V. Gupta, and K. Uchida. Strategic behavior and market power of aggregators in energy demand networks. In *2017 IEEE 56th Annual Conference on Decision and Control (CDC)*, pages 694–701, Dec 2017.
- [152] F. Oldewurtel, A. Parisio, C. N. Jones, M. Morari, D. Gyalistras, M. Gwerder, V. Stauch, B. Lehmann, and K. Wirth. Energy efficient building climate control using stochastic model predictive control and weather predictions. In *Proceedings of the 2010 American Control Conference*, pages 5100–5105, June 2010.
- [153] D. J. Olsen, M. R. Sarker, and M. A. Ortega-Vazquez. Optimal penetration of home energy management systems in distribution networks considering transformer aging. *IEEE Transactions on Smart Grid*, pages 1–1, 2017.
- [154] M. A. Ortega-Vazquez. Optimal scheduling of electric vehicle charging and vehicle-to-grid services at household level including battery degradation and price uncertainty. *IET Generation, Transmission Distribution*, 8(6):1007–1016, June 2014.

- [155] M. A. Ortega-Vazquez. Optimal scheduling of electric vehicle charging and vehicle-to-grid services at household level including battery degradation and price uncertainty. *IET Gen., Transactions, Dist.*, 8(6):1007–1016, June 2014.
- [156] M. A. Ortega-Vazquez, F. Bouffard, and V. Silva. Electric vehicle aggregator/system operator coordination for charging scheduling and services procurement. *IEEE Transactions on Power Systems*, 28(2):1806–1815, May 2013.
- [157] Andrew Ott. Unit commitment in the PJM day-ahead and real-time markets. In *FERC Technical Conference on Increasing Market and Planning Efficiency Through Improved Software and Hardware*, 2010.
- [158] Hrvoje Pandzic and Igor Kuzle. Energy storage operation in the day-ahead electricity market. In *2015 12th International Conference on the European Energy Market (EEM)*, pages 1–6, May 2015.
- [159] Dieter Patteeuw, Kenneth Bruninx, Alessia Arteconi, Erik Delarue, William Dhaeseleer, and Lieve Helsen. Integrated modeling of active demand response with electric heating systems coupled to thermal energy storage systems. *Applied Energy*, 151:306 – 319, 2015.
- [160] Ignacio Pérez-Arriaga, Christopher Knittel, R Miller, R Tabors, A Bharatkumar, M Luke, M Birk, S Burger, P Rodilla, J Pablo Chaves, et al. Utility of the future, 2016.
- [161] Ari Peskoe. Distributed Energy Resources and Public Utility Regulation. http://hejc.environment.harvard.edu/files/hejc/files/peskoe_distributedenergyresources_publicutilityregulation.pdf. [Online; accessed 2-May-2018].
- [162] A. Piccolo and P. Siano. Evaluating the impact of network investment deferral on distributed generation expansion. *IEEE Transactions on Power Systems*, 24(3):1559–1567, Aug 2009.
- [163] Mary A Piette, Oren Schetrit, Sila Kiliccote, Iris Cheung, and Becky Z Li. Costs to automate demand response-taxonomy and results from field studies and programs. Technical Report LBNL-1003924, Lawrence Berkeley National Laboratory, 2015.
- [164] Mary Ann Piette, Michael D Sohn, Ashok J Gadgil, and Alexandre M Bayen. Improved power grid stability and efficiency with a building-energy cyber-physical system. In *National Workshop on Research Directions for Future Cyber Physical Energy Systems*, June 2009.

- [165] Pierre Pinson. Wind energy: Forecasting challenges for its operational management. *Statistical Science*, 28(4):564–585, 2013.
- [166] PJM. Demand response. <http://www.pjm.com//media/markets-ops/dsr/end-use-customer-fact-sheet.ashx>, 2013.
- [167] Nadja Popovich. Today’s energy jobs are in solar, not coal. <https://www.nytimes.com/interactive/2017/04/25/climate/todays-energy-jobs-are-in-solar-not-coal.html>, April 2017. Accessed: 2018-04-29.
- [168] D. Pozo and J. Contreras. Finding multiple nash equilibria in pool-based markets: A stochastic epec approach. *IEEE Transactions on Power Systems*, 26(3):1744–1752, Aug 2011.
- [169] P. Radecki and B. Hency. Online model estimation for predictive thermal control of buildings. *IEEE Transactions on Control Systems Technology*, PP(99):1–9, 2016.
- [170] G. El Rahi, S. R. Etesami, W. Saad, N. Mandayam, and H. V. Poor. Managing price uncertainty in prosumer-centric energy trading: A prospect-theoretic stackelberg game approach. *IEEE Transactions on Smart Grid*, pages 1–1, 2017.
- [171] M. H. Rahim, A. Khalid, N. Javaid, M. Alhussein, K. Aurangzeb, and Z. A. Khan. Energy efficient smart buildings using coordination among appliances generating large data. *to appear in IEEE Access*, 2018.
- [172] Stephen J Rassenti, Vernon L Smith, and Bart J Wilson. Controlling market power and price spikes in electricity networks: Demand-side bidding. *Proceedings of the National Academy of Sciences*, 100(5):2998–3003, 2003.
- [173] D. N. Reps and J. A. Rose. Strategy for expansion of utility generation. *Transactions of the American Institute of Electrical Engineers. Part III: Power Apparatus and Systems*, 78(4):1710–1719, Dec 1959.
- [174] Andrew J Roscoe and G Ault. Supporting high penetrations of renewable generation via implementation of real-time electricity pricing and demand response. *IET Renewable Power Generation*, 4(4):369–382, 2010.
- [175] Mark Rothleder. Unit Commitment at the CAISO. In *FERC Conference on Unit Commitment Software*, 2010.

- [176] J. Van Roy, N. Leemput, F. Geth, J. Buscher, R. Salenbien, and J. Driesen. Electric vehicle charging in an office building microgrid with distributed energy resources. *IEEE Transactions on Sustainable Energy*, 5(4):1389–1396, Oct 2014.
- [177] Sullivan Royer, Stphane Thil, Thierry Talbert, and Monique Polit. Black-box modeling of buildings thermal behavior using system identification. *IFAC Proceedings Volumes*, 47(3):10850 – 10855, 2014. 19th IFAC World Congress.
- [178] N. Azizan Ruhi, K. Dvijotham, N. Chen, and A. Wierman. Opportunities for price manipulation by aggregators in electricity markets. *IEEE Transactions on Smart Grid*, pages 1–1, 2017.
- [179] T. Samad, E. Koch, and P. Stluka. Automated demand response for smart buildings and microgrids: The state of the practice and research challenges. *Proceedings of the IEEE*, 104(4):726–744, 2016.
- [180] M. E. Samper and A. Vargas. Investment Decisions in Distribution Networks Under Uncertainty With Distributed Generation, Part I: Model Formulation. *IEEE Transactions on Power Systems*, 28(3):2331–2340, Aug 2013.
- [181] M. R. Sarker, D. J. Olsen, and M. A. Ortega-Vazquez. Co-optimization of distribution transformer aging and energy arbitrage using electric vehicles. *IEEE Transactions on Smart Grid*, 8(6):2712–2722, Nov 2017.
- [182] M. R. Sarker and M. A. Ortega-Vazquez. Optimal investment strategy in photovoltaics and energy storage for commercial buildings. In *2015 IEEE Power Energy Society General Meeting*, July 2015.
- [183] Mushfiqur R. Sarker, Yury Dvorkin, and Miguel A. Ortega-Vazquez. Optimal participation of an electric vehicle aggregator in day-ahead energy and reserve markets. *IEEE Transactions on Power Systems*, 31(5):3506–3515, Sept 2016.
- [184] Mushfiqur R. Sarker, Matthew D. Murbach, Daniel T. Schwartz, and Miguel A. Ortega-Vazquez. Optimal operation of a battery energy storage system: Trade-off between grid economics and storage health. *Electric Power Systems Research*, 152:342 – 349, 2017.
- [185] Mushfiqur R. Sarker, Miguel A. Ortega-Vazquez, and Daniel S. Kirschen. Optimal coordination and scheduling of demand response via monetary incentives. *IEEE Transactions on Smart Grid*, 6(3):1341–1352, May 2015.
- [186] N. Saxena, B. Singh, and A. L. Vyas. Single-phase solar pv system with battery and exchange of power in grid-connected and standalone modes. *IET Renewable Power Generation*, 11(2):325–333, 2017.

- [187] Hossein Seifi and Mohammad Sadegh Sepasian. *Electric power system planning: issues, algorithms and solutions*. Springer Science & Business Media, 2011.
- [188] Y. Sekine. Decentralized optimization of an interconnected system. *IEEE Transactions on Circuit Theory*, 10(2):161–168, Jun 1963.
- [189] M. Shafie-khah, M. P. Moghaddam, and M. K. Sheikh-El-Eslami. Ex-ante evaluation and optimal mitigation of market power in electricity markets including renewable energy resources. *IET Generation, Transmission Distribution*, 10(8):1842–1852, 2016.
- [190] A. Y. Sheffrin, Jing Chen, and B. F. Hobbs. Watching watts to prevent abuse of power. *IEEE Power and Energy Magazine*, 2(4):58–65, July 2004.
- [191] A. Y. Sheffrin, Jing Chen, and B. F. Hobbs. Watching watts to prevent abuse of power. *IEEE Power and Energy Magazine*, 2(4):58–65, July 2004.
- [192] M. S. Shemami, M. S. Alam, and M. S. J. Asghar. Load shedding mitigation through plug-in electric vehicle-to-home (v2h) system. In *2017 IEEE Transportation Electrification Conference and Expo (ITEC)*, pages 799–804, June 2017.
- [193] Uzma Sidiqqi. Seattle City Light Planning Practices. Personal communication, 2018.
- [194] M. Singh, V. Khadkikar, A. Chandra, and R. K. Varma. Grid interconnection of renewable energy sources at the distribution level with power-quality improvement features. *IEEE Transactions on Power Delivery*, 26(1):307–315, Jan 2011.
- [195] Etienne Sorin, Lucien Bobo, and Pierre Pinson. Consensus-based approach to peer-to-peer electricity markets with product differentiation. *arXiv preprint arXiv:1804.03521*, 2018.
- [196] Tom Stanton. Getting the signals straight: Modeling, planning, and implementing non-transmission alternatives. Technical Report 15-02, National Regulatory Research Institute, 2015.
- [197] B. Stott, J. Jardim, and O. Alsac. Dc power flow revisited. *IEEE Transactions on Power Systems*, 24(3):1290–1300, Aug 2009.
- [198] David Sturzenegger, Dimitrios Gyalistras, Markus Gwerder, Carina Sagerschnig, Manfred Morari, and Roy S. Smith. Model Predictive Control of a Swiss Office Building. Technical report, ETH Zurich, www.opticontrol.ethz.ch.

- [199] K. Sun, M. R. Sarker, and M. A. Ortega-Vazquez. Statistical characterization of electric vehicle charging in different locations of the grid. In *2015 IEEE Power Energy Society General Meeting*, pages 1–5, July 2015.
- [200] F. Teixeira, J. de Sousa, and S. Faias. How market power affects the behavior of a pumped storage hydro unit in the day-ahead electricity market? In *2012 9th ICEEM*, pages 1–6, May 2012.
- [201] The Regulatory Assistance Project. *Electricity Regulation In the US: A Guide*. March 2011.
- [202] Robert Tibshirani and Guenther Walther. Cluster validation by prediction strength. *Journal of Computational and Graphical Statistics*, 14(3):511–528, 2005.
- [203] William Tokash. Innovative financing drives distributed energy storage deployment. <http://www.decentralized-energy.com/articles/2017/02/innovative-financing-drives-distributed-energy-storage-deployment.html>, February 2017.
- [204] Herman K. Trabish. Report: US generators face 2 billion in lost revenues from rooftop solar. <https://www.utilitydive.com/news/report-us-generators-face-2b-in-lost-revenues-from-rooftop-solar/415799/>, March 2016.
- [205] F. Tuffner and M. Kintner-Meyer. Using electric vehicles to meet balancing requirements associated with wind power. Technical report, Pacific Northwest National Laboratory, 2011.
- [206] B. C. Ummels, E. Pelgrum, and W. L. Kling. Integration of large-scale wind power and use of energy storage in the netherlands’ electricity supply. *IET Renewable Power Generation*, 2(1):34–46, March 2008.
- [207] U.S. Energy Information Administration. CBECS (Commercial Building Energy Consumption Surveys), 2012. <https://www.eia.gov/consumption/commercial/data/2012/>.
- [208] Francois Vanderbeck and Martin W.P. Savelsbergh. A generic view of dantzig-wolfe decomposition in mixed integer programming. *Operations Research Letters*, 34(3):296 – 306, 2006.
- [209] Marina González Vayá and Göran Andersson. Optimal bidding strategy of a plug-in electric vehicle aggregator in day-ahead electricity markets under uncertainty. *IEEE Transactions on Power Systems*, 30(5):2375–2385, September 2015.

- [210] Samuel Vazquez, Pablo Rodilla, and Carlos Batlle. Residual demand models for strategic bidding in european power exchanges: Revisiting the methodology in the presence of a large penetration of renewables. *Electric Power Systems Research*, 108:178 – 184, 2014.
- [211] E. Vrettos and G. Andersson. Scheduling and provision of secondary frequency reserves by aggregations of commercial buildings. *IEEE Transactions on Sustainable Energy*, 7(2):850–864, April 2016.
- [212] Robert Walton. Straight Outta BQDM: Consolidated Edison looks to expand its non-wires approach. <https://www.utilitydive.com/news/straight-outta-bqdm-consolidated-edison-looks-to-expand-its-non-wires-app/447433/>, July 2017.
- [213] Jing Wang, N. E. Redondo, and F. D. Galiana. Demand-side reserve offers in joint energy/reserve electricity markets. *IEEE Transactions on Power Systems*, 18(4):1300–1306, Nov 2003.
- [214] Y. Wang, L. Wu, and S. Wang. A fully-decentralized consensus-based admm approach for dc-opf with demand response. *IEEE Transactions on Smart Grid*, 8(6):2637–2647, Nov 2017.
- [215] Yishen Wang, Yury Dvorkin, Ricardo Fernandez-Blanco, Bolun Xu, Ting Qiu, and Daniel S. Kirschen. Look-ahead bidding strategy for energy storage. *IEEE Transactions on Sustainable Energy*, 8(3):1106–1117, July 2017.
- [216] Kristoffer Weywadt. Optimal bidding strategy for PHEV fleet aggregators-A bilevel model. Master’s thesis, Chalmers University, Gothenburg, Sweden, 2012.
- [217] Todd Woody. Solar: Life, liberty and the pursuit of energy independence, July 2012. Accessed: 2018-04-29.
- [218] C. Wu, H. Mohsenian-Rad, and J. Huang. Vehicle-to-aggregator interaction game. *IEEE Transactions on Smart Grid*, 3(1):434–442, March 2012.
- [219] H. Wu, M. Shahidehpour, and A. Al-Abdulwahab. Hourly demand response in day-ahead scheduling for managing the variability of renewable energy. *IET Generation, Transmission Distribution*, 7(3):226–234, March 2013.
- [220] Bolun Xu, Yury Dvorkin, Daniel S. Kirschen, Cesar A. Silva-Monroy, and J. P. Watson. A comparison of policies on the participation of storage in u.s. frequency regulation markets. In *2016 IEEE Power and Energy Society General Meeting (PESGM)*, pages 1–5, July 2016.

- [221] Z. Xu, X. Guan, Q. S. Jia, J. Wu, D. Wang, and S. Chen. Performance analysis and comparison on energy storage devices for smart building energy management. *IEEE Transactions on Smart Grid*, 3(4):2136–2147, Dec 2012.
- [222] Z. Yang, K. Long, P. You, and M. Y. Chow. Joint scheduling of large-scale appliances and batteries via distributed mixed optimization. *IEEE Transactions on Power Systems*, 30(4):2031–2040, July 2015.
- [223] Y. Ye, D. Papadaskalopoulos, and G. Strbac. Investigating the ability of demand shifting to mitigate electricity producers’ market power. *IEEE Transactions on Power Systems*, pages 1–1, 2017.
- [224] J. H. Yoon, R. Baldick, and A. Novoselac. Dynamic demand response controller based on real-time retail price for residential buildings. *IEEE Transactions on Smart Grid*, 5(1):121–129, Jan 2014.
- [225] Z. Yu, L. McLaughlin, L. Jia, M. C. Murphy-Hoye, A. Pratt, and L. Tong. Modeling and stochastic control for home energy management. In *2012 IEEE Power and Energy Society General Meeting*, pages 1–9, July 2012.
- [226] C. Yuan, M. S. Illindala, and A. S. Khalsa. Co-optimization scheme for distributed energy resource planning in community microgrids. *IEEE Transactions on Sustainable Energy*, 8(4):1351–1360, Oct 2017.
- [227] Gyeong Yun, Kap Chun Yoon, and Kang Soo Kim. The influence of shading control strategies on the visual comfort and energy demand of office buildings. *Energy and Buildings*, 84, July 2014.

Appendix A

DANTZIG-WOLFE DECOMPOSITION FOR MIXED-INTEGER LINEAR PROGRAMS

This appendix provides a brief overview of the Dantzing-Wolfe Decomposition Algorithm (DWDA). Conejo et al. provide an in-depth analysis of the algorithm and [208] generalizes it. Fig. A.1 shows a graphical representation of the algorithm.

We consider MILPs of the form

$$\begin{aligned}
 & \min \quad \mathbf{c}_0^T \mathbf{x}_0 + \mathbf{c}_1^T \mathbf{x}_1 + \mathbf{c}_2^T \mathbf{x}_2 + \dots + \mathbf{c}_N^T \mathbf{x}_N \\
 & \text{s.t.} \\
 & \begin{bmatrix} \mathbf{B}_0 & \mathbf{B}_1 & \mathbf{B}_2, \dots & \mathbf{B}_N & \\ \mathbf{0} & \mathbf{A}_1 & \mathbf{0} & \dots & \mathbf{0} \\ \mathbf{0} & \mathbf{0} & \mathbf{A}_2 & \dots & \mathbf{0} \\ \mathbf{0} & \mathbf{0} & \mathbf{0} & \ddots & \mathbf{0} \\ \mathbf{0} & \mathbf{0} & \mathbf{0} & \dots & \mathbf{A}_N \end{bmatrix} \begin{bmatrix} \mathbf{x}_0 \\ \mathbf{x}_1 \\ \mathbf{x}_2 \\ \vdots \\ \mathbf{x}_N \end{bmatrix} = \begin{bmatrix} \mathbf{b}_0 \\ \mathbf{b}_1 \\ \mathbf{b}_2 \\ \vdots \\ \mathbf{b}_N \end{bmatrix} \\
 & 0 \leq \mathbf{x}_i \leq M \quad \forall i = 0, 1, \dots, N \\
 & \mathbf{x}_i^{\text{bin}} \in \{\mathbf{0}, \mathbf{1}\}^{n_{i,\text{bin}}} \quad \forall i = 1, 2, \dots, N.
 \end{aligned}$$

Here variables \mathbf{x}_0 are not associated to any of the N subproblems. The vector $\mathbf{x}_i \quad \forall i \geq 1$ represents variables of subproblem i . The first $n_{i,c}$ entries of $n_{i,c}$ \mathbf{x}_i , \mathbf{x}_i^c , are continuous variables and the last $n_{i,\text{bin}}$, $\mathbf{x}_i^{\text{bin}}$, entries are binary variables. The portion of \mathbf{c}_i associated to $\mathbf{x}_i^{\text{bin}}$ is $\mathbf{c}_i^{\text{bin}}$. The portion of \mathbf{c}_i associated to \mathbf{x}_i^c is \mathbf{c}_i^c . Likewise, the columns of \mathbf{B}_i associated to \mathbf{x}_i^c are \mathbf{B}_i^c while the columns associated to $\mathbf{x}_i^{\text{bin}}$ are $\mathbf{B}_i^{\text{bin}}$. M is a sufficiently large number.

A.1 The master problem

The master problem

$$\min \left\{ \mathbf{c}_0^\top \mathbf{x}_0 + \sum_{k=1}^K \sum_{i=1}^N \lambda_{k,i}^c \cdot p_i^{c(k)} + \lambda_{k,i}^{\text{bin}} \cdot p_i^{\text{bin}(k)} \right\} \quad (\text{A.1a})$$

subject to :

$$\mathbf{B}_0 \mathbf{x}_0 + \sum_{k=1}^K \sum_{i=1}^N \lambda_{k,i}^c \cdot \mathbf{v}_i^{c(k)} + \lambda_{k,i}^{\text{bin}} \cdot \mathbf{v}_i^{\text{bin}(k)} = \mathbf{b}_0 \quad (\boldsymbol{\pi}_1) \quad (\text{A.1b})$$

$$\sum_{k=1}^K \lambda_{k,i}^{c(k)} = 1 \quad (\pi_i^c) \quad \forall i = 1, 2, \dots, N \quad (\text{A.1c})$$

$$\sum_{k=1}^K \lambda_{k,i}^{\text{bin}(k)} = 1 \quad (\pi_i^{\text{bin}}) \quad \forall i = 1, 2, \dots, N \quad (\text{A.1d})$$

$$0 \leq \mathbf{x}_0 \leq M \quad (\text{A.1e})$$

$$\lambda_{k,i}^{c(k)} \geq 0 \quad \forall k = 1, 2, \dots, K, \quad i = 1, 2, \dots, N \quad (\text{A.1f})$$

$$\lambda_{k,i}^{\text{bin}(k)} \in \{0, 1\} \quad \forall k = 1, 2, \dots, K, \quad i = 1, 2, \dots, N \quad (\text{A.1g})$$

handles the coupling constraints. The parameters $p_i^{c(k)} = \mathbf{c}_i^{c\top} \mathbf{x}_b^{c(k)}$, $p_i^{\text{bin}(k)} = \mathbf{c}_i^{\text{bin}\top} \mathbf{x}_b^{\text{bin}(k)}$ represent the k^{th} cost proposals. The parameters $\mathbf{v}_i^{c(k)} = \mathbf{B}_i^c \mathbf{x}_i^{c(k)}$, $\mathbf{v}_i^{\text{bin}(k)} = \mathbf{B}_i^{\text{bin}} \mathbf{x}_b^{\text{bin}(k)}$ represent the k^{th} proposals. The decision variables $\lambda_{k,i}^c$, $\lambda_{k,i}^{\text{bin}}$ assign weights to the k^{th} subproblem proposal. Constraints (A.1b) enforce the coupling constraints.

The number of times the master problem has been solved is $K - 1$ (e.g., $K = n$ after the n^{th} iteration). Thus, the number of variables in the master problem increases linearly with the number of iterations.

A.2 The subproblems

The modified subproblem i is

$$\min \{ (\mathbf{c}_i^\top - \boldsymbol{\pi}_1^\top \mathbf{B}_i) \mathbf{x}_i - \pi_i^c - \pi_i^{\text{bin}} \} \quad (\text{A.2a})$$

$$\text{s.t.} \quad (\text{A.2b})$$

$$\mathbf{A}_i \mathbf{x}_i = \mathbf{b}_i \quad (\text{A.2c})$$

$$0 \leq \mathbf{x}_i \leq M \quad (\text{A.2d})$$

$$\mathbf{x}_i^{\text{bin}} \in \{\mathbf{0}, \mathbf{1}\}^{n_{i,\text{bin}}} \quad (\text{A.2e})$$

where the objective function is referred to as the *reduced cost*. The master problem solver provides the parameters $\boldsymbol{\pi}_1$, π_i^c , and π_i^{bin} .

A.3 Initialization

We solve the subproblems with $\boldsymbol{\pi}_1 = \mathbf{0}$ and with random cost coefficients \mathbf{c}_i during initialization. The purpose of the initialization phase is to obtain feasible initial proposals.

A.4 Phase I/II Algorithm

During phase I, we solve a modified version of the sub- and master problems to find a feasible solution of the coupled problem. We reach optimality in phase II.

A.4.1 Phase I master problem

We employ the method of artificial variables explained in [50, 113] to find a feasible solution of the coupled problem. We relax the coupling constraint in the master problem (A.1b) using an artificial variable x_a and replace the objective by $\min x_a$.

A.4.2 Phase I subproblems

Phase I “steers” the solution of the subproblems to a feasible solution of the coupled problem by solving the subproblems with $\mathbf{c}_1 = \mathbf{c}_2 = \dots = \mathbf{c}_N = \mathbf{0}$. Then, the only terms in the objective function are $\boldsymbol{\pi}_1^\top \mathbf{B}_i \mathbf{x}_i$ (plus constants).

A.4.3 Phase II

The algorithm switches to phase II when the convex combination of the phase I proposals satisfy the coupling constraints with a tolerance level ε . Problems (A.1) and (A.2), describe the phase II master problem and subproblems, respectively.

A.5 Terminating condition

The DWDA has the property of providing an upper-bound (solution of the master problem) and a lower-bound (solution of the subproblems) at every iteration. Thus, one might terminate the algorithm when the difference between the upper and lower bounds reach a tolerance level. In this work, for simplicity and to convey intuition, the DWDA terminates when the solution is within 1% of the optimal as obtained with state-of-the-art solvers.

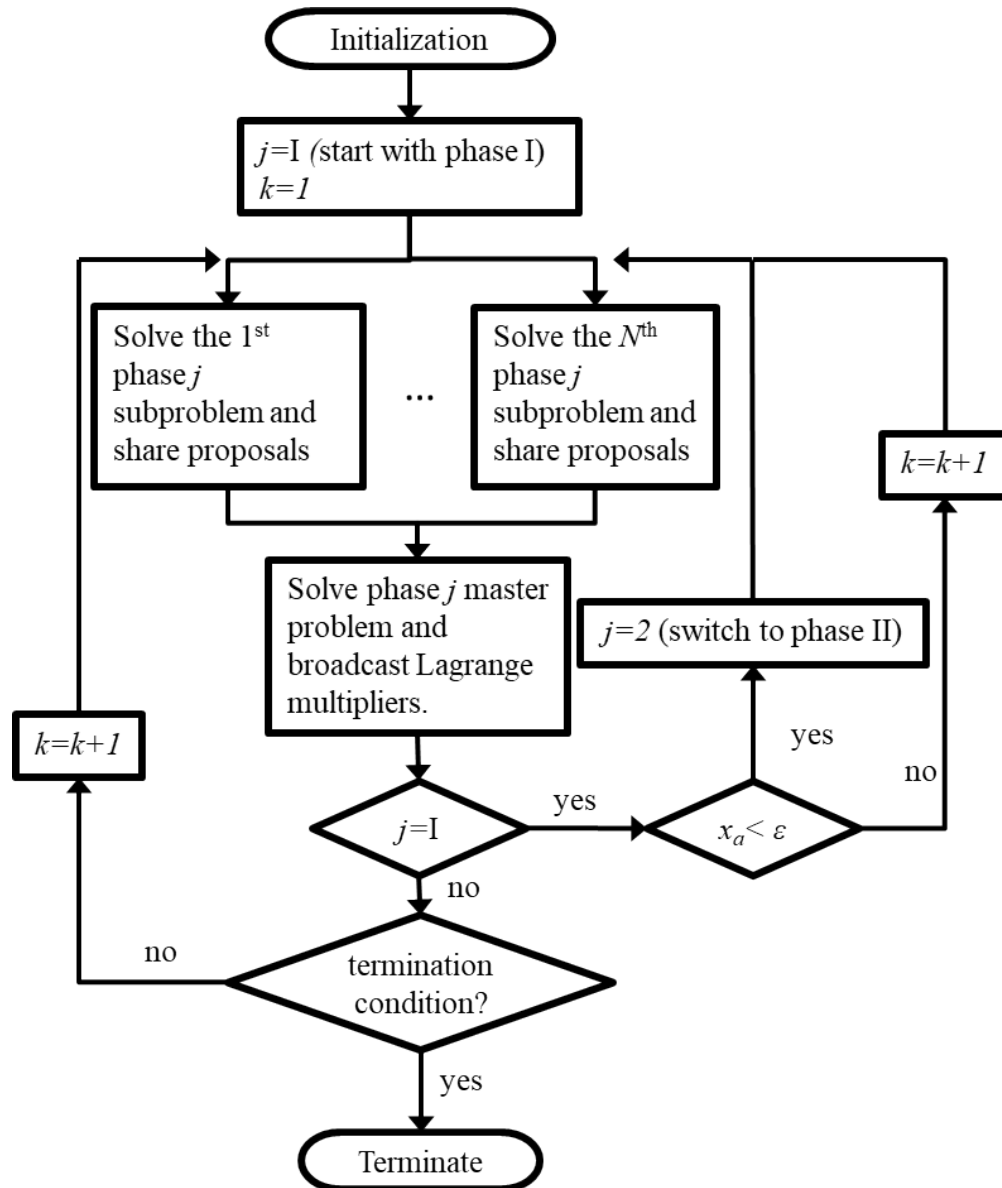


Figure A.1: Flow chart describing the Dantzig-Wolfe decomposition algorithm.

Appendix B

TRAINING DATA CLUSTERING

Let the the vector $\mathbf{w}_{k,t}$ be defined $\forall k \in \mathcal{K}$ and $t = 1, \dots, T$ as $\mathbf{w}_{k,t} = \left[\mathbf{p}_{k,1:t}^\top \ \phi_{0,t}^{\text{in}} \ \phi_{k,t}^{\text{in}} \ \phi_{k,t}^{\text{out}} \right]^\top$. Since the vectors $\mathbf{w}_{k,t}$ contain data on different units and potentially different magnitudes, normalizing the data prevents the clustering algorithm from unfairly assigning more importance to some of the elements of $\mathbf{w}_{k,t}$. Denote a normalized matrix of horizontal concatenation of all $\mathbf{w}_{k,t}$'s as

$$\mathbf{W}_t = \text{norm} \left(\left[\mathbf{w}_{1,t} \ \mathbf{w}_{2,t} \ \dots \ \mathbf{w}_{|\mathcal{K}|,t} \right] \right).$$

The matrix \mathbf{W}_t is normalized such that the mean of each row is zero and the ℓ_2 norm of each row is 1. We use the K-means algorithm [135] to group the columns of \mathbf{W}_t matrix into C_t separate clusters. The indices of $\mathbf{w}_{k,t}$'s assigned to cluster c are denoted by $\mathcal{K}_{c,t}$.

Appendix C

ESTIMATE OF THE TEMPERATURE AND LOAD LIMITS

We estimate $\theta_{c,t}^{\max}$ as the maximum indoor temperature during time period t during days in the set $\mathcal{K}_{c,t}$, i.e., $\hat{\theta}_{c,t}^{\max} = \max(\{\phi_{k,t}^{\text{in}}\}_{k \in \mathcal{K}_{c,t}})$. The minimum temperature limit, the upper and lower load bounds for each cluster are estimated using an analogous procedure, i.e., $\hat{\theta}_{c,t}^{\min} = \min(\{\phi_{k,t}^{\text{in}}\}_{k \in \mathcal{K}_{c,t}})$, $\hat{p}_{c,t}^{\min} = \min(\{p_{k,t}\}_{k \in \mathcal{K}_{c,t}})$, $\hat{p}_{c,t}^{\max} = \max(\{p_{k,t}\}_{k \in \mathcal{K}_{c,t}})$.

Appendix D

BOUNDED LEAST SQUARES ESTIMATION

Let an estimate of upper bound of the indoor temperature at time t and day k be an affine function of the initial temperature $\phi_{k,0}$, the outdoor temperature at time t , $\phi_{k,t}^{\text{out}}$, and load from the first to the t^{th} time period,

$$\hat{\theta}_{k,t}^{\text{U}}(\phi_{k,0}^{\text{in}}, \phi_{k,t}^{\text{out}}, \mathbf{p}_{k,1:t}) = \bar{\mathbf{a}}_{c,t}^{\top} \mathbf{p}_{k,1:t} + \bar{\mathbf{b}}_{c,t}^{\top} \begin{bmatrix} \phi_{k,0}^{\text{in}} & \phi_{k,t}^{\text{out}} & 1 \end{bmatrix}^{\top}.$$

Similarly, the lower bound estimate of the indoor temperature at time t is

$$\hat{\theta}_{k,t}^{\text{L}}(\phi_{k,0}^{\text{in}}, \phi_{k,t}^{\text{out}}, \mathbf{p}_{k,1:t}) = \underline{\mathbf{a}}_{c,t}^{\top} \mathbf{p}_{k,1:t} + \underline{\mathbf{b}}_{c,t}^{\top} \begin{bmatrix} \phi_{k,0}^{\text{in}} & \phi_{k,t}^{\text{out}} & 1 \end{bmatrix}^{\top}.$$

We cast the problem of finding values of $\bar{\mathbf{a}}_{c,t}$, $\underline{\mathbf{a}}_{c,t}$, $\bar{\mathbf{b}}_{c,t}$, and $\underline{\mathbf{b}}_{c,t}$ such that the square error and a measure of the tightness of the bounds are minimized as the following convex

quadratic program:

$$\begin{aligned} \arg \min_{\substack{\bar{\mathbf{a}}_{c,t}, \underline{\mathbf{a}}_{c,t}, \bar{\mathbf{b}}_{c,t}, \underline{\mathbf{b}}_{c,t} \\ \hat{\theta}_{k,t}^U, \hat{\theta}_{k,t}^L \\ J_{k,t}^U, J_{k,t}^L, J_t^A}} \beta_i \cdot \sum_{k \in \mathcal{K}_c} (J_{k,t}^U + J_{k,t}^L)^2 + (1 - \beta_i) \cdot J_t^A \end{aligned} \quad (\text{D.1a})$$

s.t.

$$\hat{\theta}_{k,t}^U = \bar{\mathbf{a}}_{c,t}^\top \mathbf{p}_{k,1:t} + \bar{\mathbf{b}}_{c,t}^\top \begin{bmatrix} \phi_{k,0}^{\text{in}} & \phi_{k,t}^{\text{out}} & 1 \end{bmatrix}^\top \quad \forall k \in \mathcal{K}_{c,t} \quad (\text{D.1b})$$

$$\hat{\theta}_{k,t}^L = \underline{\mathbf{a}}_{c,t}^\top \mathbf{p}_{k,1:t} + \underline{\mathbf{b}}_{c,t}^\top \begin{bmatrix} \phi_{k,0}^{\text{in}} & \phi_{k,t}^{\text{out}} & 1 \end{bmatrix}^\top \quad \forall k \in \mathcal{K}_{c,t} \quad (\text{D.1c})$$

$$J_{k,t}^U \geq \phi_{k,t}^{\text{in}} - \hat{\theta}_{k,t}^U \quad \forall k \in \mathcal{K}_{c,t} \quad (\text{D.1d})$$

$$J_{k,t}^L \geq \hat{\theta}_{k,t}^L - \phi_{k,t}^{\text{in}} \quad \forall k \in \mathcal{K}_{c,t} \quad (\text{D.1e})$$

$$J_t^A = \sum_{k \in \mathcal{K}_{c,t}} \hat{\theta}_{k,t}^U - \hat{\theta}_{k,t}^L \quad (\text{D.1f})$$

$$\hat{\theta}_{k,t}^U \geq \hat{\theta}_{k,t}^L \quad \forall k \in \mathcal{K}_{c,t} \quad (\text{D.1g})$$

$$\bar{\mathbf{a}}_{c,t} \leq 0 \quad (\text{D.1h})$$

$$\underline{\mathbf{a}}_{c,t} \leq 0 \quad (\text{D.1i})$$

$$J_{k,t}^U \geq 0 \quad \forall k \in \mathcal{K}_{c,t} \quad (\text{D.1j})$$

$$J_{k,t}^L \geq 0 \quad \forall k \in \mathcal{K}_{c,t} \quad (\text{D.1k})$$

The objective function of problem (D.1) is composed of two weighted components: 1) the sum of squared errors and 2) a measure of the tightness of the upper and lower estimates. The first component is weighted by β_i while the second one is weighted by $1 - \beta_i$ where $\beta_i \in (0, 1)$. When as $\beta_i \rightarrow 1$, the bounds become wider and more points fall within them. Conversely, when β_i is small, the bounds are tighter.

Equations (D.1b) and (D.1c), define the estimates of the upper and lower estimates, respectively. Eq. (D.1d) defines the upper estimate error $J_{k,t}^U$ to be the distance between the upper estimation and the measurement if this quantity is positive and zero otherwise. Similarly, Eq. (D.1e) defines the lower bound error $J_{k,t}^L$ to be the distance between the

measurement and the lower bound estimation if this quantity is positive and zero otherwise.

The measure of the tightness of the prediction band J_t^A is defined in Eq. (D.1f) as the sum of the distance between the lower and upper estimates over all samples $\mathcal{K}_{c,t}$. We restrict the upper estimate to be higher than the lower bound in Eq. (D.1g). Without loss of generality, we assume that every training day is either cooling day. Then, everything else equal, higher load must translate into lower temperature. Therefore $\bar{\mathbf{a}}_{c,t}$ and $\underline{\mathbf{a}}_{c,t}$ are restricted to be negative as in Eqs. (D.1h) and (D.1i). If the training days are all heating days, the signs in Eqs. (D.1h) and (D.1i) are reversed. Finally, we define the root mean square error of the BLSE as

$$\text{RMSE}_{c,t} = \sqrt{\frac{\sum_{k \in \mathcal{K}_{c,t}} (J_{k,t}^U + J_{k,t}^L)^2}{|\mathcal{K}_{c,t}|}}. \quad (\text{D.2})$$

The BLSE algorithm

Let $\text{BLSEF}(\beta_i)$ denote a function that takes the scalar $\beta_i \in (0, 1)$ and solves problem (D.1) and outputs the optimal values of $\bar{\mathbf{a}}_{c,t}$, $\underline{\mathbf{a}}_{c,t,i}$, $\bar{\mathbf{b}}_{c,t,i}$, $\underline{\mathbf{b}}_{c,t,i}$, $J_{t,i}^A$, and calculates the percentage of training measurements that are higher than the upper estimate or lower than the lower estimate $\pi_{t,i}^{\text{out}}$. The percentage of out of prediction band measurements is calculated as

$$\pi_{t,i}^{\text{out}} = \frac{\sum_{k \in \mathcal{K}_{c,t}} \mathbb{I}(\hat{\theta}_{k,t}^U \leq \theta_{k,t} \text{ or } \hat{\theta}_{k,t}^L \geq \theta_{k,t})}{|\mathcal{K}_{c,t}|}$$

where $\mathbb{I}(\cdot)$ is the indicator function.

Now we describe the BLSE algorithm (see Algorithm 2 below). Its inputs are: the training data set, a maximum out of band percentage α (e.g., 5%), and a vector $\boldsymbol{\beta} = \{0, \frac{1}{M-1}, \frac{2}{M-1}, \dots, 1\}$. The parameter M is an integer greater than 1 to be selected by the modeler¹. The outputs of the BLSE algorithm are the trained parameters of $\hat{\theta}_{k,t}^L$ and $\hat{\theta}_{k,t}^U$. For each time t it does the following: it goes through each element of $\boldsymbol{\beta}$, β_i , it solves $\text{BLSEF}(\beta_i)$.

¹A small M reduces the computation time of Algorithm 2 but might yield less accurate solutions. A large M , on the other hand, increases the computation time but yields a more accurate solutions. In this work we use $M = 100$

Then, among the solutions that yield an out-of-band percentage smaller than α , it selects the one that solution that yields tighter band, i.e., the smallest $J_{t,i}^A$.

Input: $\{\phi_k^{\text{in}}, \mathbf{p}_k, \phi_k^{\text{out}}, \phi_{0,k}^{\text{in}}\}_{k \in \mathcal{K}}$, α , $\beta = \{0, \frac{1}{M-1}, \frac{2}{M-1}, \dots, 1\}$, $\{\mathcal{K}_{1,t}, \dots, \mathcal{K}_{C_t,t}\}_{t=1, \dots, T}$
Output: $\{\{\bar{\mathbf{a}}_{c,t}^*, \underline{\mathbf{a}}_{c,t}^*, \bar{\mathbf{b}}_{c,t}^*, \underline{\mathbf{b}}_{c,t}^*\}_{c=1, \dots, C_t}\}_{t=1, \dots, T}$
for $t = \{1, \dots, T\}$ **do**
 for $i = \{1, \dots, M\}$ **do**
 for $c = 1 \dots, C_t$ **do**
 $(\bar{\mathbf{a}}_{c,t,i}, \underline{\mathbf{a}}_{c,t,i}, \bar{\mathbf{b}}_{c,t,i}, \underline{\mathbf{b}}_{c,t,i}, J_{t,i}^A, \pi_{t,i}^{\text{out}}) = \text{BLSEF}(\beta_i)$
 end
 $i^* = \arg \min_{\pi_{i,t}^{\text{out}} \leq \alpha} \{J_{t,i}^A\}_{i=1, \dots, M}$
 $(\bar{\mathbf{a}}_{c,t}^*, \underline{\mathbf{a}}_{c,t}^*, \bar{\mathbf{b}}_{c,t}^*, \underline{\mathbf{b}}_{c,t}^*) = (\bar{\mathbf{a}}_{c,t,i^*}, \underline{\mathbf{a}}_{c,t,i^*}, \bar{\mathbf{b}}_{c,t,i^*}, \underline{\mathbf{b}}_{c,t,i^*})$
 end
 end
end

Algorithm 2: The bounded least square estimation (BLSE) algorithm.

Note that a larger M will increase the computation time required to run Algorithm 2 but will produce a larger set $\{\pi_{i,t}^{\text{out}}\}_{i=1, \dots, M}$. A larger set of $\pi_{i,t}^{\text{out}}$'s makes it likelier that the optimal $\pi_{i^*,t}^{\text{out}}$ is closer to the desired robustness parameter α .

Appendix E

PROOFS

E.1 Proof of Lemma 1

The long-term profit made by the aggregator can be written as

$$\pi^{a,\infty} = \sum_{k=0}^{\infty} \delta^k \cdot \pi^a(\boldsymbol{\tau}^{(k)}; \boldsymbol{x}^{(k)}) = \sum_{k=0}^{v_i-1} \delta^k \cdot \pi^a(\widehat{\boldsymbol{\tau}}; \widehat{\boldsymbol{x}}) + \sum_{k=v_i}^{\infty} \delta^k \cdot \pi_i^{a'} \quad (\text{E.1})$$

where the aggregator cooperates (plays $\widehat{\boldsymbol{\tau}}_i$) until it defects from cooperation with DER i by playing $\boldsymbol{\tau}_i^D$ at time v_i . Note that the superscript (k) denotes the k^{th} time the game is played. The aggregator chooses v_i such that its long-term profit is maximized. Both the aggregator and the DER play their defection equilibrium for all subsequent time periods.

Using the identity $\sum_{k=a+1}^{b-1} \delta^k = \frac{\delta^{a+1} - \delta^b}{1 - \delta}$, (E.1) can be rewritten as

$$\pi^{a,\infty} = \frac{\pi^a(\widehat{\boldsymbol{\tau}}; \widehat{\boldsymbol{x}})}{1 - \delta} - \frac{\delta^{v_i} \cdot (\pi_i^a(\widehat{\boldsymbol{\tau}}; \widehat{\boldsymbol{x}}) - \pi_i^{a'})}{1 - \delta}.$$

Since δ is strictly less than 1 and strictly greater than zero $\delta^{v_i} \rightarrow 0$ as $v_i \rightarrow \infty$. It follows that the aggregator maximizes its profit by cooperating indefinitely (i.e., chooses $v_i^* = \infty$) if

$$\pi^a(\widehat{\boldsymbol{\tau}}; \widehat{\boldsymbol{x}}) - \pi_i^{a'} \quad (\text{E.2})$$

is greater than zero. We assume that $v_i^* = \infty$ if (E.2) is equals to zero. It follows that for the aggregator to cooperate indefinitely with DER i , the agreed DER actions and price schedule must deliver a profit greater than $\pi_i^{a'}$.

Similarly, DER i cooperates indefinitely if

$$\pi_i^{\text{der}}(\widehat{\boldsymbol{x}}_i; \widehat{\boldsymbol{\tau}}_i) - (1 - \delta) \cdot \pi_i^{\text{der}}(\boldsymbol{x}_i^{\text{D}}; \widehat{\boldsymbol{\tau}}_i) - \delta \cdot \pi_i^{\text{der}'}$$

is nonnegative. It follows that in order for DER i to cooperate indefinitely, the agreed DER actions and price schedule must deliver a profit greater than

$$(1 - \delta) \cdot \pi_i^{\text{der}}(\boldsymbol{x}_i^{\text{D}}; \widehat{\boldsymbol{\tau}}_i) + \delta \cdot \pi_i^{\text{der}'}$$

□

E.2 Proof of Lemma 2

From [34], the Nash Bargaining Solution is given by

$$(\widehat{\boldsymbol{\tau}}_i^*, \widehat{\boldsymbol{x}}_i^*) = \xi(\mathcal{B}_i) = \arg \max_{(\boldsymbol{\tau}_i, \boldsymbol{x}_i) \in \mathcal{B}_i} \left(\pi_i^{\text{der}} - \pi_i^{\text{der}'} \right) \cdot (\pi^{\text{a}} - \pi_i^{\text{a}'}). \quad (\text{E.3})$$

By the Pareto-efficiency axiom, the aggregator reaches an agreement with *every* DER and shares the maximum possible profit $\pi(\boldsymbol{x}^*)$ during every single-shot game [120].

Let

$$\mathcal{A}_i = \{(\boldsymbol{\tau}_i, \boldsymbol{d}_i) \mid \pi^{\text{a}}(\boldsymbol{\tau}; \boldsymbol{d}) \geq \pi_i^{\text{a}'}, \pi_i^{\text{s}}(\boldsymbol{d}_i; \boldsymbol{\tau}_i) \geq (1 - \delta)\pi_i^{\text{s}}(\boldsymbol{d}_i^{\text{D}}; \boldsymbol{\tau}_i) + \delta\pi_i^{\text{s}'}\}.$$

By Pareto-efficiency, the agreed prices $\widehat{\boldsymbol{\tau}}_i^*$ will be such such that long-term cooperation is sustained, i.e., $(\widehat{\boldsymbol{\tau}}_i^*, \widehat{\boldsymbol{x}}_i^*) \in \mathcal{A}_i \forall i \in \mathcal{I}$.

Denote the set of $\boldsymbol{\tau}_i$ and \boldsymbol{x}_i such that the maximum profit is split and that long-term cooperation is sustained as

$$\tilde{\mathcal{B}}_i = \{(\boldsymbol{x}_i, \boldsymbol{\tau}_i) \mid \boldsymbol{x}_i = \boldsymbol{x}_i^*, (\boldsymbol{x}_i, \boldsymbol{\tau}_i) \in \mathcal{A}_i\}.$$

By the independence of irrelevant alternatives axiom, $\xi(\mathcal{B}_i) = \xi(\tilde{\mathcal{B}}_i)$. Then, (E.3) can be replaced by

$$\xi(\mathcal{B}_i) = \arg \max_{(\boldsymbol{\tau}_i, \boldsymbol{x}_i) \in \tilde{\mathcal{B}}_i} \left(\pi_i^{\text{der}} - \pi_i^{\text{der}'} \right) \cdot (\pi^{\text{a}} - \pi_i^{\text{a}'})$$

which is equivalent to problem (4.8). □

E.3 Proof of Theorem 1

As stated in Eq. (6.4), the problem that the firm solves to formulate its strategic bids is

$$\mathbf{P1}: \mathbf{f}^* = \arg \max_{\mathbf{f}} u(\mathbf{x}(\mathbf{f})) + \sum_{t \in \mathcal{T}} \boldsymbol{\lambda}_t(\mathbf{f})^\top \mathbf{x}_t(\mathbf{f}). \quad (\text{E.4})$$

The LMPs $\boldsymbol{\lambda}_t$ are a function of the market clearing process denoted by Problem (6.2) and are defined in Definition 4. Thus, problem (4.7) is implicitly a bi-level problem: the firm determines and submits its bid \mathbf{f}^* . Subsequently, the market clears and determines $\boldsymbol{\lambda}_t$. Denote this problem as **P1**.

Similarly, Problem (6.5), which defines the socially optimal bids, is technically a bi-level problem: the system operator determines the optimal bids $\mathbf{f}^{\text{social}}$ by maximizing the social welfare function $S(\mathbf{f})$ which is a function of Problem (6.2). Denote this problem as **P2**.

Note that **P1** and **P2** are similar problems: they have the same set of decision variables, \mathbf{f} (in the upper level) and $\{\mathbf{g}_t, \mathbf{x}_t\}_{t \in \mathcal{T}}$ in (the lower level), and the same set of constraints. Their objectives are different. The objective of **P1** is to maximize the firm's profit while the objective of **P2** is to maximize social welfare.

Replacing λ_t with the definition of $\mathbf{p}_t(\mathbf{f})$ from Theorem 1 in (E.4) we get

$$u(\mathbf{x}(\mathbf{f})) - \sum_{t \in \mathcal{T}} \mathbf{1}^\top \mathbf{c}_t^{\text{gen}}(\mathbf{g}_t(\mathbf{f})) + \sum_{t \in \mathcal{T}} \mathbf{1}^\top \boldsymbol{\gamma}_t$$

which is equivalent to the social welfare from Eq. (6.1) plus a constant term $\sum_{t \in \mathcal{T}} \mathbf{1}^\top \boldsymbol{\gamma}_t$.

We have shown that the objectives of **P1** and **P2** are equivalent when the aggregator is exposed to the MPMP $\mathbf{p}_t(\mathbf{f})$. Furthermore, we showed that **P1** and **P2** are subject to the same set of constraints. Thus we conclude that when the firm is exposed to $\mathbf{p}_t(\mathbf{f})$ rather than to the LMP, **P1** and **P2** are equivalent problems. Thus, the market clears at the social optimum when the firm is exposed to $\mathbf{p}_t(\mathbf{f})$. \square

E.4 Proof of Theorem 2

Using (7.3), Problem (7.9) can be written as

$$\min_{\substack{\phi_i \in \Phi_i \\ \mathbf{x}_i \in \mathcal{X}_i(\phi_i)}} \left\{ y + \min_{\delta \in \Delta} \frac{I^W}{(1 + \rho)^\delta} \right\} \quad (\text{E.5})$$

where $y = \sum_{i \in \mathcal{N}} [C_i^O(\mathbf{x}_i) + I_i^{\text{NW}}(\phi_i)] + C^D(\mathbf{l}^P(\mathbf{x}))$ and Δ denotes the set defined by the constraints in (7.3). Problem (E.5) is equivalent to

$$\min_{\substack{\phi_i \in \Phi_i \\ \mathbf{x}_i \in \mathcal{X}_i(\phi_i)}} \min_{\delta \in \Delta} \left\{ y + \frac{I}{(1 + \rho)^\delta} \right\}. \quad (\text{E.6})$$

Problem (E.6) is a nested optimization problem that whose inner variable is δ and its outer variables are \mathbf{x}_i and ϕ_i . As shown in [40] the inner and outer variables can be minimized simultaneously in a single min function. Thus (7.9) is equivalent to (7.10) where (7.10d) implement the functions $l_a^P(\mathbf{x}) = \max_{t \in \mathcal{T}} \{l_{a,t}(\mathbf{x})\}$ via half-planes. \square

VITA

Jesus Elmer Contreras Ocaña was born in Hermosillo, México on the 16th of December of 1989. He received his B.S. in electrical engineering and B.A. in economics from The University of Texas at Austin in 2013 and his M.S. in electrical engineering from the University of Washington (UW), Seattle in 2015. He is currently a Ph.D. candidate at the UW Department of Electrical Engineering.